THERMAL BUCKLING OF FGM THIN PLATES WITH VARIABLE THICKNESS

by

Işıl Sanrı

B.S. in C.E., Çukurova University, 1997

M.S. in C.E., Boğaziçi University, 2001

Submitted to the Institute for Graduate Studies in
Science and Engineering in partial fulfillment of
the requirements for the degree of
Doctor of Philosophy

Graduate Program in Civil Engineering

Boğaziçi University

2010

to,

my dad, Remzi SANRI

my mom, Levent SANRI

ACKNOWLEDGEMENTS

I would like to take this opportunity to thank all who have contributed to the completion of this work. First and foremost, I would like to thank my supervisor Prof. Gülay Altay, for her guidance, support and motivation. She made my academic experience at Boğaziçi University very rewarding and she has been a pleasure to work with throughout this endeavor. I would also like to express my sincere gratitude to Prof. Cengiz Dökmeci, not only for his valuable help, suggestions and comments but also for his unlimited support and encouragement.

I would also like to thank the other committee members; Prof. Turan Özturan, Asst. Prof. Sami And Kılıç and Assoc. Prof. Semih Küçükarslan for agreeing to serve on my Ph.D. advisory committee and for their helpful advices and comments on my dissertation.

I also wish to express my gratitude to my friends who have believed in me and have helped me accomplish my thesis by their support. In particular, I would like to thank Dr. Seyit Çeribaşı for his endless help in guiding the software preparation and support during my entire study. Finally, I would like to thank my parents for their never ending encouragement, love and support from home town, and also my husband, who has been with me during all ups and downs of this dissertation. This thesis would not have been completed without his unlimited understanding, patience and support.

ABSTRACT

THERMAL BUCKLING OF FGM THIN PLATES WITH VARIABLE THICKNESS

The main focus of this study is the thermal buckling analysis of plates. In particular, the studies on the problem of the stability of various shapes of plates are extensive but quite little has been reported for the thermal buckling problem of plates.

In this thesis, thermal buckling of rectangular and elliptical plates is examined. Plate theories are investigated and Kirchhoff plate theory is applied to derive and formulate thermal buckling problem. Boundary conditions are assumed to be simply supported and clamped in the whole study. Rayleigh-Ritz method is used to solve the energy equations and to obtain the critical buckling loads.

The study consists of three main parts. The first part focuses on the thermal buckling of rectangular and elliptical Kirchhoff plates with constant thickness. Critical buckling temperatures for the homogenous, isotropic plates are obtained; the results are presented in graphical and tabular forms and compared with previously obtained results of the available literature.

The second part of the study covers the thermal buckling analyses of functionally graded material (FGM) Kirchhoff plates with constant thickness. FGM plates are advanced composites with properties that vary continuously through the thickness of the plate. Metal-ceramic FGM plates are proposed for the use in thermal analyses where a metal-rich interior surface of the plate gradually transitions to a ceramic-rich exterior surface of the plate. The effect of the FGM on the thermal buckling of rectangular and elliptical plates is discussed.

In the last part of the study, elliptical and rectangular FGM Kirchhoff plates with variable thicknesses are studied. The effect of parabolic thickness variation on the critical

buckling load parameter is investigated. Then, parametric studies are carried out to examine the effects of material properties and thickness variation on the critical buckling temperatures.

As a consequence, since the exact solution of thermally induced general buckling problems of plates is very difficult and in many cases even impossible, thermal buckling problem of plates is simplified and the critical buckling temperatures for homogenous and FGM plates with constant thicknesses and FGM plates with variable thicknesses are presented.

ÖZET

DEĞİŞKEN KALINLIKLI FGM INCE LEVHALARIN TERMAL BURKULMASI

Bu çalışmanın asıl amacı levhaların termal burkulma analizidir. Özellikle değişik şekillerdeki levhaların stabilite problemleriyle ilgili olan çalışmalar oldukça geniştir ancak levhaların termal burkulması üzerine yapılan çalışmalar son derece sınırlıdır.

Bu tezde dikdörtgen ve eliptik levhaların termal burkulması incelenmiştir. Plak teorileri araştırılmış ve termal burkulma probleminin formulasyonu için Kirchhoff plak teorisi kullanılmıştır. Tüm çalışmada levhalar basit mesnetli ve ankastre sınır koşullarına uygun olacak şekilde kabul edilmiştir. Enerji denklemlerinin çözümü ve kritik burkulma yüklerinin bulunması için Rayleigh-Ritz metodu kullanılmıştır.

Bu çalışma üç ana bölümden oluşmaktadır. Birinci bölüm sabit kalınlıklı dikdörtgen ve eliptik Kirchhoff plaklarının termal burkulması üzerine odaklanmıştır. Homojen, izotropik levhalar için kritik burkulma sıcaklıkları elde edilmiş, sonuçlar grafik ve tablolar halinde sunulmuş ve mevcut literatürdeki ilgili çalışmalarla karşılaştırılmıştır.

Çalışmanın ikinci bölümü bir fonksiyona bağlı olarak değişen (FGM) sabit kalınlıklı Kirchhoff plaklarının termal burkulmasını kapsamaktadır. FGM levhalar, levha kalınlığı boyunca değişen gelişmiş kompozitlerdir. Plağın metal yoğunluklu iç yüzeyinin aşamalı olarak seramik yoğunluklu dış yüzeye dönüştüğü metal-seramik FGM levhalar termal analizlerde kullanılmak üzere öngörülmüştür. FGM malzemesinin dikdörtgen ve eliptik levhaların termal burkulması üzerindeki etkisi irdelenmiştir.

Çalışmanın son bölümünde değişken kalınlıklı eliptik ve dikdörtgen FGM Kirchhoff plakları araştırılmıştır. Parabolik kalınlık değişiminin kritik burkulma yükü parametresi üzerindeki etkisi incelenmiştir. Daha sonra, malzeme özelliklerinin ve kalınlık

değişkenliğinin kritik burkulma sıcaklıkları üzerine etkilerini incelemek için parametrik çalışmalar uygulanmıştır.

Sonuç olarak, levhaların ısıya bağlı olarak genel burkulma problemlerinin kesin çözümü çok zor hatta bazı durumlarda imkansız olduğu için, levhaların termal burkulma problemi basitleştirilmiş, hem sabit hem de değişken kalınlıklı, homojen ve FGM levhaların kritik burkulma sıcaklıkları elde edilmiş ve sunulmuştur.

TABLE OF CONTENTS

LIST OF FIGURES

LIST OF TABLES

LIST OF SYMBOLS/ABBREVIATIONS

a	Plate dimension in x direction
b	Plate dimension in y direction
c	Parameter that equals the volume of plate
D	Flexural rigidity of plate
D_{eff}	Effective flexural rigidity of plate
D_0	Flexural rigidity of plate with constant thickness
E	Young's modulus of elasticity
E_c	Young's modulus of ceramic
E_{eff}	Effective Young's modulus
E_m	Young's modulus of metal
F	Total energy function
G	Shear modulus
H	Function representing the variable plate thickness
K	Thermal conduction coefficient
K_c	Thermal conduction coefficient of ceramic
K_m	Thermal conduction coefficient of metal
M_x	Bending moment in x direction
M_y	Bending moment in y direction
M_{xy}	Twisting moment in xy plane
M^*	Thermal equivalent bending moment
N_x	Normal force in x direction
N_y	Normal force in y direction
N_{xy}	Shear force acting in xy plane
N^*	Thermal force acting in xy plane
n	Power law index
p	Transverse load
Q_x	Transverse shearing force in x direction
Q_y	Transverse shearing force in y direction
r	Order of the polynomial trial function

T	Kinetic energy
T_{cr}	Critical temperature
t	Thickness of plate
t_0	Thickness of plate with constant thickness
U	Strain energy
V	Potential energy of the in-plane uniform pressure
V_c	Volume fraction of ceramic
V_m	Volume fraction of metal
$w(x,y)$	Displacement function
α	Parameter defining the constant part of the thickness
α	Thermal expansion coefficient
α_c	Thermal expansion coefficient of ceramic
α_{eff}	Effective thermal expansion coefficient
α_m	Thermal expansion coefficient of metal
α_{ij}	Unknown coefficients
β	Taper parameter
∇^2	Laplace operator
∇^4	Biharmonic operator
Π	Total potential energy of the plate
$\phi(x,y)$	Shape function
Ω	Scalar indicator of the boundary condition
ρ_{eff}	Effective mass per unit area
$\bar{\rho}_{eff}$	Effective mass density
ν	Poisson's ratio
ν_{eff}	Effective Poisson's ratio
ΔT	Temperature difference
ε_t	Thermal strain
ε_x	Normal strain in x direction
ε_y	Normal strain in y direction
γ_{xy}	Shear strain in xy plane

γ_1, γ_2	Scalar indicators
σ_x	Normal stress in x direction
σ_y	Normal stress in y direction
τ_{xy}	Shear stress in xy plane
λ	Buckling load factor
λ'	Buckling load factor for functionally graded plates

CL	Clamped
SS	Simply supported
FGM	Functionally graded material

1. INTRODUCTION

1.1. Literature Review

Plates are straight, flat surface structures whose thickness is slight compared to their dimensions. Thin and thick various shapes of plates are extensively used in civil, mechanical, nuclear and aerospace engineering and they are one of the basic structural elements. Many structures such as containers, ships, etc., require complete enclosure that can be accomplished easily by plates without use of additional covering. Because of their extensive application areas the problems related to the static and dynamic analyses of plates became more complex and the demand for solutions of plate problems increased. The plate problems have been studied by great amount of engineers and mathematicians during the last two centuries. Numerous methods have been developed for analyzing both static and dynamic behavior of plates having a wide range of shapes [1, 2].

Many papers have been published on various types of plates. The literature review shows that a plate problem can be a deflection problem, buckling problem or a vibration problem. It is also observed that, in the literature, in order to solve a plate problem, different applications are used. In many papers, a wide variety of geometries, material types, load combinations, boundary conditions and constitutive models are considered for the plates. Geometrically, plates are bound either by straight or curved lines. Statically, plates have free, simply supported and fixed boundary conditions, including elastic supports and elastic restraints or in some cases point supports.

According to this, the focus of the plate studies can be classified under five main topics. This classification is given in details in Figure 1.1. Also, there are many approximate solution techniques used for the solution of a plate problem. Galerkin Method, Rayleigh-Ritz Method, Kantorovich Method, Collocation Method, Method of Moments, Method of Least Squares, Finite Difference Method, Finite Element Method, and Boundary Elements Method are some of these approximate solution techniques encountered in the literature.

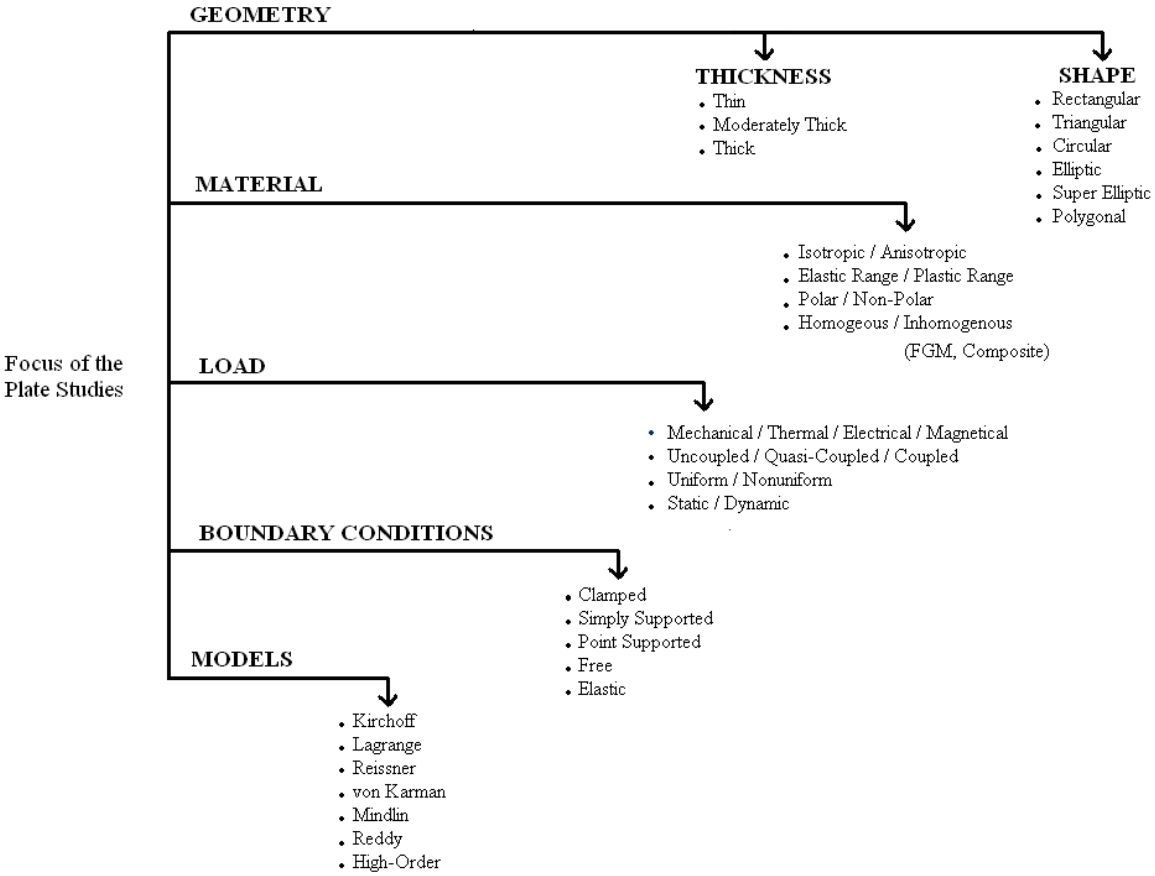

Figure 1.1. Foci of the plate studies

Among these studies, investigations on the thermal effect on the plates have received widespread attention in recent years. In many applications, it is seen that when the plate is subjected to thermal loads, that causes thermal buckling. In the light of this, there are many thermal buckling investigations which are presented in the field of thermal buckling of plates. Also, in many of applications thin walled members are subjected to thermal loads which cause thermal buckling [3, 4].

Murphy and Ferreira [5] presented the results of a thermal buckling analysis of a clamped rectangular plates based on energy considerations. In this study, a series of experiments are done to determine the buckling temperature for plates with varying edge length and the buckling analysis and the experimental results are compared with each other. Shariyat [6] worked on the thermal buckling analysis of rectangular composite multilayered plates under uniform temperature rise by using layerwise plate theory. Von Karman strain–displacement equations are employed to account for large deflections

occurrence. A FEM algorithm is used to exactly incorporate the boundary conditions. Bert and Devarakonda [7] worked on buckling of rectangular plates subjected to nonlinearly distributed in-plane loading without taking the thermal effects into consideration. They presented a solution for the half-sine load distribution on two opposite sides. In order to solve the governing differential equation of thin plate buckling, they used Galerkin method.

Kabir *et al*. [8] presented an analytical solution to thermal buckling response of moderately thick symmetric angle-ply laminated, rectangular plate which is clamped from all the edges. They applied a uniformly distributed thermal load on the plate. The first order shear deformation theory based on Reissner-Mindlin hypothesis is used. Li *et al*. [9] investigated the axisymmetric vibrations of a statically buckled polar orthotropic circular plate due to uniform temperature rise. In their study, two sets of coupled boundary value problems are solved numerically by a shooting method. Laura and Rossit [10] worked on thermal bending of thin, anisotropic, clamped elliptic plates and their study deals with the exact analytical solution of thermal bending of such plates. Liew *et al*. [11] studied the vibration analysis of circular Mindlin plates. They calculated natural frequencies of vibration for circular plates with free, simply supported and clamped edges. They analyzed plates both with and without rigid center support. For solving the governing equations they used differential quadrature method.

Kalyan and Bhaskar [12] studied on the buckling of rectangular orthotropic plates subjected to non-uniform compressive loads. In their study, for the determination of the in-plane stress distribution a rigorous superposition approach is used and then for stability the analysis is done using Galerkin's method. Further, the effects of various relevant parameters are examined with respect to partially loaded plates, plates with different load distributions on opposite edges, moderately thick plates and plates with simply supported/clamped edge conditions. Belinha and Dinis [13] extended a meshless method based in a Galerkin formulation for the use in the elastic and elasto-plastic analysis of anisotropic symmetric laminates. Several problems of laminate bending are solved and the obtained solutions are compared with finite element solutions and concluded that the meshless approach developed is an alternative to the finite element method for the solution of problems with material nonlinearity. Çeribaşı *et al.* [14] worked on the clamped

superelliptical plates under uniformly distributed surface load. Linearly elastic, homogeneous, and isotropic material is considered. Kirchhoff, the classical thin plate model, is employed to the problem and Galerkin's method is used to obtain solutions. Lee and Lee [15] investigated the behaviors of thermally post-buckled anisotropic plates. The finite element method is used for the analysis of thermal post-buckling and natural vibration of thermally post-buckled plates. The finite element model is based on the first-order shear deformable plate theory (FSDT) and von Karman strain-displacement relation to account for large deflection. In their study, critical buckling temperature and the corresponding mode shape are determined from Euler buckling problem. Park *et al.* [16] performed the vibration analysis of the thermally postbuckled composite plate embedded with shape memory alloy fibers. In order to account for the temperature-dependent material properties of shape memory alloy fibers, the incremental method considering the initial displacement and initial stress is adopted.

Shen *et al*. [17] worked on the response of Reissner–Mindlin plates exposed to thermo-mechanical loading which is resting on a Pasternak-type elastic foundation. The formulations are based on the Reissner–Mindlin plate theory, considering the first order shear deformation effect and including the plate–foundation interaction and thermal effects. The Modal Superposition Approach and State Variable Approach are both used to determine the dynamic response of the moderately thick plate with all four edges simply supported. Shen [18] presented a thermal buckling analysis for a simply supported, moderately thick rectangular plate subjected to uniform or non-uniform tent-like temperature loading which is resting on a softening nonlinear elastic foundation. The formulations are based on the Reissner-Mindlin plate theory considering the first-order shear-deformation effect, and including plate-foundation interaction and thermal effects. The analysis uses a deflection-type perturbation technique to determine the thermal buckling loads and post-buckling equilibrium paths. Shen [19] studied on the thermal post-buckling analysis for a shear-deformable rectangular plate subjected to uniform or non-uniform tent-like temperature loading and resting on a two-parameter elastic foundation. Again, the formulations are based on the Reissner-Mindlin plate theory considering the first order shear deformation effect and including thermal effects. The analysis uses a deflection-type perturbation technique to determine the thermal buckling loads and post-buckling equilibrium paths. Shen [20] worked on the post-buckling analysis for a

moderately thick rectangular plate subjected to combined axial compression and uniform temperature loading, and resting on a softening nonlinear elastic foundation. Formulations are based on Reissner-Mindlin plate theory considering first-order shear deformation effects and the analysis uses a deflection-type perturbation technique to determine buckling loads and post-buckling equilibrium paths.

Ganapathi and Touratier [21] worked on a nonlinear finite element formulation for studying the post-buckling behavior of laminated plates induced by a uniform/non-uniform temperature field. The thermal stress analysis is carried out for the nonuniformly distributed temperature loading over the plate before solving the buckling problem. The formulation is based on the Reissner-Mindlin first order shear deformation theory. Deflection-load relationships are obtained through an iterative method. Detailed numerical results are presented for cross-ply and angle-ply laminated composite plates with different boundary conditions. Prabhu and Dhanaraj [22] researched the thermal buckling of laminated composite plates using the finite element method based on the Reissner-Mindlin first order shear deformation theory. Thermal buckling analysis of symmetric cross-ply, symmetric angle-ply and quasi-isotropic laminates subjected to uniform temperature distribution is done. Huang and Tauchert [23] investigated the buckling behavior of moderately thick symmetric angle-ply laminates having clamped edges, subjected to a uniform temperature rise. The Reissner-Mindlin theory is employed and the exact solution to the coupled differential equations is obtained using the general double Fourier series approach. Calculated values of the critical temperature are compared with corresponding finite element results.

Giorgi and Naso [24] studied on the mathematical models describing deformations and thermal variations of a thin homogeneous thermo-viscoelastic plate. A hereditary non-Fourier constitutive law for the heat flux and some heat power constitutive equation with linear memory are considered. The resulting models are derived according to the standard approximation procedure for the Reissner-Mindlin plate model. Lee *et al.* [25] worked on the thermal post-buckling analysis of patched laminated panels under uniform and non-uniform temperature distributions. A finite element method based on the Hellinger–Reissner principle with independent strain, which is free of shear locking is performed. The cylindrical arc-length method is adopted to obtain a non-linear solution. Shen [26]

studied on the post-buckling analysis for a simply supported, shear deformable laminated plate with piezoelectric actuators subjected to the combined action of mechanical, electric and thermal loads. The temperature field considered is assumed to be a uniform distribution over the plate surface and through the plate thickness. The governing equations of a laminated plate are based on Reddy's higher order shear deformation plate theory that includes thermo-piezoelectric effects. A perturbation technique is employed to determine buckling loads and post-buckling equilibrium paths.

Shen [27] investigated a thermal post-buckling analysis for a simply supported, shear-deformable laminated plate with piezoelectric actuators subjected to the combined action of thermal and electric loads. The governing equations of a laminated plate are based on Reddy's higher-order shear-deformation plate theory that includes thermo-piezoelectric effects. The analysis uses a mixed Galerkin-perturbation technique to determine thermal buckling temperature and post-buckling equilibrium paths. Shen [28] researched thermal post-buckling analysis for a simply supported, shear deformable laminated plate subjected to a uniform temperature rise and resting on an elastic foundation. The formulations are based on Reddy's higher order shear deformation plate theory including the plate-foundation interaction and thermal effects. A perturbation technique and an iterative numerical procedure are employed to determine the buckling temperature and thermal post-buckling load-deflection curves. Shen [29] presented a post-buckling analysis for a simply supported, shear deformable composite laminated plate subjected to combined axial and thermal loads and resting on an elastic foundation. Initially compressed plates and of compressive post-buckling of initially heated plates are considered. The formulations are based on Reddy's higher order shear deformation plate theory, including the plate-foundation interaction and thermal effects. The analysis uses a perturbation technique to determine the buckling loads and the post-buckling equilibrium paths.

Cheng and Kitipornchai [30] found the exact explicit eigenvalues based on Reddy’s third-order theory, the first-order theory and the classical theory for compression buckling, thermal buckling and vibration of laminated plates via analogy with membrane vibration. Shen [31] worked on the thermal post-buckling analysis for a simply supported, shear-deformable composite laminated plate subjected to uniform or non-uniform parabolic

temperature loading and resting on a two-parameter elastic foundation. Reddy's third-order shear-deformation plate theory with von Karman nonlinearity is used. The analysis uses a mixed Galerkin-perturbation technique to determine thermal buckling loads and post-buckling equilibrium paths. Yapici [32] studied on the thermal buckling analysis of symmetric and antisymmetric angle-ply laminated hybrid composite plates with an inclined crack subjected to a uniform temperature rise. The first-order shear deformation theory in conjunction with the variational energy method is employed in mathematical formulations. The eight-node Lagrange finite-element technique is used for determining the thermal buckling temperatures of hybrid laminates. The effect of crack size and stacking sequences on the temperatures is investigated.

Singha and Ganapathi [33] presented the system parameters effects on supersonic panel flutter behavior of laminated composite skew plates using a shear deformable finite element approach. The first-order high Mach number approximation to linear potential flow theory is employed for evaluating the aerodynamic pressure. The solutions of complex eigenvalue problem, formulated based on Lagrange's equation of motion are obtained using the standard method for finding eigenvalues. Zhu *et al*. [34] worked on the nonlinear thermal buckling of symmetrically laminated cylindrically orthotropic shallow spherical shell under temperature field and uniform pressure including transverse shear. The analytic formulas for determining the critical buckling loads under different temperature fields are obtained by using the modified iteration method. Pradeep and Ganesan [35] presented the thermal buckling and vibration behavior of multi-layer all side clamped rectangular viscoelastic sandwich plates. A decoupled thermo-mechanical analysis is made by using finite element method. Aydogdu [36] researched the thermal buckling analysis of rectangular cross-ply laminated beams subjected to different sets of boundary conditions. Three different combinations of clamped and hinged edge boundary conditions are considered. The analysis is based on a three-degree-of-freedom shear deformable beam theory. The governing equations are obtained by means of minimum energy principle. The critical thermal buckling temperatures are obtained by applying the Ritz method.

Matsunaga [37] worked on the free vibration and stability problems of angle-ply laminated composite and sandwich plates subjected to thermal loading. A two-dimensional

global higher-order deformation theory is used. Avci *et al*. [38] studied on the thermal buckling analysis of symmetric and antisymmetric cross-ply laminated hybrid composite plates with an inclined crack subjected to a uniform temperature rise. The first-order shear deformation theory in conjunction with variational energy method is employed in the mathematical formulation. Zakeri and Alinia [39] developed governing equations for determining thermal buckling of imperfect sandwich plates by using the large deflection theory and considering first shear deformation principles. Matsunaga [40] studied on a two-dimensional global higher-order deformation theory for thermal buckling of angle-ply laminated composite and sandwich plates. Several sets of truncated *m*th order approximate theories are applied to solve the eigenvalue problems of simply supported laminated composite and sandwich plates.

Sahin [41] worked on thermal buckling analysis of symmetric and antisymmetric laminated hybrid composite plates with a hole subjected to a uniform temperature rise for different boundary conditions. The first-order shear deformation theory in conjunction with variational energy method is employed in mathematical formulation. The eight-node Lagrangian finite element technique is used for obtaining the thermal buckling temperatures of hybrid laminates. Avci *et al*. [42] studied on the thermal buckling analysis of symmetric and antisymmetric cross-ply laminated hybrid composite plates with a hole subjected to a uniform temperature rise for different boundary conditions. The first-order shear deformation theory in conjunction with variational energy method is employed in the mathematical formulation. The eight-node Lagrangian finite element technique is used for finding the thermal buckling temperatures of hybrid laminates. Avci *et al*. [43] studied on the thermal buckling analysis of symmetric and antisymmetric laminated composite plates with clamped and simply supported edges, and containing a hole. The first-order shear deformation theory in conjunction with the variational energy method is employed in mathematical formulation. The eight-node Lagrangian finite element technique is used to find thermal buckling temperatures of isotropic, glass-epoxy and boron-epoxy laminates.

Shen and Li [44] investigated the post-buckling responses of shear deformable laminated plates supported by a tensionless elastic foundation and subjected to in-plane compressive edge loads or a uniform temperature rise. The formulations are based on the higher order shear deformation plate theory with a von Kármán-type of kinematic non-

linearity. The thermal effects are included and a two step perturbation technique is used to determine the post-buckling response of the plate. Vangipuram and Ganesan [45] studied on the free vibration and damping characteristics of plates consisting of composite stiff-layers and an isotropic viscoelastic core under thermal loads using finite element method. The temperature dependence of viscoelastic core properties and effects of pre-stresses are taken into account. Morimoto *et al*. [46] presented the thermal buckling analysis of an isotropic inhomogeneous rectangular plate subjected to the arbitrary thermal loads. The fundamental equations system is derived by introducing the technique of the newly defined position of the reference plane, which allows us to analyze the problem using an elementary plate theory.

Girish and Ramachandra [47] worked on the post-buckling and postbuckled vibrations of symmetrically laminated composite plate subjected to a uniform temperature distribution through the thickness. The structural model is based on a higher-order shear deformation theory incorporating von Kármán nonlinear strain–displacement relations and initial geometric imperfections. Also, a multi term Galerkin's approximation is adopted. The critical buckling temperatures are obtained from the solution of the corresponding linear eigenvalue problems. Zhang and Xing [48] presented a mathematical model of thin plates in the sense of the Kirchhoff's hypothesis. The Ritz method in the spatial domain and the differentiating method in the temporal domain are used to approximate the mathematical model in a system of rectangular Cartesian coordinates. The influences of thermal excitation frequency, mechanical relaxation time and thermal relaxation time on amplitude and phase difference of steady-state vibration of a square plate are investigated. Wang *et al*. [49] obtained solutions for super elliptical plates by using two dimensional polynomials at degree of 12 for frequency and buckling factors. They presented a wide range of solutions for such plates with either simply supported or clamped edges.

Singha *et al*. [50] presented a study on the thermal post-buckling behavior of laminated composite plates. Temperature dependent thermal and elastic properties of the material are taken into account in the analysis. Gossard *et al*. [51] presented an approximate method to calculate the deflections of flat or initially imperfect plates subjected to thermal buckling. The analyses are done based on a large deflection theory and a tent like temperature distribution is applied over the rectangular plate surface.

Theoretical results are also compared with the experimental results and it is seen that they are in good agreement with each other. Nath and Shukla [52] investigated the buckling and post-buckling analysis of the moderately thick angle ply laminated composite rectangular plates subjected to combined in-plane mechanical load and temperature gradient across the thickness. First order shear deformation theory is employed in the formulation of the problem. The boundary conditions consisting of clamped, simply supported and their combinations are considered. Shiau *et al*. [53] studied thermal buckling behavior of composite laminated plates by making the use of finite element method.

It is also apparent from the literature survey that most of the researches have been reported on the buckling and post-buckling analysis of functionally graded plates (FGM) subjected to mechanical or thermal loading. Most of the researches on FGMs have been restricted to thermal stress analysis, fracture mechanics and optimization. It is seen that very little work has been done to consider the stability analysis, buckling and vibrational behavior of FGM structures.

Among those studies, thermal and mechanical buckling of simply supported FGM rectangular plates is studied by Javaheri and Eslami [54, 55, 56] based on the classical and higher order shear deformation plate theories. Na and Kim [57, 58] used solid finite elements to calculate the buckling temperature of FGM plates with fully clamped edges. Thermal buckling and post-buckling behaviors due to uniform and non-uniform temperature rise are studied. Najafizadeh and Heydari [59, 60] considered axisymmetric buckling of simply supported and clamped circular FGM plates under a uniform temperature rise or a radial compression based on the higher order shear deformation theory. The results are compared with the buckling loads of plates obtained for functionally graded circular plate based on the first order shear deformation plate theory and classical plate theory. Ganapathi and Prakash [61] presented the buckling loads for simply supported FGM skew plates subjected to in-plane mechanical loads and heat conduction by using the first-order shear deformation theory in conjunction with the finite element approach. In their analysis, the material properties are based on the Mori-Tanaka scheme and the rule of mixture, respectively. This work was then extended to the case of thermal post-buckling of FGM skew plates by Prakash *et al*. [62]. In the analysis, von Karman's assumptions are used. The temperature field is assumed to be uniform over the plate

surface and varies in the thickness direction only. The nonlinear governing equations derived based on von Karman's assumptions are solved employing the direct iterative technique. Yang and Shen [63] investigated the nonlinear bending behavior of the functionally graded plate subjected to the uniform load with the temperature rise. Furthermore, Yang and Shen [64] studied the post-buckling behavior of FGM thin plates under fully clamped boundary conditions. This work was then extended to the case of shear deformable FGM plates with various boundary conditions and various possible initial geometric imperfections by Yang *et al*. [65]. In this study, the formulations are based on Reddy's higher-order shear deformation plate theory and von Karman-type geometric nonlinearity.

Saidi and Baferani [66] worked on the thermal buckling analysis of moderately thick functionally graded annular sector plates. Wu [67] studied the thermal buckling behavior of simply supported FGM rectangular plates under uniform temperature rise and gradient through the thickness based on the first order shear deformation plate theory. Wu *et al*. [68] obtained the post-buckling behavior of FGM rectangular plates under various boundary conditions subjected to uniaxial compression or uniform temperature rise based on the first order shear deformation plate theory. Park and Kim [69] studied the thermal post-buckling and vibration behaviors of simply supported FGM plates with temperature dependent material properties by using finite element method. Shariat and Eslami [70, 71] performed the thermal buckling of imperfect FGM rectangular plates under three types of thermal loading as uniform temperature rise, non-linear temperature rise through the thickness and axial temperature rise based on the first order shear deformation plate theory and the classical thin plate theory, respectively. The results are reduced and compared with the results of perfect functionally graded and imperfect isotropic plates. Shariat and Eslami [72], also, presented the buckling analysis of rectangular thick functionally graded plates under mechanical and thermal loads. The plate is assumed to be under three types of mechanical loadings, namely; uniaxial compression, biaxial compression, and biaxial compression and tension and two types of thermal loadings, namely, uniform temperature rise and non-linear temperature rise through the thickness. The equilibrium and stability equations are derived using the third order shear deformation plate theory. Resulting equations are employed to obtain the closed-form solution for the critical buckling load for each loading case.

Recently, Shen [73] provided a post-buckling analysis for simply supported, mid-plane symmetric FGM plates with fully covered or embedded piezoelectric actuators subjected to the combined action of mechanical, thermal and electronic loads. The governing equations are based on a higher order shear deformation plate theory that includes thermo-piezoelectric effects. In this study, the material properties are considered to be temperature dependent and the effect of temperature rise and applied voltage on the post-buckling response is reported. It is seen that this work was then extended by Shen and Li [74] to the case of post-buckling analysis of sandwich plates with FGM face sheets subjected to mechanical and thermal loads. The results reveal that the temperature changes, the volume fraction distribution of FGM face sheets, and the substrate-to-face sheet thickness ratio have a significant effect on the buckling load and post-buckling behavior of sandwich plates. Also, they confirm that for the case of heat conduction, the post-buckling path is no longer of the bifurcation type.

Moreover, buckling of FGM plates without or with piezoelectric layers subjected to various non-uniform in-plane loads, along with heat and applied voltage is considered by Chen and Liew [75] and Chen *et al*. [76] using the first order shear deformation theory. Shen [77] provided a thermal post-buckling analysis for simply supported, midplane symmetric FGM plates under in-plane non-uniform parabolic temperature distribution and heat conduction and concluded that for the case of heat conduction, the post-buckling path for geometrically perfect plates is no longer of the bifurcation type. Liew *et al.* [78] examined the post-buckling behavior of FGM rectangular hybrid plates that are integrated with surface-bonded piezoelectric actuators and are subjected to the combined action of uniform temperature change, in-plane forces, and constant applied actuator voltage. A Galerkin differential quadrature iteration algorithm is proposed for solution of the non-linear partial differential governing equations. In their study, the effects of applied actuator voltage, in-plane forces, volume fraction exponents, temperature change, and the character of boundary conditions on the buckling and post-buckling characteristics of the plates are also shown.

Kim [79] developed a theoretical method to investigate vibration characteristics of initially stressed functionally graded rectangular plates made up of metal and ceramic in thermal environment. The third-order shear deformation plate theory to account for rotary

inertia and transverse shear strains is adopted to formulate the theoretical model. The Rayleigh–Ritz procedure is applied to obtain the frequency equation. The analysis is based on an expansion of the displacements in the double Fourier series that satisfy the boundary conditions. The effect of material compositions, plate geometry, and temperature fields on the vibration characteristics is examined. Kitipornchai *et al*. [80] investigated the random free vibration of functionally graded laminates. They applied general boundary conditions on the plates and considered the temperature change.

Reddy [81] researched the linear and nonlinear static analyses of the functionally graded plate under thermo-mechanical loads. Theoretical formulation, Navier's solution and finite element model for the functionally graded plate are presented. Lanhe [82] presented the analytical solution for the thermal buckling of the thick functionally graded plate and derived equilibrium and stability equations of a moderately thick rectangular plate made of functionally graded materials under thermal loads based on the first order shear deformation theory. The derived equilibrium and buckling equations are then solved analytically for a plate with simply supported boundary conditions. Two types of thermal loading, uniform temperature rise and gradient through the thickness are considered, and the buckling temperatures are derived. Yang *et al*. [83] worked on the effect of randomness on the elastic buckling of FGM rectangular plates which are resting on an elastic foundation and subjected to uniform in-plane edge compressions. First-order shear deformation plate theory and a mean-centered first-order perturbation procedure are used to examine the stochastic characteristics of the buckling load.

Morimoto *et al*. [84] studied on the thermal buckling analysis of functionally graded rectangular plates subjected to partial heating. The plate that they worked on is simply supported for out of plane deformation and perfectly clamped for in plane deformation. The critical buckling temperatures of plates are calculated by using the Galerkin method. Park *et al*. [85] studied on a post-buckling analysis presented for a simply supported, shear deformable functionally graded plate with piezoelectric actuators subjected to the combined action of mechanical, electrical and thermal loads. The governing equations are based on a higher order shear deformation plate theory that includes thermo-piezoelectric effects. A two step perturbation technique is employed to determine buckling loads and post-buckling equilibrium paths. The effects played by

temperature rise, volume fraction distribution, applied voltage, the character of in-plane boundary conditions, as well as initial geometric imperfections are studied.

Furthermore, Sohn and Kim [86] investigated the static and dynamic stabilities of functionally graded panels which are subjected to combined thermal and aerodynamic loads. Panels are considered as rectangular plates which are based on the first-order shear deformation theory. The von Karman strain–displacement relation is used to account for geometric nonlinearity, which is caused by a large deformation. Equations of motion are derived by the principle of virtual work and numerical solutions are obtained by a finite element method. The Newton–Raphson method is applied to get solutions of the nonlinear governing equations. Navazi and Haddadpour [87] studied on the aero-thermoelastic stability of functionally graded plates and used Galerkin method in order to derive the equations. The effects of compressive in-plane loads and both uniform and through the thickness non-linear temperature distributions are considered. Hamilton's principle is used to determine the coupled partial differential equations of motion. Zhao *et al*. [88] presented an analysis on the mechanical and thermal buckling of functionally graded plates. The first-order shear deformation plate theory is used in the analyses.

It is observed that the number of the researches about the buckling of plates with variable thicknesses is not too much. It is also concluded from the literature survey that most of the researches have been reported on the vibration analysis of tapered plates.

The first study on the transverse vibrations of an elliptic plate with variable thickness is done by Singh and Tyagi [89]. A clamped elliptic plate whose thickness varies parabolically is solved by using Galerkin method and the transverse vibration mode shapes of the elliptic plate are obtained. Then, Singh and Chakraverty [90] worked on the transverse vibration of circular and elliptical plates with quadratically varying thickness. Approximate values of the frequencies of transverse vibrations of the plates with clamped edges are computed using the Rayleigh-Ritz method. Later, Singh and Saxena [91] presented a study on the transverse vibration of a quarter of a circular plate with variable thickness. The Rayleigh-Ritz method is employed to find the first three frequencies of free flexural vibration of a plate in the form of a quadrant of a circle and of thickness varying quadratically with radial distance. The same problem is solved by Singh and Saxena [92]

for a quarter of an elliptic plate. Again, Rayleigh-Ritz method is used and the analyses are done for a quadrant of an ellipse with linear and quadratic thickness variations. Singh and Hassan [93] employed Rayleigh- Ritz method to obtain approximations to frequencies and mode shapes of circular plates with variable thickness. The boundary conditions are assumed as clamped, simply supported or completely free. Axisymmetric vibrations of a circular plate of linearly varying thickness under the action of a hydrostatic in-plane force and resting on elastic foundation of Winkler type are discussed by Gupta and Lal [94] on the basis of the classical theory of plates. Here, transverse displacements and moments are also computed.

Recently, Gupta *et al*. [95] presented a free vibration analysis of non-homogenous circular plates with variable thickness by using the first order shear deformation plate theory of Mindlin. Gupta and Khanna [96] studied the effect of linear thickness variations in both directions on the vibration of visco-elastic rectangular plate. The plate is clamped on all four edges and Rayleigh-Ritz method is used in the analysis. Bayer *et al*. [97] presented a vibration analysis of clamped elliptical plates with variable thickness. In their study, both, Rayleigh-Ritz and moment method are chosen as approximate solution techniques. Çeribaşı and Altay [98] investigated free vibration of simply supported and clamped super elliptical plates. For the solution of the plates, Rayleigh-Ritz method is employed. Very recently, Gupta and Bhardwaj [99] used boundary characteristic orthogonal polynomials method to study the vibration of orthotropic plates with variable thickness resting on elastic foundation. The study of non-homogeneity as well as variable thickness in elliptic and circular plates is undertaken by Chakraverty *et al*. [100]. In their study, non-homogeneity of plate material and thickness variation is assumed to be quadratic.

Moreover, Wang *et al*. [101] presented an elastic buckling analysis of tapered circular plates. Here, in the buckling analysis of linearly and parabolically tapered plates, an optimization search technique is also implemented into the algorithm to seek the optimal values of the taper parameters. A power series method is developed by Kobayashi and Sonoda [102] in order to solve the buckling problem of uniaxially compressed rectangular plates with linearly tapered thickness. It is assumed that the compressed edges are simply supported and the unloaded edges are arbitrarily restrained. Nerantzaki and

Katsikadelis [103] applied an analog equation solution to the plates with variable thicknesses for the buckling analysis. Numerical results are also given to illustrate the effectiveness of the proposed method. Eisenberger and Alexandrov [104] presented accurate solutions for bifurcation buckling loads of rectangular thin plates with variable thickness that varies in the directions parallel to the two sides. In this study, the plates are subjected to biaxial compression and various combinations of boundary conditions are considered. The calculation of the critical loads is carried out by using Kantorovich method.

1.2. Objectives

It is known that plates and plate-type structures have gained special importance and notably increased applications in recent years. A large number of structural components in engineering structures can be classified as plates. Practical applications of plates in civil, mechanical, marine, nuclear and aerospace engineering are numerous. Typical examples in civil engineering structures are floor and foundation slabs, lock-gates, thin retaining walls, bridge decks and slab bridges. Plates are also indispensible in shipbuilding and aerospace industries. They are also frequently parts of machineries and other mechanical devices. Plates of various shapes and of non-uniform thickness are widely used in engineering structures. Plates with variable thickness are often used in slab design, machine design, nuclear reactor technology, naval structures and acoustical components. Besides, in-homogenous materials such as FGMs are developed to be used as thin-walled members of plates.

During the review of the literature, within the papers recorded by “ISI-Web of Science”, no work dealing with thermal buckling of FGM plates with variable thickness has been found. Therefore, the current work is motivated by the lack of contributions on the thermal buckling studies of such plates.

In this study, the analyses are divided into three parts. In all parts, the analyses are done for both rectangular and elliptical plates and the thermal buckling analyses are performed by Rayleigh-Ritz method. Also, the plates are assumed to be fully clamped and simply supported in each case.

The first part of the study, Chapter 3, examines the thermal buckling behavior of homogenous isotropic rectangular and elliptical thin plates with constant thickness. Examples of thermal buckling of biaxially and uniaxially loaded plates are given. The results of the buckling analyses and the critical buckling temperatures are tabulated. Also, the influence of the aspect ratio of the plate on the critical buckling temperature is illustrated. The results are compared with the available matching studies in literature.

In the second part of the study, Chapter 4, thermal buckling analyses are conducted for FGM plates with constant thickness. Since FGMs are mainly used as heat resistant materials and they are employed as structural members in extremely high temperature environments, it is essential to understand the thermal buckling behavior of FGM plates. Material properties are assumed to be temperature dependent and graded in the thickness direction according to a power law distribution in terms of the volume fractions of the constituents. According to this, as a result of the thermal buckling analysis, critical buckling temperatures of FGM plates under linear temperature change are tabulated and illustrated.

Finally, since the buckling load is highly dependent on the thickness variations, thermal buckling analyses of FGM plates with variable thicknesses are presented in Chapter 5. Here, a parabolic variation of plate thickness is considered and the critical buckling temperatures for FGM plates with variable thicknesses are given.

2. FUNDAMENTAL EQUATIONS OF THIN PLATES

2.1. General Definitions

Plates are straight, plane, two dimensional structural components of which one dimension, referred to as thickness t, is much smaller than the other dimension. If the thickness is no greater than one-tenth of the in-plane dimensions, the plate is called thin plate. If the thickness to span ratio is between 0.1 and 0.2, the plate is called moderately thick plate. They are in many respects similar to thin plates with the exception that the effects of transverse shear forces on the normal stress components are also taken into account. When the thickness to span ratio exceeds approximately 0.2, a plate problem becomes a corresponding problem of three-dimensional elasticity and the plate is called thick plate [1]. Geometrically the plates are bound either by straight or curved lines. They are subjected to loads causing bending and stretching deformations.

Thin plates are poor in resisting compression, although they are quite capable of carrying tensile loadings. Usually buckling or wrinkling phenomena observed in compressed plates take place rather suddenly and are very dangerous. When a flat plate is under the action of edge compression in its middle plane, the plate is deformed but remains completely flat when the edge forces are sufficiently small unless there is an initial geometric imperfection. By increasing the load, an important change in the character of the deformation takes place. It becomes unstable and begins to buckle at a certain critical value of the in-plane force. Therefore, in this condition, the originally stable equilibrium becomes unstable and the plate is said to have buckled. The in-plane compressive load which is sufficient to keep the plate in a slightly bent form is the critical load or the buckling load. Once the buckling load is exceeded, the load deflection relationship exhibits a stable character due to membrane forces which come into play. The behavior of flat plates after buckling is of considerable interest. The post-buckling analysis of plates is usually difficult and it is basically a nonlinear problem. Actually, the buckling mode would change in the post-buckling range and these changes occur when the energy stored in the plate is sufficient to carry the plate from one buckled form to the other.

2.2. Plate Theories

The governing equations of plates can be derived by either using vector mechanics or energy principles. In vector mechanics, the forces and moments on an element are summed to obtain the equation of equilibrium. In energy methods, the principles of virtual work or their derivatives are used, such as the minimum potential energy. Although both methods give the same equations, the energy methods are advantageous in providing information on the form of the boundary conditions.

Of the numerous plate theories that have been developed, two are widely accepted and used in engineering. The two-dimensional plate theories can be classified into these two categories:

- Classical (Kirchhoff) Plate Theory
- Shear Deformation (Mindlin) Plate Theory

Plate theories are developed by assuming the form of the displacement or stress field as linear combinations of unknown functions and the thickness coordinate. For the bending case, lines normal to midsurface in the undeformed geometry remain normal to this surface in the deformed geometry. In other words, lines connecting to the surfaces of the plate and normal to the xy plane in the undeformed geometry, translate vertically as rigid lines while maintaining the same coordinate values x and y. Additionally, these lines rotate as rigid elements as a result of bending.

2.2.1. Classical (Kirchhoff) Plate Theory

The shape of a plate is defined by describing the geometry of its middle surface which divides the plate thickness, t, into two at each point. The small deflection plate theory which is generally attributed to Kirchhoff can be summarized by the following assumptions [1]:

- The material of the plate is linear elastic, homogeneous, and isotropic.

- The plate is initially flat.

- The middle surface of the plate remains unstrained during bending.

- The constant thickness of the plate, *t*, is small compared to its other dimensions; that is, the smallest lateral dimension of the plate is at least ten times larger than its thickness.

- The transverse deflections are small compared to the plate thickness. A maximum deflection of one-tenth of the thickness is considered the limit of the small deflection theory.

- Slopes of the deflected middle surface are small compared to unity.

- Sections taken normal to the middle surface before deformation remain plane and normal to the deflected middle surface. Consequently, shear deformations are neglected.

- The stresses normal to the middle surface are negligible.

Using these assumptions, all stress components can be expressed by deflection, *w*, of the plate, which is a function of the two coordinates in the plane of the plate. This function has to satisfy a linear partial differential equation, which, together with the boundary conditions, completely defines *w*. Thus, the solution of this equation gives all necessary information for calculating stresses at any point of the plate.

2.2.2. Shear Deformation (Mindlin) Plate Theory

In addition to classical (Kirchhoff) plate theory, there are a number of shear deformation plate theories. The simplest is the first order shear deformation plate theory which is also known as the Mindlin plate theory. The Mindlin plate theory assumes that the transverse shear strain is constant with respect to the thickness coordinate. In addition to its inherent simplicity and low computational cost, the first order plate theory often provides a

sufficiently accurate description of the global response (e.g. deflections, buckling loads, and natural vibration frequencies) for thin to moderately thick plates [105].

In the second and higher order shear deformation plate theories, higher order polynomials are used in the expansion of the displacement components through the thickness of the plate.

2.3. Basic Plate Equations

A thin plate of thickness t is considered, whose median plane lies in the x-y plane, with z denoting the distance from this lane. The displacements in the x, y and z directions of points on the median plane are denoted by u, v and w, respectively. According to this, the displacements can be expressed as:

$$\begin{aligned} u &= u_0(x,y) - z\frac{\partial w}{\partial x} \\ v &= v_0(x,y) - z\frac{\partial w}{\partial y} \\ w &= w_0(x,y) \end{aligned} \tag{2.1}$$

The strain-displacement relation is given in Eq. (2.2), where ε_x and ε_y are normal strains and γ_{xy} is the shear strain.

$$\begin{aligned} \varepsilon_x &= \frac{\partial u}{\partial x} \\ \varepsilon_y &= \frac{\partial v}{\partial y} \\ \gamma_{xy} &= \frac{\partial v}{\partial x} + \frac{\partial u}{\partial y} \end{aligned} \tag{2.2}$$

Denoting $u_0=u$ and $v_0=v$ in Eq. (2.1), the following expressions for the strains in terms of displacements are obtained. As a result of this, the strain-displacement relation in Eq. (2.2) becomes:

$$\begin{aligned}\varepsilon_x &= \frac{\partial u}{\partial x} - z\frac{\partial^2 w}{\partial x^2} \\ \varepsilon_y &= \frac{\partial v}{\partial y} - z\frac{\partial^2 w}{\partial y^2} \\ \gamma_{xy} &= \left(\frac{\partial v}{\partial x} + \frac{\partial u}{\partial y}\right) - 2z\frac{\partial^2 w}{\partial x \partial y}\end{aligned} \tag{2.3}$$

For an isotropic material, stress-strain relation is given in Eq. (2.4), where E is the Young's modulus and ν denotes the Poisson's ratio:

$$\begin{aligned}\varepsilon_x &= \frac{1}{E}\left[\sigma_x - \nu\sigma_y\right] \\ \varepsilon_y &= \frac{1}{E}\left[\sigma_y - \nu\sigma_x\right] \\ \gamma_{xy} &= \frac{\tau_{xy}}{G} \qquad G = \frac{E}{2(1+\nu)}\end{aligned} \tag{2.4}$$

From Eq. (2.4), the total stress components are given by Eq. (2.5). So, from Hooke's law, the non-zero stress components are:

$$\begin{aligned}\sigma_x &= \frac{E}{1-\nu^2}\left(\varepsilon_x + \nu\varepsilon_y\right) \\ \sigma_y &= \frac{E}{1-\nu^2}\left(\varepsilon_y + \nu\varepsilon_x\right) \\ \tau_{xy} &= G\gamma_{xy} = \frac{E}{2(1+\nu)}\gamma_{xy}\end{aligned} \tag{2.5}$$

The stress distributed over the thickness of the plate result in-plane forces and moments per unit length. It is convenient in plate theory to deal with forces and moments per unit of length rather than with the stresses themselves. Therefore, the following quantities are introduced:

$$\begin{Bmatrix} N_x \\ N_y \\ N_{xy} \end{Bmatrix} = \int_{-t/2}^{t/2} \begin{Bmatrix} \sigma_x \\ \sigma_y \\ \tau_{xy} \end{Bmatrix} dz \qquad \begin{Bmatrix} M_x \\ M_y \\ M_{xy} \end{Bmatrix} = \int_{-t/2}^{t/2} \begin{Bmatrix} \sigma_x \\ \sigma_y \\ \tau_{xy} \end{Bmatrix} z\, dz \tag{2.6}$$

The above quantities may be expressed in terms of displacements by the help of Eq. (2.3) and Eq. (2.5). Substituting these equations into Eq. (2.6), the following results are obtained.

$$\begin{aligned} N_x &= \frac{Et}{(1-\nu^2)}\left(\frac{\partial u}{\partial x}+\nu\frac{\partial v}{\partial y}\right) & M_x &= -D\left(\frac{\partial^2 w}{\partial x^2}+\nu\frac{\partial^2 w}{\partial y^2}\right) \\ N_y &= \frac{Et}{(1-\nu^2)}\left(\frac{\partial v}{\partial y}+\nu\frac{\partial u}{\partial x}\right) & M_y &= -D\left(\frac{\partial^2 w}{\partial y^2}+\nu\frac{\partial^2 w}{\partial x^2}\right) \\ N_{xy} &= \frac{Et}{2(1+\nu)}\left(\frac{\partial v}{\partial x}+\frac{\partial u}{\partial y}\right) & M_{xy} &= -D(1-\nu)\frac{\partial^2 w}{\partial x \partial y} \end{aligned} \tag{2.7}$$

Here, the bending rigidity of the plate per unit of length is:

$$D = \frac{Et^3}{12(1-\nu^2)} \tag{2.8}$$

The determination of the six quantities defined in Eq. (2.6) is most conveniently carried out in two steps. In the first of these, the two dimensional equilibrium and compatibility equations in the *x-y* plane are used to determine the forces *N*, and in the second step, the equilibrium equation of forces in the *z* direction and of bending and twisting moments are written in terms of displacements so as to determine the deflection *w* and hence from Eq. (2.7), the moments *M* [106].

The equations of equilibrium in the plane of the plate are given as:

$$\begin{aligned} \frac{\partial \sigma_x}{\partial x}+\frac{\partial \tau_{xy}}{\partial y} &= 0 \\ \frac{\partial \tau_{xy}}{\partial x}+\frac{\partial \sigma_y}{\partial y} &= 0 \end{aligned} \tag{2.9}$$

Also, the differential equations of equilibrium in the plane of the plate can be presented by Eq. (2.10):

$$\frac{\partial N_x}{\partial x}+\frac{\partial N_y}{\partial y}=0\ ;\qquad \frac{\partial N_{xy}}{\partial x}+\frac{\partial N_y}{\partial y}=0 \tag{2.10}$$

The second part of the solution, namely the determination of the transverse displacement *w*, is the more direct concern of plate theory. The equilibrium equations of forces in the *z* direction and of moments about the *x* and *y* axis acting on an element of volume (*dx dy dz*) of the plate as shown in Figure 2.2 are, respectively, as follows:

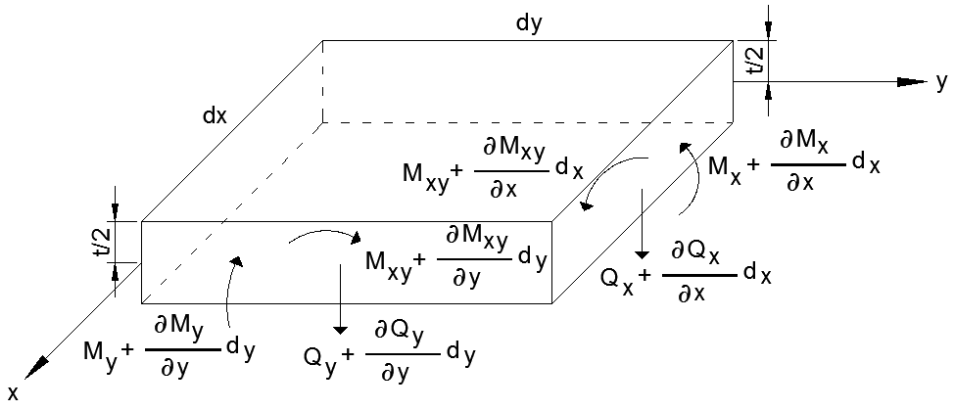

Figure 2.1. Element of plate used in the derivation of the equilibrium conditions

$$\begin{aligned}
&\frac{\partial Q_x}{\partial x}+\frac{\partial Q_y}{\partial y}+p=0\\
&\frac{\partial M_{xy}}{\partial x}-\frac{\partial M_y}{\partial y}+Q_y=0\\
&\frac{\partial M_{xy}}{\partial y}-\frac{\partial M_x}{\partial x}+Q_x=0
\end{aligned} \tag{2.11}$$

where, Q_x and Q_y are the shear forces per unit length acting on a surface whose normal is indicated by the subscript and p= p(x, y) is the distributed transverse loading per unit of area. With the substitution of Q_x and Q_y from the second and third of Eq. (2.11) into the first of these, the equilibrium equation of forces in the *z* direction becomes;

$$\frac{\partial^2 M_x}{\partial x^2}-2\frac{\partial^2 M_{xy}}{\partial x\partial y}+\frac{\partial^2 M_y}{\partial y^2}=-p \tag{2.12}$$

The governing equation for the deflection *w* is now obtained by substituting the expressions for the moments which are given in Eq. (2.7). So, the governing equation of the mathematical model of the plate problem in differential equation form is:

$$\frac{\partial^2}{\partial x^2}\left[D(\frac{\partial^2 w}{\partial x^2}+\nu\frac{\partial^2 w}{\partial y^2}) \right]+2(1-\nu)\frac{\partial^2}{\partial x\partial y}\left[D\frac{\partial^2 w}{\partial x\partial y} \right]+\frac{\partial^2}{\partial y^2}\left[D(\frac{\partial^2 w}{\partial y^2}+\nu\frac{\partial^2 w}{\partial x^2}) \right]=p \qquad (2.13)$$

If the problem is a buckling problem, the governing equation of this mathematical model given as a differential equation in Cartesian coordinates becomes:

$$\nabla^2(D\nabla^2 w)-(1-\nu)\left(\frac{\partial^2 D}{\partial x^2}\frac{\partial^2 w}{\partial y^2}-2\frac{\partial^2 D}{\partial x\partial y}\frac{\partial^2 w}{\partial x\partial y}+\frac{\partial^2 D}{\partial y^2}\frac{\partial^2 w}{\partial x^2} \right)-N\nabla^2 w=p \qquad (2.14)$$

where, N is the uniform boundary compression per unit length of the edge and ∇^2 is the second order Laplace operator which is given as:

$$\nabla^2=\frac{\partial^2}{\partial x^2}+\frac{\partial^2}{\partial y^2} \qquad (2.15)$$

The governing equation can also be expressed in variational form. The total energy function of a vibrating plate with in-plane uniform compressive load is as follows [105]:

$$F=U-\gamma_1 T+\gamma_2 V \qquad (2.16)$$

where, U is the strain energy due to bending, T is the kinetic energy of the plate considered and V is the potential energy of the in-plane uniform compressive load. Here, the scalar indicators, γ_1 and γ_2, are chosen according to the type of the plate problem. If the problem is a vibration problem, then, γ_1=1 and γ_2=0. If the problem is a buckling problem, then, γ_1=0 and γ_2=1. These energy expressions are presented down below in the open form:

$$U = \frac{D}{2}\iint_A \left\{ \left(\nabla^2 w\right)^2 + 2\left(1-\nu\right)\left[\left(\frac{\partial^2 w}{\partial x \partial y} \right)^2 - \frac{\partial^2 w}{\partial x^2}\frac{\partial^2 w}{\partial y^2} \right] \right\} dx\, dy$$

$$T = \frac{1}{2}\rho t w^2 \iint_A w^2\, dx\, dy \tag{2.17}$$

$$V = -\frac{1}{2}\iint_A N\left\{ \left(\frac{\partial w}{\partial x} \right)^2 + \left(\frac{\partial w}{\partial y} \right)^2 \right\} dx\, dy$$

2.4. Boundary Conditions

Boundary conditions for the simply supported case, where the edge deflections and the edge moments are zero, are given as:

$$w = 0; \qquad M_x = 0 \quad \text{and} \quad M_y = 0 \tag{2.18}$$

For the clamped case condition, the edge deflection remains zero and the slopes at the edges are zero as follows:

$$w = 0; \qquad \frac{\partial w}{\partial x} = 0 \quad \text{and} \quad \frac{\partial w}{\partial y} = 0 \tag{2.19}$$

2.5. Rayleigh-Ritz Method

There are many approximate solution techniques used for the solution of plate problems. These techniques can be grouped as the weighted residual techniques and the variational techniques [107]. The weighted residual techniques are Galerkin Method, Kantorovich Method, Collocation Method, Method of Moments, Method of Least Squares, Finite Difference Method, Finite Element Method and Boundary Elements Method. As the variational technique, Rayleigh-Ritz Method is the most widely used one.

Advantages of Rayleigh-Ritz method lie in the relative ease with which complex boundary conditions can be handled. It is a powerful tool yielding high accuracy in the deflection analysis, provided that suitable shape functions are employed. Rayleigh-Ritz

method can be used for plates of various shapes and of variable thicknesses. Since the method is easier than the other methods conceptually and mathematically and also powerful to obtain accurate results for plates of various shapes and thicknesses, Rayleigh-Ritz method is chosen to be used in this thesis.

In this method, the idea is to assume a certain functional form for the displacement field that satisfies the kinematic boundary conditions of the problem and as many of the remaining boundary conditions as possible. Satisfaction of the kinematic boundary conditions by the assumed displacement field is essential since the virtual displacement calculated from this displacement field must not violate the kinematic constraints of the problem. The total potential energy is then calculated based on the assumed displacement field. Minimization of the total potential energy with respect to this displacement field then allows the determination of the unknown constants contained in the assumed displacement field [108].

The objective of the variational methods is to find from a group of admissible functions those which represent the deflections of the elastic body, pertinent to its stable equilibrium condition.

The principle of minimum potential energy makes use of the change of the total potential during arbitrary variation of the deflection. Introducing δu, δv, and δw as the virtual displacements of the elastic body, the new position u+ δu, v+ δv, w+ δw produces an increase in the strain energy stored. The change in the total potential energy can be evaluated as:

$$\delta\Pi = \Pi(u+\delta u, v+\delta v, w+\delta w) - \Pi(u,v,w) \tag{2.20}$$

Since the equilibrium configuration is represented by those admissible functions which make the total potential of the system minimum, it can be stated that,

$$\delta\Pi = \delta U + \delta V = \delta(U+V) = 0 \tag{2.21}$$

Components of the compatible infinitesimal virtual displacements (δu, δv, δw) should satisfy the geometrical boundary conditions of the elastic system, and be capable of representing all possible displacement patterns. If these admissible displacement functions are chosen properly a very good accuracy may be attained.

The Rayleigh-Ritz method employs the principle of minimum potential energy. Of all the displacements that satisfy the boundary conditions, those making the total potential energy of the structure a minimum are the sought deflections pertinent to the stable equilibrium conditions.

The deflected middle surface may be represented in the form of a series:

$$w(x,y)=\alpha_1 f_1(x,y)+\alpha_2 f_2(x,y)+.....+\alpha_n f_n(x,y)=\sum_{i=1}^{n}\alpha_i f_i(x,y) \qquad (2.22)$$

where, $f_i(x,y),(i=1,2,3,.....,n)$ are continuous functions that satisfy individually at least the geometrical boundary conditions and are capable of representing the deflected plate surface. The unknown constants $\alpha_1,\alpha_2,\alpha_3.....,\alpha_n$ are determined from the minimum potential energy principle as:

$$\frac{\partial E}{\partial \alpha_1}=0,\frac{\partial E}{\partial \alpha_2}=0,.....,\frac{\partial E}{\partial \alpha_n}=0 \qquad (2.23)$$

With this minimization procedure, n simultaneous algebraic equations, in terms of the unknown coefficients $\alpha_1,\alpha_2,\alpha_3.....,\alpha_n$ will be obtained. The number of equations is equal to the number of unknown parameters, so $\alpha_1,\alpha_2,\alpha_3.....,\alpha_n$ can be calculated.

The potential energy, *U*, of a plate from Eq. (2.17) is:

$$U=\frac{D}{2}\iint_A\left\{\left(\nabla^2 w\right)^2+2\left(1-\nu\right)\left[\left(\frac{\partial^2 w}{\partial x\partial y}\right)^2-\frac{\partial^2 w}{\partial x^2}\frac{\partial^2 w}{\partial y^2}\right]\right\}dx\,dy \qquad (2.24)$$

For fixed plates and simply supported plates, the second term on the right hand side of the integral expression becomes zero [109]. Thus the expression for potential energy becomes:

$$U = \frac{D}{2}\iint_A \left(\nabla^2 w\right)^2 dx\,dy \tag{2.25}$$

The total potential energy of a plate subjected to lateral load q_0 is expressed in the following form:

$$\Pi = \frac{D}{2}\iint_A \left\{\left(\nabla^2 w\right)^2 + 2(1-\nu)\left[\left(\frac{\partial^2 w}{\partial x \partial y}\right)^2 - \frac{\partial^2 w}{\partial x^2}\frac{\partial^2 w}{\partial y^2}\right] - \frac{2q_0 w}{D}\right\} dx\,dy \tag{2.26}$$

The above expression may be simplified for a clamped plate as:

$$\Pi = \frac{D}{2}\iint_A \left\{\left(\nabla^2 w\right)^2 - \frac{2q_0 w}{D}\right\} dx\,dy \tag{2.27}$$

In order to form an expression for the buckling problem of a plate, potential energy should be added to the strain energy. Total energy equation becomes:

$$F = \frac{D}{2}\iint_A \left\{\left(\nabla^2 w\right)^2 + 2(1-\nu)\left[\left(\frac{\partial^2 w}{\partial x \partial y}\right)^2 - \frac{\partial^2 w}{\partial x^2}\frac{\partial^2 w}{\partial y^2}\right]\right\} dx\,dy - \frac{1}{2}\iint_A N\left\{\left(\frac{\partial w}{\partial x}\right)^2 + \left(\frac{\partial w}{\partial y}\right)^2\right\} dx\,dy \tag{2.28}$$

with respect to undetermined coefficients $\alpha_1, \alpha_2, \alpha_3 ....., \alpha_n$.

In this thesis, for the calculations of buckling parameters by Rayleigh-Ritz method, a software algorithm is prepared by the help of Mathematica 5.2 and the example of an elliptical plate program is presented in Appendix A1.

3. THERMAL BUCKLING OF RECTANGULAR AND ELLIPTICAL PLATES

In this part of the study, thermal buckling problem of rectangular and elliptical plates are considered. Kirchhoff plate model is conducted for homogenous and isotropic material. The plates are subjected to biaxial in-plane compression forces and considered as fully clamped and fully simply supported. In addition to this, a rectangular plate subjected to uniaxial in-plane compression forces and a half elliptic plate subjected to biaxial in-plane compression forces are also analyzed with respect to the same boundary conditions. Besides, in order to see the convergence of the applied solution technique, another thermal buckling problem of a plate with a different geometry is also solved and the obtained critical temperatures are compared with the other studies in the literature. Rayleigh-Ritz method is carried out in the analysis. Critical temperatures of the plates are obtained and the results are arranged in the tabular form. For the purpose of understanding the behavior of the structure with respect to the parameters, some of the solutions are also presented in the graphical form.

3.1. Thermal Buckling of Plates

Solution for the deflection and stress in planes subjected to temperature variation requires reformulation of the stress-strain relationship. For homogenous isotropic materials, a change in temperature $\Delta T=T-T_0$ produces uniform linear strain in every direction. Here, T and T_0 are the final and the initial temperatures, respectively. Thermal strains can be expressed as [106];

$$\varepsilon_t = \alpha(\Delta T) \tag{3.1}$$

where, α is the thermal expansion coefficient. Over a moderate temperature change, α remains constant. Also for isotropic materials, a change in temperature produces no shear strains which means $\gamma_t=0$

The total x and y strains, ε_x and ε_y, are obtained by adding to the thermal strains, the strains due to stress resulting from external forces. According to this, the strain equation becomes:

$$\begin{aligned}
\varepsilon_x &= \frac{1}{E}\left[\sigma_x - \nu\sigma_y\right] + \alpha\left(\Delta T\right) \\
\varepsilon_y &= \frac{1}{E}\left[\sigma_y - \nu\sigma_x\right] + \alpha\left(\Delta T\right) \\
\gamma_{xy} &= \frac{\tau_{xy}}{G} \qquad G = \frac{E}{2(1+\nu)}
\end{aligned} \tag{3.2}$$

From Eq. (3.2), the total stress components are given by Eq. (3.3). Here, it should be noted that an increase in temperature ΔT is algebraically positive.

$$\begin{aligned}
\sigma_x &= \frac{E}{1-\nu^2}\left[\varepsilon_x + \nu\varepsilon_y - (1+\nu)\alpha\left(\Delta T\right)\right] \\
\sigma_y &= \frac{E}{1-\nu^2}\left[\varepsilon_y + \nu\varepsilon_x - (1+\nu)\alpha\left(\Delta T\right)\right] \\
\tau_{xy} &= G\gamma_{xy} = \frac{E}{2(1+\nu)}\gamma_{xy}
\end{aligned} \tag{3.3}$$

The stress resultants may be expressed in terms of displacements with the aid of Eq. (2.3) and Eq. (3.3), with the following results:

$$\begin{aligned}
N_x &= \frac{Et}{(1-\nu^2)}\left(\frac{\partial u}{\partial x} + \nu\frac{\partial v}{\partial y}\right) - \frac{N^*}{1-\nu} & M_x &= -D\left(\frac{\partial^2 w}{\partial x^2} + \nu\frac{\partial^2 w}{\partial y^2}\right) - \frac{M^*}{1-\nu} \\
N_y &= \frac{Et}{(1-\nu^2)}\left(\frac{\partial v}{\partial y} + \nu\frac{\partial u}{\partial x}\right) - \frac{N^*}{1-\nu} & M_y &= -D\left(\frac{\partial^2 w}{\partial y^2} + \nu\frac{\partial^2 w}{\partial x^2}\right) - \frac{M^*}{1-\nu} \\
N_{xy} &= \frac{Et}{2(1+\nu)}\left(\frac{\partial u}{\partial y} + \frac{\partial v}{\partial x}\right) & M_{xy} &= -D(1-\nu)\frac{\partial^2 w}{\partial x \partial y}
\end{aligned} \tag{3.4}$$

where, N^* and M^* are termed the thermal stress resultants and presented as;

$$N^* = \alpha E \int_{-t/2}^{t/2} \Delta T \, dz$$
$$M^* = \alpha E \int_{-t/2}^{t/2} \Delta T \, z \, dz \tag{3.5}$$

According to this, the governing equation for the deflection w under the thermal effects becomes:

$$\frac{\partial^2}{\partial x^2}\left[D(\frac{\partial^2 w}{\partial x^2} + \nu \frac{\partial^2 w}{\partial y^2}) \right] + 2(1-\nu)\frac{\partial^2}{\partial x \partial y}\left[D\frac{\partial^2 w}{\partial x \partial y} \right] + \frac{\partial^2}{\partial y^2}\left[D(\frac{\partial^2 w}{\partial y^2} + \nu \frac{\partial^2 w}{\partial x^2}) \right] = p - \frac{1}{1-\nu}\nabla^2 M^* \tag{3.6}$$

For the plates of uniform thickness, this governing equation for deflection of plates under elevated temperature reduces to:

$$D\nabla^4 w = p - \frac{1}{1-\nu}\nabla^2 M^* \tag{3.7}$$

The basic equations describing the behavior of plates are derived on the assumption that the stress resultants N_x, N_y and N_{xy} in the plane of the plate are small enough not to influence materially the transverse deformations. If this is not the case, the basic equation for the bending plates of uniform thickness is as Eq. (3.8) in place of Eq. (3.7).

$$D\nabla^4 w = p - \frac{1}{1-\nu}\nabla^2 M^* + N_x \frac{\partial^2 w}{\partial x^2} + 2N_{xy}\frac{\partial^2 w}{\partial x \partial y} + N_y \frac{\partial^2 w}{\partial y^2} \tag{3.8}$$

3.2. Thermal Buckling Problem of Biaxially Loaded Rectangular and Elliptical Plates

3.2.1. Basic Assumptions and Equations

In this problem, the analyses are done for homogenous rectangular and elliptical plates which are compressed in their plane, in the directions of x and y, by N_x and N_y, respectively. Boundary conditions are considered as fully simply supported and fully

clamped. The configurations of the analyzed rectangular and elliptical plates are given in Figure 3.1.

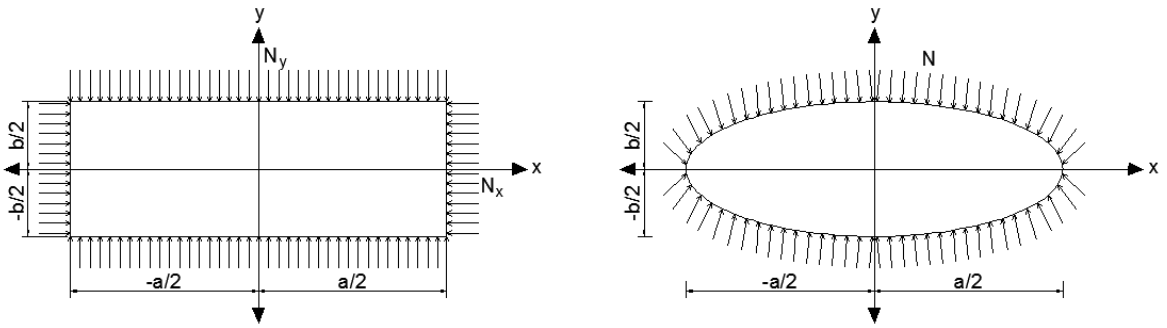

Figure 3.1. Configurations of the biaxially loaded plates

The boundary shape equation of the given rectangular and elliptical plates can be represented by Eq. (3.9) and Eq. (3.10), respectively. If the external boundary condition is simply supported, then in the equations below Ω=1. If the edges are clamped then, Ω=2.

$$\phi(x,y)=\left[\left(x^2-\frac{a^2}{4}\right)\left(y^2-\frac{b^2}{4}\right)\right]^{\Omega} \tag{3.9}$$

$$\phi(x,y)=\left[\frac{x^2}{(a/2)^2}+\frac{y^2}{(b/2)^2}-1\right]^{\Omega} \tag{3.10}$$

In order to write the displacement function, *w*, it is assumed to be:

$$w(x,y)=\sum_{i}^{r}\sum_{j}^{r}\alpha_{ij}\phi(x,y)\,x^i y^j \tag{3.11}$$

where, $i+j\le r$, so r is the degree of the polynomial trial function and α_{ij} are the coefficients to be determined. The existence of $\phi(x,y)$ in the equation guarantees that every element of these trial functions satisfy the boundary conditions of the problem. Knowing that the deflection function of the chosen system is en even function, the elements of the trial function which has odd powers of *x* and *y* are eliminated. It should be noted that selection of the trial functions has crucial importance in approximation and time

consuming. A trial function for displacement function of rectangular plates, w, with three terms for *r=2* is simplified and may be represented by Eq. (3.12).

$$w=\left(x^2-\frac{a^2}{4}\right)\left(y^2-\frac{b^2}{4}\right)^{\Omega}(\alpha_{00}x^0y^0+\alpha_{20}x^2y^0+\alpha_{02}x^0y^2) \tag{3.12}$$

For the other *r* values used in the analyses, the displacement functions take the forms presented in Table 3.1.

Table 3.1. Displacement functions used in the analyses

r	Displacement function, *w*
2	$\left(x^2-\frac{a^2}{4}\right)\left(y^2-\frac{b^2}{4}\right)^{\Omega}(\alpha_{00}x^0y^0+\alpha_{20}x^2y^0+\alpha_{02}x^0y^2)$
4	$\left(x^2-\frac{a^2}{4}\right)\left(y^2-\frac{b^2}{4}\right)^{\Omega}(\alpha_{00}x^0y^0+\alpha_{20}x^2y^0+\alpha_{02}x^0y^2+\alpha_{22}x^2y^2+\alpha_{40}x^4y^0+\alpha_{04}x^0y^4)$
6	$\left(x^2-\frac{a^2}{4}\right)\left(y^2-\frac{b^2}{4}\right)^{\Omega}(\alpha_{00}x^0y^0+\alpha_{20}x^2y^0+\alpha_{02}x^0y^2+\alpha_{22}x^2y^2+\alpha_{40}x^4y^0+\alpha_{04}x^0y^4+\alpha_{24}x^2y^4+\alpha_{42}x^4y^2+\alpha_{60}x^6y^0+\alpha_{06}x^0y^6)$

3.2.2. Solution by Rayleigh-Ritz Method

In the calculations, Rayleigh-Ritz method is used in conjunction with the potential energy *U* and can be written as:

$$U=\frac{D}{2}\iint_A\left\{\left(\nabla^2w\right)^2+2(1-\nu)\left[\left(\frac{\partial^2w}{\partial x\partial y}\right)^2-\frac{\partial^2w}{\partial x^2}\frac{\partial^2w}{\partial y^2}\right]\right\}dx\,dy \tag{3.13}$$

The areas of the rectangular and elliptical plates are expressed as:

$$A_{rectangular}=\int_{-a/2}^{a/2}\int_{-b/2}^{b/2}dx\,dy \tag{3.14}$$

$$A_{elliptical} = \int_{-a/2}^{a/2} \int_{-b/2\sqrt{1-(2x/a)^2}}^{b/2\sqrt{1-(2x/a)^2}} dx\,dy \tag{3.15}$$

The total energy function, F, is expressed again in Eq. (3.16) where U is the strain energy due to bending, T is the kinetic energy of the plate and V is the potential energy of the in-plane uniform pressure, N. These energy expressions are presented before in the open form in Eq. (2.17).

$$F = U - \gamma_1 T + \gamma_2 V \tag{3.16}$$

Here, as it is explained before, the scalar indicators, γ_1 and γ_2, are chosen according to the type of the plate problem. Since, the problem is a buckling problem, then, γ_1=0 and γ_2=1.

In order to apply Rayleigh-Ritz method, first of all an appropriate deflection shape is selected as it is shown in Eq. (3.12). Then, the strain and the potential energy equations are computed into the total energy equation. According to this, for the buckling problem of the given rectangular and elliptical plates subjected to biaxial in-plane compression forces, the total energy equation becomes:

$$F = \frac{D}{2}\iint_A \left\{ \left(\nabla^2 w\right)^2 + 2(1-\nu)\left[\left(\frac{\partial^2 w}{\partial x \partial y}\right)^2 - \frac{\partial^2 w}{\partial x^2}\frac{\partial^2 w}{\partial y^2} \right] \right\} dx\,dy - \frac{1}{2}\iint_A \left[N_x \left(\frac{\partial w}{\partial x}\right)^2 + N_y \left(\frac{\partial w}{\partial y}\right)^2 \right] dx\,dy \tag{3.17}$$

Eq. (3.17) is minimized with respect to unknown coefficients, α_{00}, α_{20} and α_{02}. This procedure yields a set of homogeneous linear simultaneous equations in α_i and in this way the problem is reduced to an eigenvalue problem.

3.2.3. Numerical Results

In order to find the critical temperatures for the plates, before the thermal analyses, the buckling loads of the plates have to be obtained. The buckling problem for isotropic

rectangular and elliptical plates is solved by using Rayleigh-Ritz method in accordance with the methodology given. As it is mentioned before, all the plates are solved as clamped and simply supported while applying the approximate solution method.

In the analysis, three different shape functions are used which are namely the expansions of Eq. (3.11) for r=2, 4, and 6. It is seen that as the number of the unknown terms are increased in the shape functions, the results get more convenient. Therefore, here, the results for r=6 are presented which correspond to the analysis done with 10 unknown terms. Also, for the entire study, *a* is kept constant as 1, and *b* is chosen for 8 different numbers from 1 to 3 in order to obtain results for various *a/b* ratios. During the analyses, Poisson's ratio is chosen as 0.3, Young's modulus is $2x10^{11}$ Pa and the thermal expansion coefficient is taken as $2x10^{-6}$ (1/°C). Also, the in-plane compressive forces are taken equal to each other as $N_x = N_y = -N$.

For both rectangular and elliptical plates, the results are compared with the results obtained in Ref. [49]. In order to make comparison all values are normalized by the parameter $\lambda=Na^2/D$. The comparisons for the rectangular and elliptical plates are given in Table 3.2 and Table 3.3, respectively.

Table 3.2. Comparison of the results of the buckling problem of rectangular plates

Buckling Load Factors for Simply Supported Rectangular Plates ($\lambda=Na^2/D$)								
a/b	1	1,125	1,25	1,375	1,5	2	2,5	3
Ref. [49]	19,72	22,34	25,26	28,5	32,04	49	71,34	98,6
Present	19,74	22,36	25,29	28,53	32,08	49,35	71,55	98,7
Buckling Load Factors for Clamped Rectangular Plates ($\lambda=Na^2/D$)								
a/b	1	1,125	1,25	1,375	1,5	2	2,5	3
Ref. [49]	52,3	59,66	68,66	79,26	91,43	154,74	239,9	342,57
Present	52,35	59,72	68,73	79,35	91,52	154,89	240,15	345,64

Table 3.3. Comparison of the results of the buckling problem of elliptical plates

Buckling Load Factors for Simply Supported Elliptical Plates (λ=Na²/D)								
a/b	1	1,125	1,25	1,375	1,5	2	2,5	3
Ref. [49]	16,78	19,13	21,99	25,36	29,19	48,76	74,15	104,65
Present	16,79	19,15	22,02	25,39	29,23	48,82	74,25	104,8
Buckling Load Factors for Clamped Elliptical Plates (λ=Na²/D)								
a/b	1	1,125	1,25	1,375	1,5	2	2,5	3
Ref. [49]	58,67	66,85	76,68	88,1	101,06	166,84	253,06	358,67
Present	58,73	66,91	76,74	88,17	101,13	166,94	253,18	358,87

As it is seen from the tables above, the results are so close to each other. Therefore, for the solution of thermal buckling of these plates, the basic equations and assumptions given are followed in the analysis. By using these buckling load factors and the thermal stress resultants, the critical temperatures for homogenous rectangular and elliptical plates are obtained, and the results are given in Table 3.4 and 3.5, respectively. In all calculations, a/b ratio is changed and due to the variation of a/b, the critical temperatures are found. Also, the plates are again considered as simply supported and clamped in each case.

Table 3.4. Critical buckling temperatures for rectangular plates

	T_{cr} (ºC)							
a/b	1	1,125	1,25	1,375	1,5	2	2,5	3
Simply Supported Edges	63,27	71,67	81,06	91,44	102,82	158,17	229,33	316,35
Clamped Edges	167,79	191,41	220,29	254,33	293,33	496,44	769,71	1107,8

Table 3.5. Critical buckling temperatures for elliptical plates

	T_{cr} (ºC)							
a/b	1	1,125	1,25	1,375	1,5	2	2,5	3
Simply Supported Edges	53,81	61,38	70,58	81,38	93,69	156,47	237,98	335,90
Clamped Edges	188,24	214,45	245,96	282,60	324,13	535,06	811,47	1150,2

According to the solution, for the simply supported and clamped uniformly heated plates, the influence of the aspect ratio (a/b) and t/a ratio of the plate on the buckling temperature are also given. Figure 3.2 shows the influence of the aspect ratio on the buckling temperature for the rectangular and elliptical plates on the same figure for both simply supported and clamped boundaries.

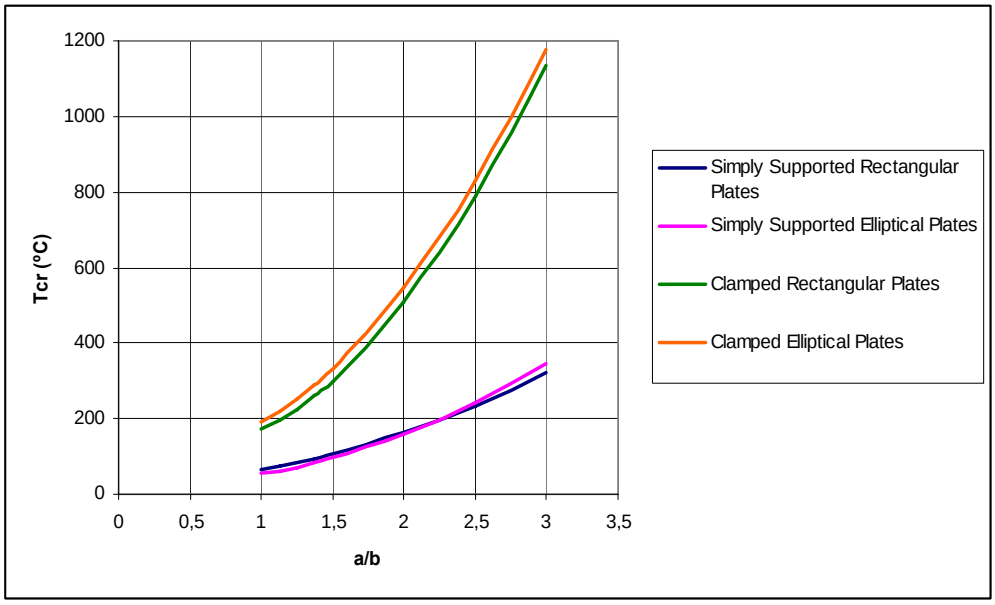

Figure 3.2. Influence of the aspect ratio of the rectangular and elliptical plates on the buckling temperature

Figure 3.3 shows the influence of the t/a ratio on the buckling temperature, again for the rectangular and elliptical plates, respectively. In order to show the influence of the t/a ratio on the buckling temperature, aspect ratio is kept constant as 1.0.

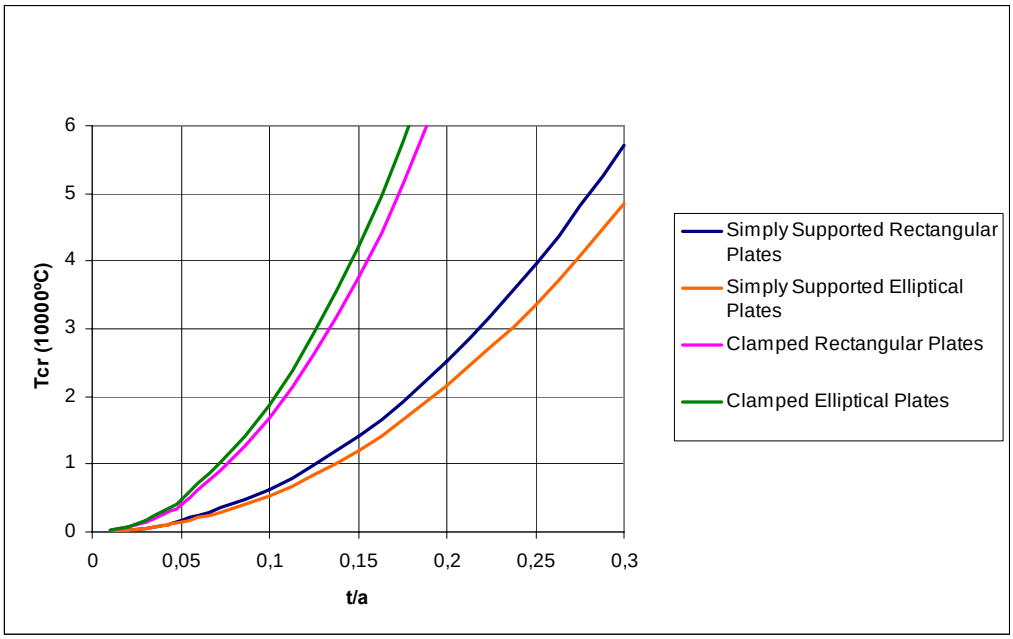

Figure 3.3. Critical buckling temperature vs. t/a ratio of the rectangular and elliptical plates

In order to see the convergence of the applied solution technique, another thermal buckling problem of a plate with a different geometry is solved and the obtained critical temperatures are compared with the other studies.

An isotropic square plate with (b/t=100) ratio, E = $2x10^{11}$ GPa, ν = 0.27 and α = $2x10^{-6}$ 1/ºC is considered. The critical buckling temperatures for the given plate are found for both simply supported edges and the clamped edges. A uniform temperature rise is considered and the results are compared with various references given in Table 3.6. The plate solved for thermal buckling is given in Figure 3.4.

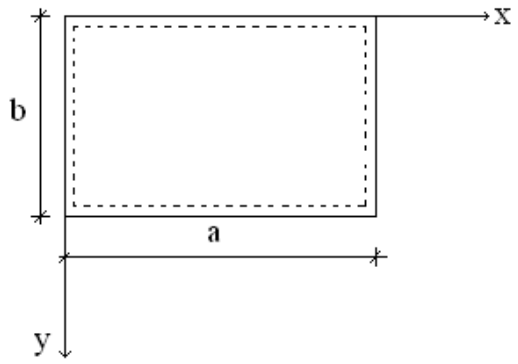

Figure 3.4. Plate subjected to uniform heating

Table 3.6. A comparison among the results of various references for a square isotropic plate

	Tcr (ºC)					
	Present Study	Ref. [50]	Ref. [51]	Ref. [52]	Ref. [22]	Ref. [6]
Simply Supported Edges	64,79	63,266	63,27	63,3	63,21	62,14
Clamped Edges	172,025	167,856	168,71	168	169,07	166,91

The present results show that the results are so close to each other. In the analysis, the shape function for r=4 is used which corresponds to the analysis done with 6 unknown terms. As it is mentioned before when the number of the unknown terms are increased in the shape functions, the results get more convenient. So, it is possible to obtain more accurate results if the term number is increased in the solution method for this problem.

3.3. Thermal Buckling Problem of Uniaxially Loaded Rectangular Plates

3.3.1. Basic Assumptions and Equations

In this problem, the analyses done for the thermal buckling problem of the plates subjected to biaxial in-plane compression forces are repeated for a homogenous rectangular plate subjected to uniaxial in-plane compression forces. For the edges of $x=\mp$ a/2, the problem is solved for both simply supported and clamped boundary conditions whereas for the edges of $y=\mp$ b/2, the edges are assumed to be free. The configuration of the analyzed rectangular plate is given in Figure 3.5.

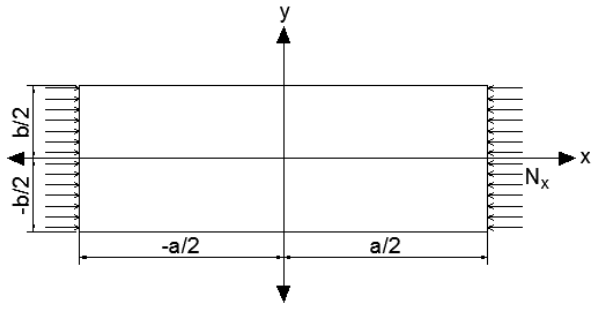

Figure 3.5. Configuration of the uniaxially loaded rectangular plate

According to the given assumptions, the boundary shape equation of the rectangular plate changes and becomes:

$$\phi(x,y)=\left[\left(x^2-\frac{a^2}{4}\right)\right]^{\Omega} \tag{3.18}$$

The displacement function, w, is again taken to be:

$$w(x,y)=\sum_{i}^{r}\sum_{j}^{r}\alpha_{ij}\phi(x,y)\,x^i y^j \tag{3.19}$$

The methodology of the Rayleigh-Ritz method is followed as given in the preceding problem. Here, it should be noted that when the plates are subjected to uniaxial in-plane forces, N_y in Eq. (3.17) becomes zero. Therefore, for the buckling problem of the given rectangular plate subjected to uniaxial in-plane compression forces, the total energy equation becomes:

$$F=\frac{D}{2}\iint_A\left\{\left(\nabla^2 w\right)^2+2(1-\nu)\left[\left(\frac{\partial^2 w}{\partial x\partial y}\right)^2-\frac{\partial^2 w}{\partial x^2}\frac{\partial^2 w}{\partial y^2}\right]\right\}dx\,dy-\frac{1}{2}\iint_A\left[N_x\left(\frac{\partial w}{\partial x}\right)^2\right]dx\,dy \tag{3.20}$$

3.3.2. Numerical Results

Since the buckling loads of the plate have to be obtained before the thermal analysis, the buckling problem for isotropic homogenous rectangular plate is solved by using Rayleigh-Ritz method. As mentioned before, the given plate is solved both for clamped and simply supported case. In the analyses, the results for r=6 are presented which correspond to the analysis done with 10 unknown terms. In order to obtain results for various *a/b* ratios, *a* is kept constant as 1, and *b* is chosen for 8 different numbers from 1 to 3. During the analyses, Poisson's ratio is chosen as 0.3, Young's modulus is $2\text{x}10^{11}$ Pa and the thermal expansion coefficient is taken as $2\text{x}10^{-6}$ (1/°C). Also, the in-plane compressive forces are taken to be N_x = -N. As a result of the critical buckling load analysis, buckling

load factors for simply supported and clamped rectangular plates are presented in Table 3.7.

Table 3.7. Buckling load factors for simply supported and clamped rectangular plates

$\lambda=Na^2/D$								
a/b	1	1,125	1,25	1,375	1,5	2	2,5	3
Simply Supported Plate	9,4	9,36	9,32	9,29	9,26	9,17	9,11	9,08
Clamped Plate	38,79	38,7	38,63	38,55	38,49	38,25	38,05	37,88

In order to obtain the critical buckling temperatures for the given plate, the basic equations and assumptions given for the thermal buckling of plates are used in the analysis. Thermal stress resultants are obtained in accordance with Eq. (3.4) and Eq. (3.5) and then by using the buckling load factors presented in Table 3.7, the critical temperatures for homogenous rectangular plate are obtained. In the analyses, a/b ratio is changed and due to the variation of a/b, the critical temperatures are found. The results are given in Table 3.8.

Table 3.8. Critical buckling temperatures for the rectangular plates

T_{cr} (ºC)								
a/b	1	1,125	1,25	1,375	1,5	2	2,5	3
Simply Supported Plate	30,13	30	29,87	29,78	29,68	29,39	29,2	29,1
Clamped Plate	124,33	124,04	123,81	123,56	123,36	122,6	121,95	121,41

According to the results obtained for the simply supported and clamped plates, the influence of the aspect ratio (a/b) of the plate on the buckling temperature is presented. Figure 3.6 and Figure 3.7 show the influence of the aspect ratio on the buckling temperature for the simply supported and clamped rectangular plates, respectively.

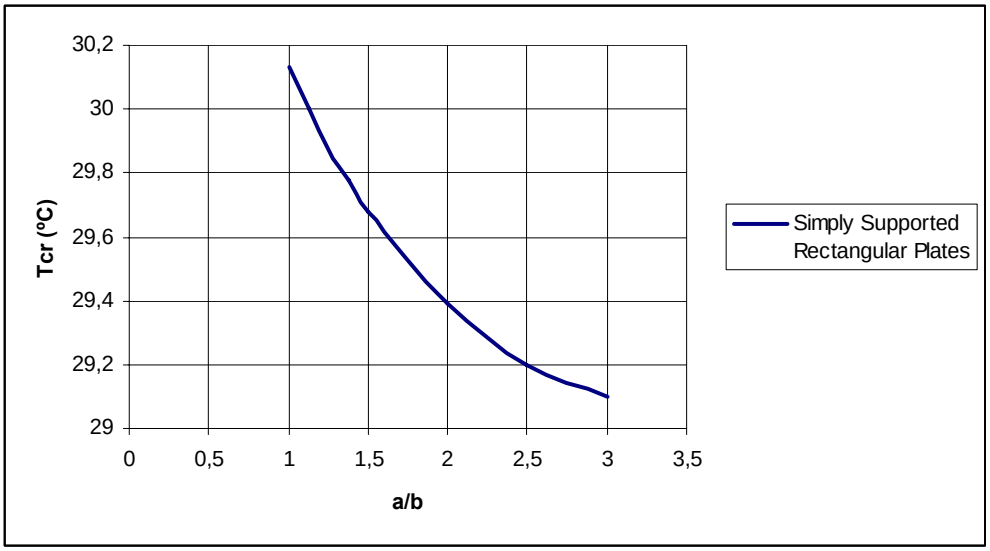

Figure 3.6. Influence of the aspect ratio of the simply supported rectangular plate on the buckling temperature

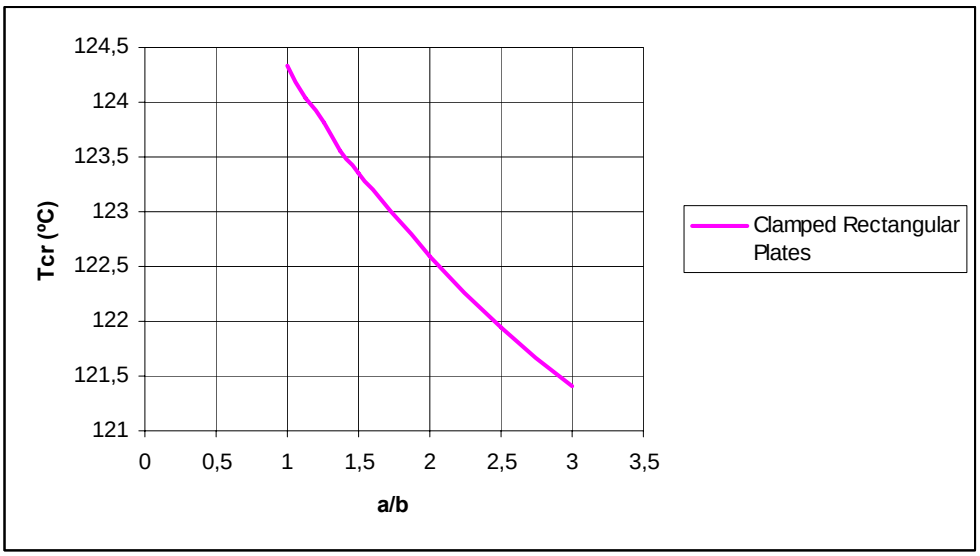

Figure 3.7. Influence of the aspect ratio of the clamped rectangular plate on the buckling temperature

3.4. Thermal Buckling Problem of Half Elliptic Plates

3.4.1. Basic Assumptions and Equations

In this problem, the critical buckling temperature analysis is employed for a half elliptic plate. The plate is again assumed to be fully simply supported and fully clamped. The configuration of the analyzed half elliptic plate is given in Figure 3.8.

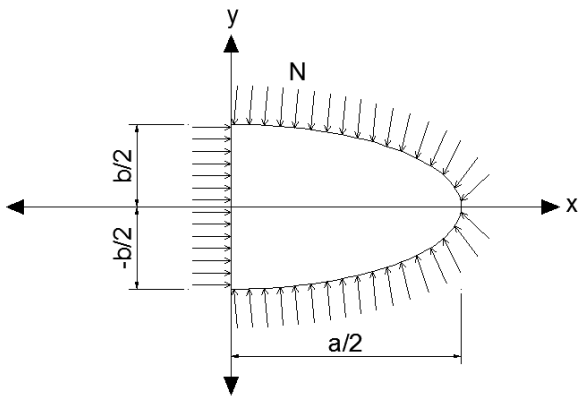

Figure 3.8. Configuration of the analyzed half elliptic plate

The methodology followed in the previous problems is also followed in this problem. In order to find the critical buckling temperatures for the given plate, first of all, critical buckling load analysis is done. For this problem, the boundary shape equation of the given half elliptic plate becomes:

$$\phi(x,y)=\left[\frac{x^2}{(a/2)^2}+\frac{y^2}{(b/2)^2}-1\right]^{\Omega} x^{\Omega} \tag{3.21}$$

In order to apply Rayleigh-Ritz method, an appropriate displacement function is selected. The displacement function, *w*, is chosen as given in Eq. (3.22). Since the accuracy of the results depend highly on the number of the unknown terms in the displacement function, the analyses are done with 10 terms which means *r* is chosen to be 6.

$$w(x,y)=\sum_{i}^{r}\sum_{j}^{r}\alpha_{ij}\phi(x,y)\,x^i y^j \tag{3.22}$$

The total energy equation for the buckling problem of the given half elliptic plate becomes:

$$F=\frac{D}{2}\iint_A\left\{\left(\nabla^2 w\right)^2+2(1-\nu)\left[\left(\frac{\partial^2 w}{\partial x\partial y}\right)^2-\frac{\partial^2 w}{\partial x^2}\frac{\partial^2 w}{\partial y^2}\right]\right\}dx\,dy-\frac{1}{2}\iint_A\left[N_x\left(\frac{\partial w}{\partial x}\right)^2+N_y\left(\frac{\partial w}{\partial y}\right)^2\right]dx\,dy \qquad (3.24)$$

It should be noted that, according to the configuration of the half elliptic plate in this problem, the area is expressed as:

$$A_{half\ elliptic}=\int_0^{a/2}\int_{-b/2\sqrt{1-(2x/a)^2}}^{b/2\sqrt{1-(2x/a)^2}}dx\,dy \qquad (3.25)$$

3.4.2. Numerical Results

Thermal buckling analyses for the given half elliptic plate are done again both for simply supported and clamped cases. As mentioned before, Rayleigh-Ritz method is used in order to obtain the critical buckling loads. The results are obtained for various a/b ratios. In the calculations, Poisson's ratio is chosen as 0.3, Young's modulus is $2\text{x}10^{11}$ Pa and the thermal expansion coefficient is taken as $2\text{x}10^{-6}$ (1/°C). As the first step of the analyses, buckling load factors are obtained and presented in Table 3.9.

Table 3.9. Buckling load factors for simply supported and clamped half elliptic plates

$\lambda=Na^2/D$								
a/b	1	1,125	1,25	1,375	1,5	2	2,5	3
Simply Supported Plate	52,55	55,22	58,38	62,08	66,32	88,76	118,94	155,38
Clamped Plate	171,08	177,22	184,96	194,46	205,78	269,33	359,74	474,33

After obtaining the buckling load factors for the given plate, thermal stress resultants are found and critical buckling temperatures are achieved. These temperatures for the simply supported and clamped half elliptic plates are given in Table 3.10.

Table 3.10. Critical buckling temperatures for the half elliptic plates

Tcr (ºC)								
a/b	1	1,125	1,25	1,375	1,5	2	2,5	3
Simply Supported Plate	168,43	176,99	187,11	198,97	212,56	284,49	381,22	498,01
Clamped Plate	548,33	568,01	592,82	623,27	659,55	863,24	1153,01	1520,19

The graphical representation of the change between the temperatures and the aspect ratios of the plates is also presented in Figure 3.9 and Figure 3.10.

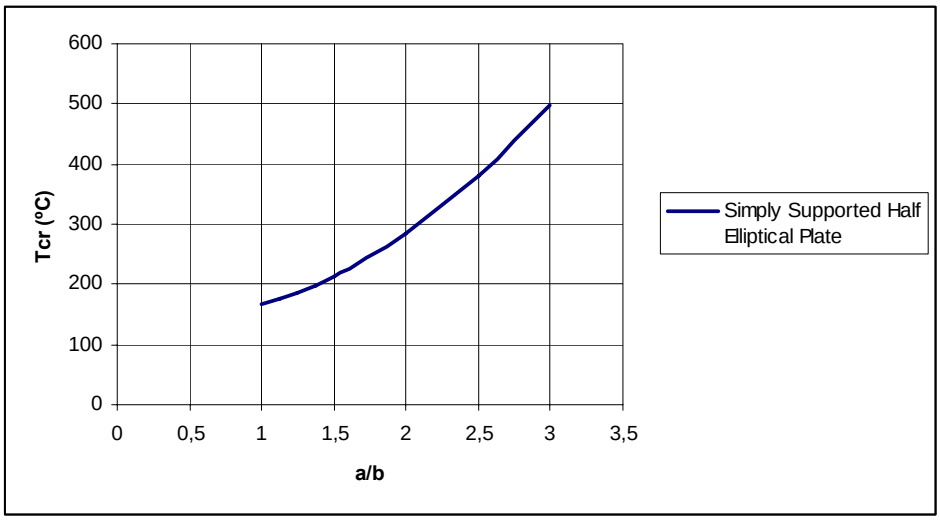

Figure 3.9. Influence of the aspect ratio of the simply supported half elliptic plate on the buckling temperature

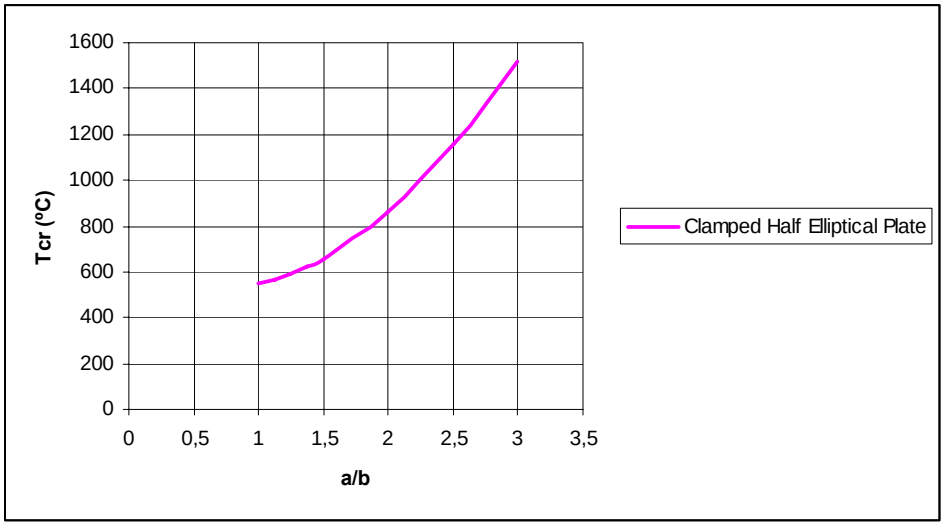

Figure 3.10. Influence of the aspect ratio of the clamped half elliptic plate on the buckling temperature

4. THERMAL BUCKLING OF RECTANGULAR AND ELLIPTICAL FGM PLATES

In this part of the study, thermal buckling problem of elastic, functionally graded material (FGM) Kirchhoff plates are investigated. Rectangular and elliptical plates are analyzed and simply supported and clamped boundaries are assumed. Rayleigh-Ritz method is used to solve the partial differential equation of plates. The Poisson's ratios of the plates are assumed to be constant, but their Young's modules and thermal expansion coefficient vary in the thickness direction functionally. Thermal buckling analyses are done and the critical temperatures of such plates are obtained. The objective here is to investigate the influence of volume fractions and the component materials on the behavior of plates and also see the effect of FGM on the critical buckling temperature.

This work is motivated by the increased demand to the FGM and the necessity to understand the behavior of FGM members under thermal effects. Here, the results are examined with respect to the parameters a/b ratios and n which are the plate aspect ratio and the power law index, respectively. The demand of material properties can be satisfied by organizing the material composition by the power low exponent. According to this, the numerical work is conducted for various exponents.

4.1. Functionally Graded Materials (FGMs)

The most lightweight composite materials with high strength/weight and stiffness/weight ratios have been used successfully in aircraft industry and other engineering applications. However, the traditional composite material is incapable to employ under the high-temperature environments. In general, the metals have been used in engineering field for many years on account of their excellent strength and toughness. In the high-temperature condition, the strength of the metal is reduced similar to the traditional composite material. The ceramic materials have excellent characteristics in heat resistance. However, the applications of ceramic are usually limited due to their low toughness.

Recently, a new class of composite materials known as functionally graded materials (FGMs) has drawn considerable attention [110]. A typical FGM, with a high bending–stretching coupling effect, is an inhomogeneous composite made from different phases of material constituents which are usually ceramic and metal. FGMs are microscopically inhomogenous and by gradually varying the volume fraction of constituent materials, their material properties exhibit a smooth and continuous change from one surface to another, thus eliminating interface problems and mitigating thermal stress concentrations. This is due to the fact that the ceramic constituents of FGMs are able to withstand high-temperature environments due to their better thermal resistance characteristics, while the metal constituents provide stronger mechanical performance and reduce the possibility of catastrophic fracture. In a high-temperature environment, for example in the engine combustion chamber of an air vehicle or a nuclear fusion reaction container, the relatively higher mismatch in thermal expansion coefficients induces high residual stresses. Consequently, the composite may incur cracking or debonding. Therefore, the concept of FGMs satisfies the demand of ultra-high-temperature environment and to eliminate the stress singularities.

Due to the continuous change in material properties of an FGM, the interfaces between two materials disappear but the characteristics of two or more different materials of the composite are preserved. Subsequently the stress singularity at the interface of a composite can be eliminated and thus the bonding strength is enhanced. On the other hand, in conventional laminated composite structures, homogeneous elastic laminae are bonded together to obtain enhanced mechanical and thermal properties. However, the abrupt change in material properties across the interface between different materials can result in large inter-laminar stresses. Also, in conventional composites, large plastic deformations at the interface may initiate the propagation of cracks in the material.

4.1.1. Material Properties of FGMs

The functionally graded plates are typically made from a controlled mixture of ceramics and metal or a combination of different metals. The material in the top surface ($z=t/2$) and in the bottom surface ($z=-t/2$) is ceramic and metal rich, respectively. The ceramic constituent of the material provides the high temperature resistance due to its low

thermal conductivity. The ductile metal constituent prevents fracture caused by stresses due to the high temperature gradient in a very short period of time. The material properties change in the thickness direction. For the validity of classical thin plate theory, the transverse deflections are assumed to be small compared to plate dimensions.

FGM plates are composed of more than one material; therefore, effective material properties of the mixture govern the plate behavior. Through-the-thickness composition of the material is assumed to be governed by a volume fraction rule. Recently, in addition to volume fraction rule micro-mechanical homogenization techniques like Mori-Tanaka have been started to be used for representing effective mechanical properties [110]. The volume fractions of ceramic, Vc, and metal, Vm, corresponding to the power law are expressed as [111]:

$$V_{\mathrm{c}}(z)=\left(\frac{2z+t}{2t}\right)^{n};\qquad V_{\mathrm{c}}=\int_{-t/2}^{t/2}V_{\mathrm{c}}(z)\,dz$$
$$V_{m}=1-V_{c} \tag{4.1}$$

where, z is the thickness coordinate variable; and $-t/2\leq z\leq t/2$, where t is the thickness of the plate and n is the power law index that takes values greater than or equal to zero ($0\leq n\leq\infty$). The variation of the composition of ceramics and metal is linear for $n=1$ and as it is seen from Eq. (4.1), the value of n equal to zero represents a fully ceramic plate. Also, for the high values of n, the dominant constituent material first exhibit changes in small increments and then rapidly changes at the opposite side. On the other hand, for the low values of n, the material properties change quickly near the surface. The variations of the volume fractions through the thickness are illustrated in Figure 4.1.

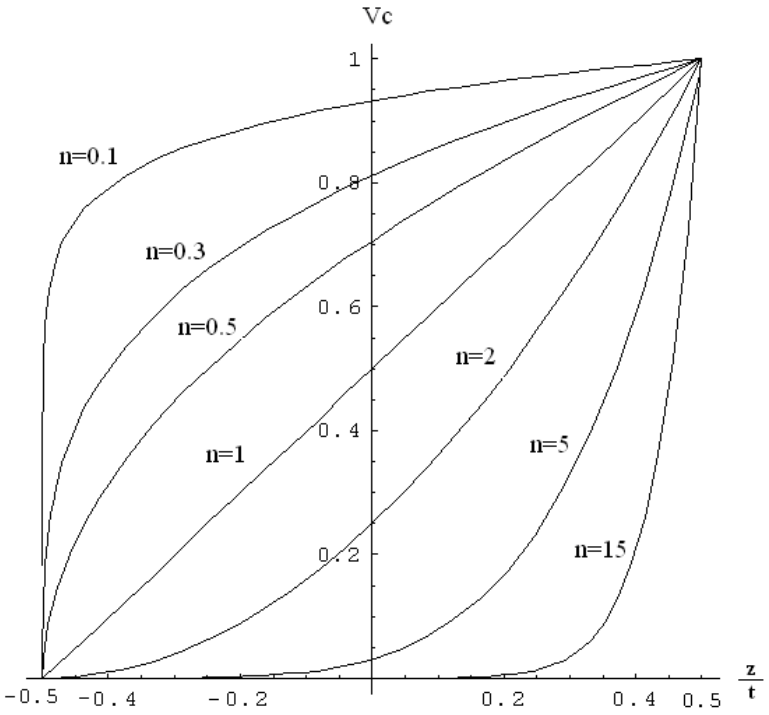

Figure 4.1. Through the thickness distribution of the volume fraction of ceramic [112]

The mechanical and thermal properties of FGMs are determined from the volume fraction of the material constituents. It is assumed that the non-homogenous material properties such as the Young's modulus E and the coefficient of thermal expansion α change in the thickness direction z, whereas Poisson's ratio ν is assumed to be constant.

$$\begin{aligned} E(z) &= E_c V_c + E_m(1-V_c) \\ \alpha(z) &= \alpha_c V_c + \alpha_m(1-V_c) \\ \nu(z) &= \nu_0 \end{aligned} \tag{4.2}$$

where, subscripts *m* and *c* refer to the metal and ceramic constituents, respectively. When Eq. (4.1) is substituted into Eq. (4.2), material properties of the FGM plate are determined. So, according to the rule of mixture:

$$\begin{aligned} E(z) &= (E_c - E_m)\left(\frac{2z+t}{2t}\right)^n + E_m \\ \alpha(z) &= (\alpha_c - \alpha_m)\left(\frac{2z+t}{2t}\right)^n + \alpha_m \\ \nu(z) &= \nu_0 \end{aligned} \tag{4.3}$$

In addition to this, the thermal conduction coefficient, *K*, of an FGM plate can also be written as:

$$K(z) = (K_c - K_m)(\frac{2z+t}{2t})^n + K_m \tag{4.4}$$

It should also be noted that the effective properties obtained by using Eq. (4.2) are position dependent in the thickness (z) direction. The position independent effective mass per unit area, ρ_{eff}, of the plate can be obtained by integrating over the thickness as:

$$\rho_{eff} = \int_{-t/2}^{t/2} \overline{\rho}_{eff}(z)\, dz \tag{4.5}$$

In the same way, the effective bending rigidity of the plate, D_{eff}, can be obtained as it is given in Eq. (4.6) where ν_{eff} is the effective Poisson's ratio of the FGM plate.

$$D_{eff} = \int_{-t/2}^{t/2} \frac{E_{eff}(z)}{1-\nu_{eff}^{\,2}(z)}\, z^2\, dz \tag{4.6}$$

It is seen in the literature that, the effect of Poisson's ratio is neglected in many studies under the case of FGM. The effect of Poisson's ratio on the deformation is negligible, but the effect of Young's modulus is highly effective [113]. Therefore, Poisson's ratio is assumed to be constant and Young's modulus is assumed to vary in the thickness direction.

4.2. Thermal Buckling Problem of Rectangular and Elliptical FGM Plates

4.2.1. Basic Assumptions and Equations

The geometrical shapes of the studied plates are rectangular and elliptical. The configuration of these studied plates is given in Figure 3.1. In order to deal with the plate bending problem a complete set of independent, continuous functions which are capable of representing the plate deflections are selected as follows. Here, Eq. (4.7) represents the

function of the rectangular plate whereas Eq. (4.8) represents the function of the elliptical plate.

$$w(x,y)=\sum_{i}^{r}\sum_{j}^{r}\alpha_{ij}\left[\left(x^2-\frac{a^2}{4}\right)\left(y^2-\frac{b^2}{4}\right)\right]^{\Omega}x^i y^j \tag{4.7}$$

$$w(x,y)=\sum_{i}^{r}\sum_{j}^{r}\alpha_{ij}\left[\frac{x^2}{(a/2)^2}+\frac{y^2}{(b/2)^2}-1\right]^{\Omega}x^i y^j \tag{4.8}$$

As it is mentioned before, if the external boundary condition is simply supported, then in the equations above, Ω=1. If the edges are clamped then, Ω=2. Each term of these expressions must satisfy all the boundary conditions of the problem. While applying Rayleigh-Ritz method, in the static analysis, shape functions at the length of r=6 are used. It should be noted that $i+j\leq r$. Knowing that the displacement function of the studied loading and boundary conditions is an even function, the odd powered terms are removed from the function. According to this, for the buckling problem of the given rectangular and elliptical plates, the total energy equation to be solved is:

$$F=\frac{D}{2}\iint_{A}\left\{\left(\nabla^2 w\right)^2+2(1-\nu)\left[\left(\frac{\partial^2 w}{\partial x\partial y}\right)^2-\frac{\partial^2 w}{\partial x^2}\frac{\partial^2 w}{\partial y^2}\right]\right\}dx\,dy-\frac{1}{2}\iint_{A}\left[N_x\left(\frac{\partial w}{\partial x}\right)^2+N_y\left(\frac{\partial w}{\partial y}\right)^2\right]dx\,dy \tag{4.9}$$

According to this, Rayleigh-Ritz method is conducted by minimizing the total energy equation with respect to the undetermined coefficients. During the analyses one dimension of the plates are kept constant (a=1). In order to analyze the thermal buckling of FGM plates, the first step is to solve the buckling problem for isotropic, homogenous rectangular and elliptical plates. The boundary conditions are assumed as fully clamped and simply supported for both of the studied plates.

For the solution of FGM plates, effective material properties are obtained by using Eq. (4.1) and Eq. (4.2) due to the variation of the power law index, *n*. It is assumed that plate layers are made from a mixture of ceramics and metals, the mixing ratio of which are varied continuously and smoothly in the z-direction. It is also considered that the effective

Young's modulus and thermal expansion coefficient of the FGM layers are temperature-dependent, whereas Poisson's ratio depends weakly on temperature change and is assumed to be constant. Here, for the numerical calculations, the properties used in the analyses for the ceramic and metal materials are given. In order to illustrate the proposed approach Young's modulus and the coefficient of thermal expansion for metal are E_m=70 GPa and α_m=23x10^{-6} 1/ºC and for the ceramic E_c=380 GPa and α_c=7.4x10^{-6} 1/ºC, respectively. Poisson's ratio is chosen to be 0.3.

As a result of the analyses, thermal buckling load factor, λ, changes due to the change in the material properties and λ_{eff} is used for the rest of the analyses. According to this, critical buckling temperatures are obtained for the rectangular and elliptical FGM plates with the boundary conditions assumed.

4.2.2. Numerical Results

Once the buckling loads for the isotropic, homogenous plates are obtained as they are presented in Table 3.1 and Table 3.2, for the solution of FGM plates, the volume fractions of the ceramic and metal are found due to the variation of the power law index, *n*. Since functionally graded structures are most commonly used in high temperature environment where significant changes in mechanical properties of the constituent materials are to be expected, it is essential to take into consideration this temperature-dependency for accurate prediction of the mechanical response. Thus, the effective Young's modulus, E_{eff}, and thermal expansion coefficient, α_{eff}, are assumed to be temperature dependent. According to these, the effective Young's moduli, E_{eff}, and effective thermal expansion, α_{eff}, coefficients are obtained again due to the variation of the power law index, *n*. The results are presented in Table 4.1.

Table 4.1. Effective values of the Young's modulus and the thermal expansion coefficient

n	Vc	Vm	Ec (GPa)	Em (GPa)	Eeff (GPa)	αc (1/ºC)	αm (1/ºC)	αeff (1/ºC)
0,1	0,909	0,091	380	70	351,79	7,4E-06	23E-06	8,82E-06
0,3	0,769	0,231	380	70	308,39	7,4E-06	23E-06	1,1E-05
0,5	0,667	0,333	380	70	276,77	7,4E-06	23E-06	1,26E-05
1	0,5	0,5	380	70	225	7,4E-06	23E-06	1,52E-05
2	0,333	0,667	380	70	173,23	7,4E-06	23E-06	1,78E-05
5	0,167	0,833	380	70	121,77	7,4E-06	23E-06	2,04E-05
15	0,062	0,938	380	70	89,22	7,4E-06	23E-06	2,2E-05

Since the effective values of Young's moduli and the thermal expansion coefficients are found, it is possible to obtain the buckling load factors for FGM plates. The obtained buckling load factors are shown as λ' and are presented as:

$$\lambda' = Na^2 \frac{12(1-\nu^2)}{t^3} \tag{4.10}$$

The buckling load factors of the all edges simply supported and clamped rectangular FGM plates are given in Table 4.2 and Table 4.3, respectively. Also, the results for the elliptical FGM plates are presented in Table 4.4 and Table 4.5, respectively, for the same boundary conditions. As it is seen from the tables, in order to see the influence of the aspect ratio, the results are obtained for a wide range of a/b ratios.

Table 4.2. Buckling load factors for simply supported FGM rectangular plates

	n						
	0,1	0,3	0,5	1	2	5	15
	Eeff (GPa)						
	351,79	308,39	276,77	225	173,23	121,77	89,22
a/b	**λ'**						
1	6944,33	6087,62	5463,44	4441,50	3419,56	2403,74	1761,20
1,125	7866,02	6895,60	6188,58	5031,00	3873,42	2722,78	1994,96
1,25	8896,77	7799,18	6999,51	5690,25	4380,99	3079,56	2256,37
1,375	10036,57	8798,37	7896,25	6419,25	4942,25	3474,10	2545,45
1,5	11285,42	9893,15	8878,78	7218,00	5557,22	3906,38	2862,18
2	17360,84	15219,05	13658,60	11103,75	8548,90	6009,35	4403,01
2,5	25170,57	22065,30	19802,89	16098,75	12394,61	8712,64	6383,69
3	34721,67	30438,09	27317,20	22207,50	17097,80	12018,70	8806,01
5	90272,83	79135,96	71021,95	57737,25	44452,55	31247,40	22894,74
10	350674,83	307412,40	275892,64	224286,75	172680,86	121383,99	88937,17

Table 4.3. Buckling load factors for clamped FGM rectangular plates

	n						
	0,1	0,3	0,5	1	2	5	15
	Eeff						
	351,79	308,39	276,77	225	173,23	121,77	89,22
a/b	**λ'**						
1	18416,21	16144,22	14488,91	11778,75	9068,59	6374,66	4670,67
1,125	21008,90	18417,05	16528,70	13437,00	10345,30	7272,10	5328,22
1,25	24178,53	21195,64	19022,40	15464,25	11906,10	8369,25	6132,09
1,375	27914,54	24470,75	21961,70	17853,75	13745,80	9662,45	7079,61
1,5	32195,82	28223,85	25329,99	20592,00	15854,01	11144,39	8165,41
2	54488,75	47766,53	42868,91	34850,25	26831,59	18860,96	13819,29
2,5	84482,37	74059,86	66466,32	54033,75	41601,18	29243,07	21426,18
3	121592,70	106591,92	95662,78	77769,00	59875,22	42088,58	30838,00
5	329785,54	289100,21	259458,04	210926,25	162394,46	114153,29	83639,29
10	1332080,98	1167743,41	1048011,75	851980,50	655949,25	461091,85	337838,67

Table 4.4. Buckling load factors for simply supported FGM elliptical plates

	n						
	0,1	0,3	0,5	1	2	5	15
	Eeff						
	351,79	308,39	276,77	225	173,23	121,77	89,22
a/b	**λ'**						
1	5906,55	5177,87	4646,97	3777,75	2908,53	2044,52	1498,00
1,125	6736,78	5905,67	5300,15	4308,75	3317,35	2331,90	1708,56
1,25	7746,42	6790,75	6094,48	4954,50	3814,52	2681,38	1964,62
1,375	8931,95	7830,02	7027,19	5712,75	4398,31	3091,74	2265,30
1,5	10282,82	9014,24	8089,99	6576,75	5063,51	3559,34	2607,90
2	17174,39	15055,60	13511,91	10984,50	8457,09	5944,81	4355,72
2,5	26120,41	22897,96	20550,17	16706,25	12862,33	9041,42	6624,59
3	36867,59	32319,27	29005,50	23580,00	18154,50	12761,50	9350,26
5	96981,47	85016,96	76299,95	62028,00	47756,05	33569,55	24596,17
10	369217,68	323667,64	290481,19	236146,50	181811,81	127802,49	93639,96

Table 4.5. Buckling load factors for clamped FGM elliptical plates

	n						
	0,1	0,3	0,5	1	2	5	15
	Eeff						
	351,79	308,39	276,77	225	173,23	121,77	89,22
a/b	**λ'**						
1	20660,63	18111,74	16254,70	13214,25	10173,80	7151,55	5239,89
1,125	23538,27	20634,37	18518,68	15054,75	11590,82	8147,63	5969,71
1,25	26996,36	23665,85	21239,33	17266,50	13293,67	9344,63	6846,74
1,375	31017,32	27190,75	24402,81	19838,25	15273,69	10736,46	7866,53
1,5	35576,52	31187,48	27989,75	22754,25	17518,75	12314,60	9022,82
2	58727,82	51482,63	46203,98	37561,50	28919,02	20328,28	14894,39
2,5	89066,19	78078,18	70072,63	56965,50	43858,37	30829,73	22588,72
3	126246,88	110671,92	99324,45	80745,75	62167,05	43699,60	32018,38
5	344602,93	302089,59	271115,59	220403,25	169690,91	119282,24	87397,24
10	1400096,06	1227367,53	1101522,46	895482,00	689441,54	484634,86	355088,46

Once the buckling load factors for each case are achieved, the critical buckling temperatures of FGM plates can be found. The methodology for the thermal buckling of

plates is applied for the FGM plates as well. The only difference is, due to the material properties, the thermal expansion coefficient and the Young's modulus change in the thermal analysis. It is evident that E_{eff} and α_{eff} are both temperature and position dependent. The given method is simple and convenient to apply for predicting the overall material properties and responses.

The critical temperature results under the uniform temperature rise for the simply supported and the clamped rectangular and elliptical FGM plates are given in Table 4.6, Table 4.7, Table 4.8 and Table 4.9.

Table 4.6. Critical buckling temperatures for simply supported rectangular FGM plates

	n								
	Ceramic	0,1	0,3	0,5	1	2	5	15	Metal
a/b	**Tcr (ºC)**								
1	17,1	14,35	11,50	10,04	8,32	7,11	6,20	5,75	5,5
1,125	19,37	16,25	13,03	11,37	9,43	8,05	7,03	6,51	6,23
1,25	21,91	18,38	14,74	12,87	10,66	9,11	7,95	7,37	7,05
1,375	24,71	20,73	16,63	14,51	12,03	10,27	9,96	8,31	7,95
1,5	27,79	23,31	18,69	16,32	13,53	11,55	10,08	9,35	8,94
2	42,75	35,87	28,76	25,11	20,81	17,77	15,51	14,38	13,75
2,5	61,98	52,00	41,70	36,40	30,17	25,77	22,48	20,85	19,94
3	85,5	71,73	57,52	50,21	41,62	35,54	31,01	28,76	27,51

Table 4.7. Critical buckling temperatures for clamped rectangular FGM plates

	n								
	Ceramic	0,1	0,3	0,5	1	2	5	15	Metal
a/b	**Tcr (ºC)**								
1	45,35	38,05	30,51	26,63	22,08	18,85	16,45	15,25	14,59
1,125	51,73	43,40	34,80	30,38	25,16	21,51	18,77	17,40	16,64
1,25	59,54	49,95	40,05	34,97	28,98	24,75	21,60	20,03	19,15
1,375	68,74	57,67	46,24	40,37	33,46	28,58	24,93	23,12	22,11
1,5	79,28	66,51	53,33	46,56	38,60	32,96	28,76	26,67	25,51
2	134,17	112,57	90,26	78,80	65,32	55,78	48,67	45,13	43,17
2,5	208,03	174,54	139,95	122,18	101,28	86,48	75,46	69,97	66,93
3	299,41	251,21	201,42	175,84	145,77	124,47	108,61	100,71	96,33

Table 4.8. Critical buckling temperatures for simply supported elliptical FGM plates

	n								
	Ceramic	0,1	0,3	0,5	1	2	5	15	Metal
a/b	Tcr (ºC)								
1	14,54	12,20	9,78	8,54	7,08	6,05	5,28	4,89	4,65
1,125	16,59	13,92	11,16	9,74	8,08	6,90	6,02	5,58	5,34
1,25	19,07	16,00	12,83	11,20	9,29	7,93	6,92	6,42	6,14
1,375	21,99	18,45	14,80	12,92	10,71	9,14	7,98	7,40	7,08
1,5	25,32	21,24	17,03	14,87	12,33	10,53	9,18	8,52	8,15
2	42,29	35,48	28,45	24,84	20,59	17,58	15,34	14,22	13,61
2,5	64,32	53,96	43,27	37,77	31,31	26,74	23,33	21,63	20,69
3	90,78	76,17	61,07	53,32	44,20	37,74	32,93	30,54	29,21

Table 4.9. Critical buckling temperatures for clamped elliptical FGM plates

	n								
	Ceramic	0,1	0,3	0,5	1	2	5	15	Metal
a/b	Tcr (ºC)								
1	50,87	42,68	34,22	29,88	24,77	21,15	18,45	17,11	16,37
1,125	57,96	48,62	38,99	34,04	28,22	24,10	21,02	19,50	18,65
1,25	66,48	55,77	44,72	39,04	32,36	27,64	24,11	22,36	21,39
1,375	76,38	64,08	51,38	44,86	37,18	31,75	27,70	25,69	24,57
1,5	87,61	73,51	58,94	51,45	42,65	36,42	31,78	29,47	28,19
2	144,65	121,36	97,31	84,95	70,42	60,13	52,47	48,65	46,54
2,5	219,57	184,22	147,71	128,95	106,89	91,28	79,65	73,85	70,64
3	311,92	261,70	209,84	183,19	151,86	129,67	113,15	104,92	100,36

As it is seen from the tables, again, a wide range of a/b ratio is considered. According to the results obtained, the variation of the critical temperatures vs. dimensionless geometrical parameters a/b are plotted for each case. Seven arbitrary values of the power law index, n= 0.1, 0.3, 0.5, 1, 2, 5, 15 are taken in the calculations. The value of n=0 represents a fully ceramic plate and the variation of the composition of ceramics and metal is linear for n=1.

In Figure 4.2 and Figure 4.3, critical buckling temperatures of the simply supported and clamped rectangular FGM plates under linear temperature change are given, respectively.

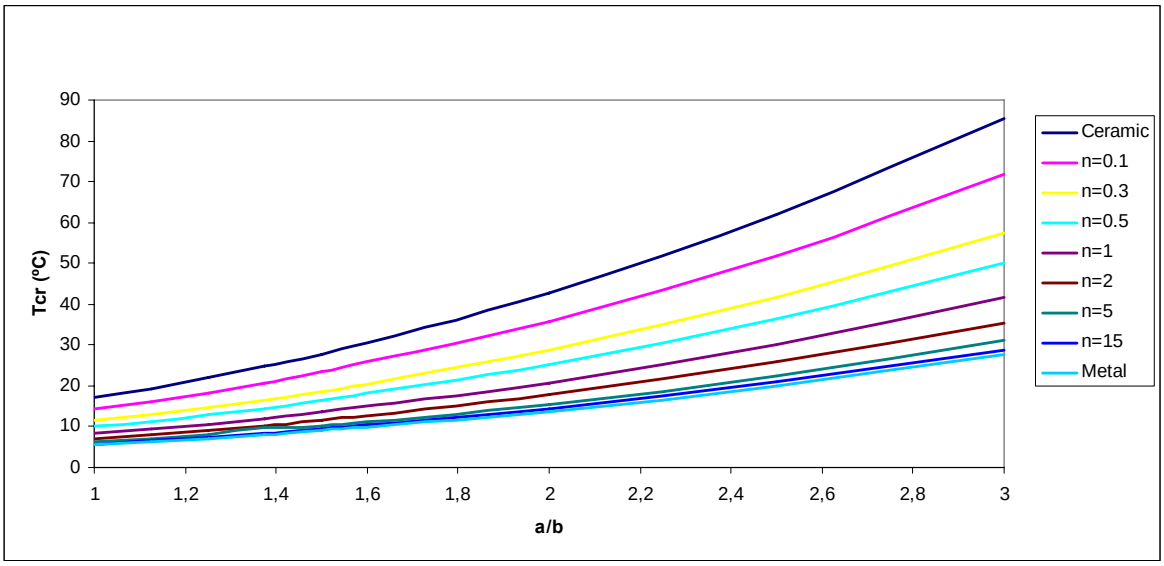

Figure 4.2. Critical buckling temperature of simply supported rectangular FGM plates under linear temperature change across the thickness vs. a/b

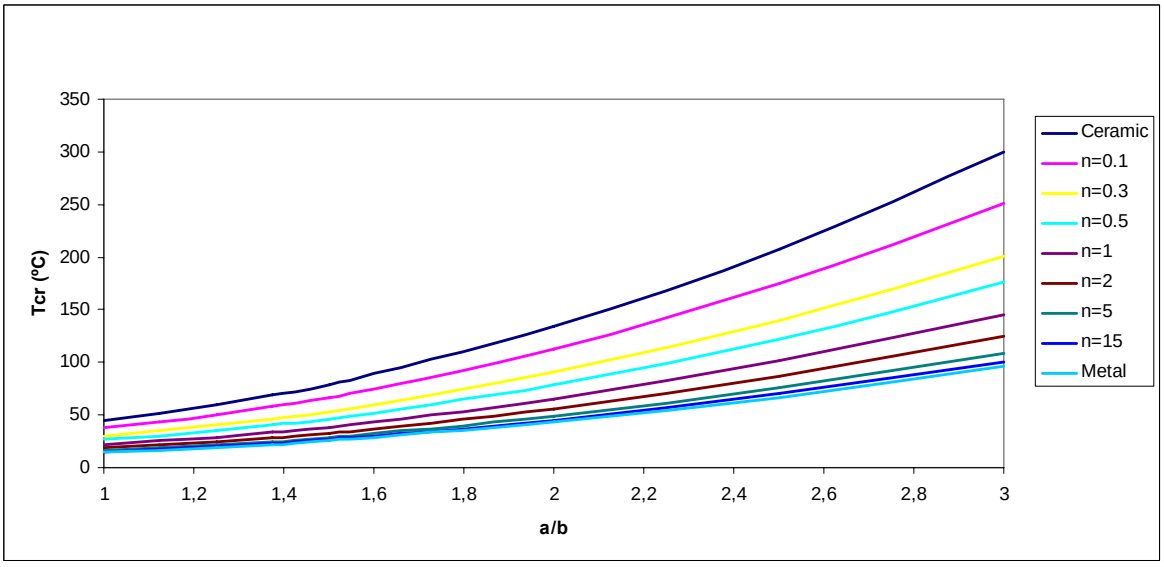

Figure 4.3. Critical buckling temperature of clamped rectangular FGM plates under linear temperature change across the thickness vs. a/b

In Figure 4.4 and Figure 4.5, this time, critical buckling temperatures of the simply supported and clamped elliptical FGM plates under linear temperature change are given, respectively.

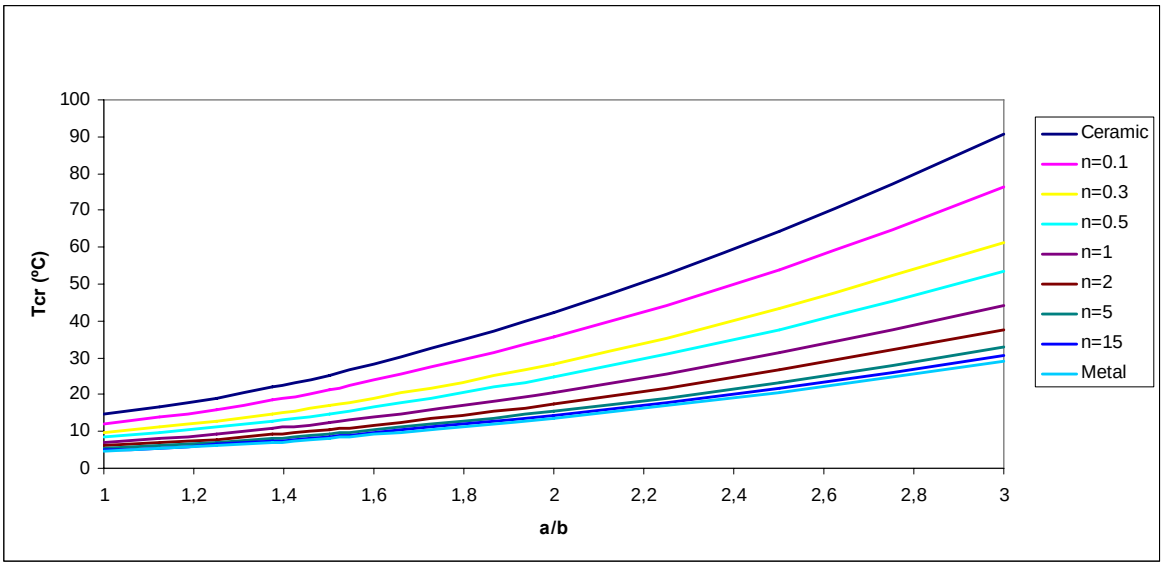

Figure 4.4. Critical buckling temperature of simply supported elliptical FGM plates under linear temperature change across the thickness vs. a/b

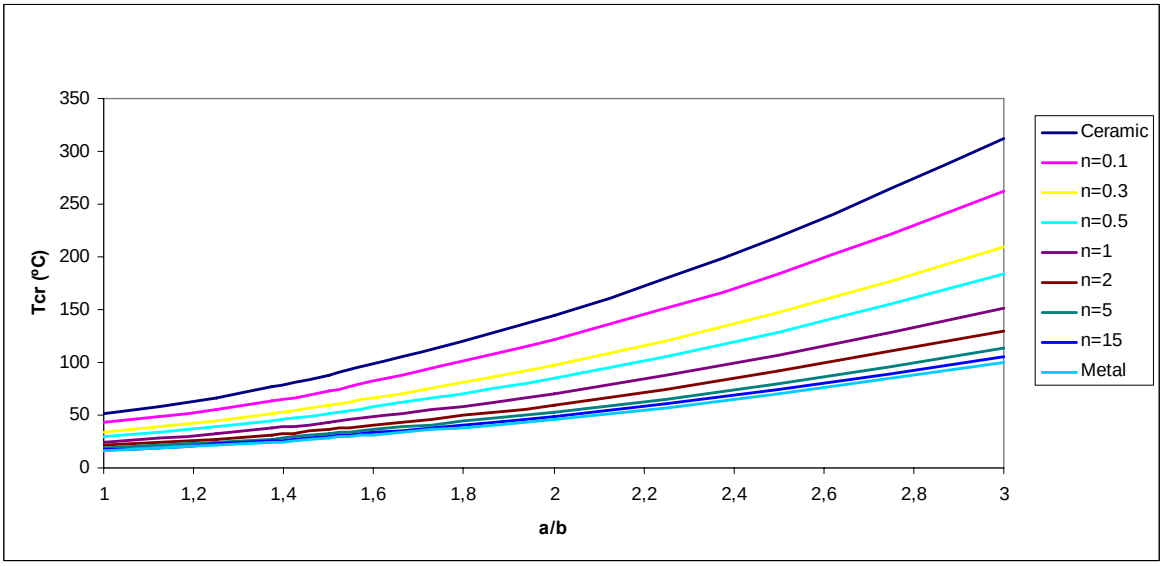

Figure 4.5. Critical buckling temperature of clamped elliptical FGM plates under linear temperature change across the thickness vs. a/b

5. THERMAL BUCKLING OF FGM PLATES WITH VARIABLE THICKNESS

In this part of the study, thermal buckling loads of rectangular and elliptical thin FGM plates with thicknesses that vary parabolically are investigated. The analysis presented here is to study the effect of parabolic thickness variations in both directions on the thermal buckling of FGM plates. Elliptical and rectangular FGM plates are analyzed. For the assumption of the boundary conditions, the edges are assumed to be fully simply supported and fully clamped for the elliptical FGM plates. In addition to this, rectangular FGM plates are studied under two different boundary conditions. In the first case, rectangular plates having three edges clamped and one edge simply supported are considered whereas in the second case, rectangular plates having two edges simply supported and two edges clamped are analyzed. Rayleigh-Ritz method is used to solve the partial differential equations of the rectangular and elliptical plates. The Poisson's ratios of the plates are assumed to be constant, but their Young's moduli and thermal expansion coefficient vary in the thickness direction functionally due to the material properties of FGMs. The study is carried out for several plate aspect ratios. Thermal buckling results of rectangular and elliptical FGM plates with parabolically varying thicknesses are generated and the critical temperatures of such plates are obtained.

5.1. Plates with Variable Thicknesses

Non-uniform plates are used in many engineering applications. It is important that the use of variable thickness can help the designer reduce the weight of the structure. For cases where reduction of weight is of high importance, these types of plates can be one of the best choices.

The plate thickness is assumed to vary according to the following relation [97]. It should be noted that sign plus and sign minus denote the clamped and simply supported cases, respectively.

$$t(x,y) = c\,t_0\left[\alpha \mp \beta(x^2+y^2)\right] \tag{5.1}$$

where, t_0 is the thickness of a plate with constant thickness, α is a parameter defining the constant part of the thickness, β is the taper parameter controlling the variation of thickness and c is a parameter insuring that all plates considered are of equal volume defined as:

$$c = \frac{2}{2\alpha \mp \beta} \tag{5.2}$$

Volume of an elliptical plate with constant thickness is πabt_0 and this corresponds to the following which gives the volume of an elliptical plate with varying thickness in the dimensionless form:

$$V = 4\int_0^1 \left\{ \int_0^{\sqrt{1-x^2}} \left(\int_{-t/2}^{t/2} dz \right) dy \right\} dx = 4\int_0^1 \left\{ \int_0^{\sqrt{1-x^2}} t(x,y)\,dy \right\} dx = \pi c t_0(\alpha + \beta/2) = \pi t_0 \tag{5.3}$$

In case of thickness variation, since the flexural rigidity also varies, it should be rewritten as:

$$D(x,y) = D_0 c^3 H \tag{5.4}$$

where, the flexural rigidity of the plate with constant thickness, D_0, and the function representing the variable plate thickness, H:

$$D_0 = E{t_0}^3 / \left[12(1-\nu^2)\right] \tag{5.5}$$

$$H = \left[\alpha + \beta(x^2+y^2)\right]^3 \tag{5.6}$$

5.2. Thermal Buckling Problem of Elliptical FGM Plates with Variable Thickness

5.2.1. Basic Assumptions and Equations

Since the problem is concerned with the elliptical plates, continuous functions which are capable of representing the plate deflections are selected as follows.

$$w(x,y)=\sum_{i}^{r}\sum_{j}^{r}\alpha_{ij}\left[\frac{x^2}{(a/2)^2}+\frac{y^2}{(b/2)^2}-1\right]^{\Omega}x^i y^j \tag{5.7}$$

If the external boundary condition is simply supported, then in the equation above, Ω=1. If the edges are clamped then, Ω=2. In order to apply the Rayleigh-Ritz method, firstly an appropriate deflection shape function, which is Eq. (5.7), at the length of r=4 is selected. Since the thickness is not uniform, the parabolic variation of the plate thickness is considered with respect to the Eq. (5.2), (5.4) and (5.6). After substituting these equations into the total energy equation for the buckling problem of an elliptical plate, the equation in the following form is obtained:

$$F=\frac{D}{2}\iint_{A}\left\{c^3\left(\alpha+\beta(x^2/a^2+y^2/b^2)\right)^3\left(\nabla^2 w\right)^2+2(1-\nu)\left[\left(\frac{\partial^2 w}{\partial x\partial y}\right)^2-\frac{\partial^2 w}{\partial x^2}\frac{\partial^2 w}{\partial y^2}\right]\right\}dx\,dy-\frac{1}{2}\iint_{A}\left[N_x\left(\frac{\partial w}{\partial x}\right)^2+N_y\left(\frac{\partial w}{\partial y}\right)^2\right]dx\,dy \tag{5.8}$$

During the calculations of the differential equations, there are difficulties arising from integration over an elliptical area. Therefore, the integration over the elliptical region should be taken in accordance with the elliptical function given in Eq. (5.9) which means while *x* take the values from –a/2 to a/2, y takes the values represented in Eq. (5.10).

$$\frac{x^2}{(a/2)^2}+\frac{y^2}{(b/2)^2}-1=0 \tag{5.9}$$

$$y=\mp(b/2)\sqrt{1-(x^2/(a^2/4)}} \tag{5.10}$$

According to this, Rayleigh-Ritz method is conducted by considering the thickness variation. This effect is governed by two more parameters than the constant thickness cases which are the controlling parameter of constant part of the plate (α) and the controlling parameter of the thickness variation (β). During the analyses one dimension of the plates are kept constant (a=1). The boundary conditions are assumed as fully clamped and simply supported.

For the solution of FGM plates, effective material properties are obtained by using Eq. (4.1) and Eq. (4.2) due to the variation of the power law index, *n*. Again, it is assumed that plate layers are made from a mixture of ceramics and metals, the mixing ratio of which are varied continuously and smoothly in the z-direction. As it is mentioned before, the effective Young's modulus and thermal expansion coefficient of the FGM layers are temperature-dependent, whereas Poisson's ratio depends weakly on temperature change and is assumed to be constant. As a result of the analyses, thermal buckling load factor, λ, changes due to the change in the material properties and the variation of the α and β parameters. According to this, λ_{eff} is calculated for the different values of a/b ratios and used in the calculation of the critical buckling temperature of the elliptical FGM plate with variable thickness. By the help of the obtained buckling factors, critical buckling temperatures are calculated by using Eq. (3.4) and Eq. (3.5).

5.2.2. Numerical Results

The analyses for the critical buckling temperature of the elliptical FGM plates with a parabolic variation of its plate thickness start with the calculation of the buckling parameters. The buckling parameters depending on the α and β parameters are calculated by Rayleigh-Ritz method for fully simply supported and fully clamped elliptical plates for different a/b ratios ($1 \leq a/b \leq 10$). It should be noted that results of variable thickness calculations are obtained for Poisson's ratio of 0.3. The critical buckling parameters for the simply supported and clamped cases are presented in Table 5.1 and Table 5.2, respectively.

Table 5.1. Buckling parameters for the simply supported elliptical plate with variable thickness

		a/b									
		1	1,11	1,25	1,43	1,67	2	2,5	3,33	5	10
α	**β**	**λ=Na²/D**									
2,0	0,0	16,79	18,86	22,02	26,98	35,04	48,82	74,26	127,91	276,27	1060,45
2,0	0,2	19,11	21,47	25,07	30,72	39,92	55,67	84,80	146,37	316,92	1219,21
2,0	0,4	21,94	24,64	28,78	35,27	45,85	63,99	97,61	168,84	366,49	1413,14
2,0	0,6	25,40	28,54	33,33	40,86	53,14	74,22	113,37	196,52	427,66	1652,79
2,0	0,8	29,71	33,38	38,99	47,81	62,21	86,96	133,02	231,07	504,13	1952,80
2,0	1,0	35,16	39,50	46,14	56,60	73,67	103,06	157,86	274,81	601,12	2333,88
1,8	0,0	16,79	18,86	22,02	26,98	35,04	48,82	74,26	127,91	276,27	1060,45
1,8	0,2	19,40	21,79	25,45	31,18	40,52	56,51	86,10	148,64	321,94	1238,86
1,8	0,4	22,64	25,44	29,71	36,41	47,34	66,08	100,83	174,49	378,97	1462,01
1,8	0,6	26,73	30,03	35,08	43,01	55,94	78,16	119,43	207,17	451,23	1745,22
1,8	0,8	31,97	35,92	41,96	51,46	66,96	93,64	143,32	249,20	544,32	2110,64
1,8	1,0	38,82	43,61	50,95	62,50	81,37	113,89	174,58	304,26	666,52	2591,14
1,6	0,0	16,79	18,86	22,02	26,98	35,04	48,82	74,26	127,91	276,27	1060,45
1,6	0,2	19,77	22,21	25,93	31,78	41,29	57,60	87,76	151,57	328,38	1264,04
1,6	0,4	23,58	26,49	30,93	37,92	49,30	68,84	105,07	181,94	395,43	1526,45
1,6	0,6	28,54	32,07	37,45	45,92	59,75	83,50	127,68	221,67	483,33	1871,13
1,6	0,8	35,16	39,50	46,14	56,60	73,67	103,06	157,86	274,81	601,12	2333,88
1,6	1,0	44,20	49,66	58,02	71,19	92,71	129,83	199,20	347,69	763,04	2971,20
1,4	0,0	16,79	18,86	22,02	26,98	35,04	48,82	74,26	127,91	276,27	1060,45
1,4	0,2	20,25	22,75	26,57	32,56	42,32	59,03	89,97	155,44	336,93	1297,48
1,4	0,4	24,86	27,93	32,62	39,99	52,00	72,62	110,91	192,19	418,09	1615,26
1,4	0,6	31,14	34,98	40,86	50,11	65,21	91,18	139,52	242,50	529,47	2052,30
1,4	0,8	39,96	44,90	52,45	64,35	83,78	117,28	179,81	313,49	687,02	2671,82
1,4	1,0	52,82	59,35	69,35	85,09	110,86	155,35	238,65	417,36	918,10	3582,57
1,2	0,0	16,79	18,86	22,02	26,98	35,04	48,82	74,26	127,91	276,27	1060,45
1,2	0,2	20,93	23,52	27,46	33,65	43,74	61,03	93,05	160,83	348,83	1344,01
1,2	0,4	26,73	30,03	35,08	43,01	55,94	78,16	119,43	207,17	451,23	1745,22
1,2	0,6	35,16	39,50	46,14	56,60	73,67	103,06	157,86	274,81	601,12	2333,88
1,2	0,8	47,95	53,88	62,95	77,24	100,61	140,94	216,37	378,00	830,47	3236,97
1,2	1,0	68,51	76,98	89,95	110,41	143,91	201,84	310,56	544,50	1201,63	4702,40
1,0	0,0	16,79	18,86	22,02	26,98	35,04	48,82	74,26	127,91	276,27	1060,45
1,0	0,2	21,94	24,64	28,78	35,27	45,85	63,99	97,61	168,84	366,49	1413,14
1,0	0,4	29,71	33,38	38,99	47,81	62,21	86,96	133,02	231,07	504,13	1952,80
1,0	0,6	42,15	47,36	55,32	67,87	88,38	123,75	189,80	331,11	726,18	2826,02
1,0	0,8	63,52	71,37	83,40	102,35	133,39	187,05	287,67	504,00	1111,25	4345,20
1,0	1,0	104,00	116,87	136,59	167,70	218,73	307,15	473,61	833,32	1847,41	7259,47

Table 5.2. Buckling parameters for the clamped elliptical plate with variable thickness

		a/b									
		1	1,11	1,25	1,43	1,67	2	2,5	3,33	5	10
α	**β**	**λ=Na²/D**									
1,0	0,0	58,73	65,92	76,74	93,55	120,67	166,98	253,47	442,55	995,53	4047,11
1,0	0,2	46,99	52,74	61,38	74,78	96,39	133,24	202,07	352,78	794,19	3228,95
1,0	0,4	38,45	43,15	50,21	61,14	78,74	108,74	164,79	287,73	648,23	2635,67
1,0	0,6	32,04	35,96	41,83	50,92	65,53	90,42	136,96	239,20	539,27	2192,66
1,0	0,8	27,13	30,44	35,41	43,07	55,40	76,40	115,67	202,09	455,90	1853,62
1,0	1,0	23,28	26,12	30,37	36,93	47,48	65,43	99,04	173,11	390,76	1588,66
0,8	0,0	58,73	65,92	76,74	93,55	120,67	166,98	253,47	442,55	995,53	4047,11
0,8	0,2	44,60	50,06	58,26	70,97	91,46	126,39	191,64	334,59	753,38	3063,11
0,8	0,4	35,02	39,30	45,73	55,67	71,68	98,95	149,90	261,77	589,96	2398,76
0,8	0,6	28,24	31,69	36,86	44,85	57,70	79,58	120,49	210,50	474,80	1930,48
0,8	0,8	23,28	26,12	30,37	36,93	47,48	65,43	99,04	173,11	390,76	1588,66
0,8	1,0	19,53	21,91	25,48	30,97	39,79	54,80	82,93	145,05	327,64	1331,88
0,6	0,0	58,73	65,92	76,74	93,55	120,67	166,98	253,47	442,55	995,53	4047,11
0,6	0,2	41,01	46,03	53,57	65,24	84,04	116,10	175,98	307,25	692,04	2813,79
0,6	0,4	30,27	33,96	39,51	48,08	61,86	85,34	129,24	225,75	509,06	2069,83
0,6	0,6	23,28	26,12	30,37	36,93	47,48	65,43	99,04	173,11	390,76	1588,66
0,6	0,8	18,49	20,74	24,11	29,31	37,64	51,84	78,46	137,25	310,07	1260,41
0,6	1,0	15,07	16,91	19,65	23,87	30,64	42,17	63,83	111,76	252,67	1026,85
0,4	0,0	58,73	65,92	76,74	93,55	120,67	166,98	253,47	442,55	995,53	4047,11
0,4	0,2	35,02	39,30	45,73	55,67	71,68	98,95	149,90	261,77	589,96	2398,76
0,4	0,4	23,28	26,12	30,37	36,93	47,48	65,43	99,04	173,11	390,76	1588,66
0,4	0,6	16,64	18,67	21,70	26,37	33,86	46,62	70,55	123,48	279,07	1134,26
0,4	0,8	12,55	14,07	16,35	19,86	25,48	35,06	53,08	93,01	210,42	854,93
0,4	1,0	9,84	11,04	12,82	15,57	19,97	27,47	41,61	73,01	165,29	671,29
0,2	0,0	58,73	65,92	76,74	93,55	120,67	166,98	253,47	442,55	995,53	4047,11
0,2	0,2	23,28	26,12	30,37	36,93	47,48	65,43	99,04	173,11	390,76	1588,66
0,2	0,4	12,55	14,07	16,35	19,86	25,48	35,06	53,08	93,01	210,42	854,93
0,2	0,6	7,97	8,94	10,38	12,60	16,15	22,22	33,69	59,19	134,06	544,24
0,2	0,8	5,61	6,29	7,31	8,87	11,37	15,65	23,77	41,83	94,81	384,60
0,2	1,0	4,24	4,76	5,52	6,70	8,60	11,84	18,01	31,75	71,98	291,81

After the buckling parameters for the homogenous plates with variable thicknesses are obtained as they are presented in Table 5.1 and Table 5.2, for the solution of FGM plates, the volume fractions of the ceramic and metal are found due to the variation of the power law index, *n*. According to these values, the effective Young's moduli, E_{eff}, and effective thermal expansion, α_{eff}, coefficients are obtained due to the variation of the power law index, *n*. For the numerical calculations, Young's modulus and the coefficient of thermal expansion for metal are taken as E_m=70 GPa and α_m=23x10^{-6} 1/ºC and for the

ceramic E_c=380 GPa and α_c=7.4x10^{-6} 1/ºC, respectively. Poisson's ratio is again chosen to be 0.3. The results of these calculations are presented in Table 5.3.

Table 5.3. Effective values of the Young's modulus and the thermal expansion coefficient

n	Vc	Vm	Eeff (GPa)	α_{eff} (1/ºC)
0,1	0,909	0,091	351,79	8,82E-06
0,3	0,769	0,231	308,39	1,1E-05
0,5	0,667	0,333	276,77	1,26E-05
1	0,5	0,5	225	1,52E-05
2	0,333	0,667	173,23	1,78E-05
5	0,167	0,833	121,77	2,04E-05
15	0,062	0,938	89,22	2,2E-05

After obtaining the effective values of Young's moduli and the thermal expansion coefficients, it is possible to obtain the buckling load factors for elliptical FGM plates. Since the effect of the parabolic thickness variation is taken into account, the buckling load factors for different thickness variations and a/b ratios are calculated. The obtained buckling load factors are shown as λ' and are presented in tables in accordance with the α and β parameters. In the calculations, the controlling parameter of the constant part of the plate is taken as α=1 while the controlling parameter of the thickness variation, β, changes. Here, tables from 5.4 to 5.9 represent the results for the fully simply supported case whereas tables from 5.10 to 5.15 represent the results for the fully clamped case.

Table 5.4. Buckling load factors for simply supported elliptical FGM plate (α=1, β=0)

	n						
	0,1	0,3	0,5	1	2	5	15
a/b	λ'						
1	5906,55	5177,87	4646,97	3777,75	2908,53	2044,52	1498,00
1,11	6634,76	5816,24	5219,88	4243,50	3267,12	2296,58	1682,69
1,25	7746,42	6790,75	6094,48	4954,50	3814,52	2681,38	1964,62
1,43	9491,29	8320,36	7467,25	6070,50	4673,75	3285,35	2407,16
1,67	12326,72	10805,99	9698,02	7884,00	6069,98	4266,82	3126,27
2	17174,39	15055,60	13511,91	10984,50	8457,09	5944,81	4355,72
2,5	26123,93	22901,04	20552,94	16708,50	12864,06	9042,64	6625,48
3,33	44997,46	39446,16	35401,65	28779,75	22157,85	15575,60	11412,13
5	97189,02	85198,91	76463,25	62160,75	47858,25	33641,40	24648,81
10	373055,71	327032,18	293500,75	238601,25	183701,75	129131,00	94613,35

Table 5.5. Buckling load factors for simply supported elliptical FGM plate (α=1, β=0,2)

	n						
	0,1	0,3	0,5	1	2	5	15
a/b	**λ'**						
1	7718,27	6766,08	6072,33	4936,50	3800,67	2671,63	1957,49
1,11	8668,11	7598,73	6819,61	5544,00	4268,39	3000,41	2198,38
1,25	10124,52	8875,46	7965,44	6475,50	4985,56	3504,54	2567,75
1,43	12407,63	10876,92	9761,68	7935,75	6109,82	4294,83	3146,79
1,67	16129,57	14139,68	12689,90	10316,25	7942,60	5583,15	4090,74
2	22511,04	19733,88	17710,51	14397,75	11084,99	7792,06	5709,19
2,5	34338,22	30101,95	27015,52	21962,25	16908,98	11885,97	8708,76
3,33	59396,22	52068,57	46729,85	37989,00	29248,15	20559,65	15063,90
5	128927,52	113021,85	101433,44	82460,25	63487,06	44627,49	32698,24
10	497128,52	435798,24	391114,76	317956,50	244798,24	172078,06	126080,35

Table 5.6. Buckling load factors for simply supported elliptical FGM plate (α=1, β=0,4)

	n						
	0,1	0,3	0,5	1	2	5	15
a/b	**λ'**						
1	10451,68	9162,27	8222,84	6684,75	5146,66	3617,79	2650,73
1,11	11742,75	10294,06	9238,58	7510,50	5782,42	4064,68	2978,16
1,25	13716,29	12024,13	10791,26	8772,75	6754,24	4747,81	3478,69
1,43	16819,08	14744,13	13232,37	10757,25	8282,13	5821,82	4265,61
1,67	21884,86	19184,94	17217,86	13997,25	10776,64	7575,31	5550,38
2	30591,66	26817,59	24067,92	19566,00	15064,08	10589,12	7758,57
2,5	46795,11	41022,04	36815,95	29929,50	23043,05	16197,85	11868,04
3,33	81288,12	71259,68	63953,24	51990,75	40028,26	28137,39	20616,07
5	177347,89	155468,65	139528,06	113429,25	87330,44	61387,91	44978,48
10	686975,51	602223,99	540476,46	439380,00	338283,54	237792,46	174228,82

Table 5.7. Buckling load factors for simply supported elliptical FGM plate (α=1, β=0,6)

	n						
	0,1	0,3	0,5	1	2	5	15
a/b	**λ'**						
1	14827,95	12998,64	11665,86	9483,75	7301,64	5132,61	3760,62
1,11	16660,77	14605,35	13107,83	10656,00	8204,17	5767,03	4225,46
1,25	19461,02	17060,13	15310,92	12447,00	9583,08	6736,32	4935,65
1,43	23875,99	20930,43	18784,38	15270,75	11757,12	8264,53	6055,36
1,67	31091,20	27255,51	24460,93	19885,50	15310,07	10762,03	7885,26
2	43534,01	38163,26	34250,29	27843,75	21437,21	15069,04	11040,98
2,5	66769,74	58532,42	52530,95	42705,00	32879,05	23111,95	16933,96
3,33	116481,19	102111,01	91641,31	74499,75	57358,19	40319,26	29541,63
5	255462,86	223946,65	200984,84	163390,50	125796,16	88426,94	64789,78
10	994165,58	871516,31	782157,56	635854,50	489551,44	344124,46	252137,50

Table 5.8. Buckling load factors for simply supported elliptical FGM plate (α=1, β=0,8)

	n						
	0,1	0,3	0,5	1	2	5	15
a/b	**λ'**						
1	22345,70	19588,93	17580,43	14292,00	11003,57	7734,83	5667,25
1,11	25107,25	22009,79	19753,07	16058,25	12363,43	8690,72	6367,63
1,25	29339,29	25719,73	23082,62	18765,00	14447,38	10155,62	7440,95
1,43	36005,71	31563,72	28327,41	23028,75	17730,09	12463,16	9131,67
1,67	46925,27	41136,14	36918,35	30012,75	23107,15	16242,90	11901,06
2	65802,32	57684,35	51769,83	42086,25	32402,67	22777,08	16688,60
2,5	101199,43	88714,55	79618,43	64725,75	49833,07	35029,58	25665,92
3,33	177302,16	155428,56	139492,08	113400,00	87307,92	61372,08	44966,88
5	390926,64	342698,39	307560,66	250031,25	192501,84	135316,91	99145,73
10	1528597,91	1340016,23	1202621,00	977670,00	752719,00	529115,00	387678,74

Table 5.9. Buckling load factors for simply supported elliptical FGM plate (α=1, β=1)

	n						
	0,1	0,3	0,5	1	2	5	15
a/b	**λ'**						
1	36586,16	32072,56	28784,08	23400,00	18015,92	12664,08	9278,88
1,11	41113,70	36041,54	32346,11	26295,75	20245,39	14231,26	10427,14
1,25	48051,00	42122,99	37804,01	30732,75	23661,49	16632,56	12186,56
1,43	58995,18	51717,00	46414,33	37732,50	29050,67	20420,83	14962,19
1,67	76947,03	67454,14	60537,90	49214,25	37890,60	26634,75	19515,09
2	108052,30	94721,99	85009,91	69108,75	53207,59	37401,66	27403,92
2,5	166611,26	146056,59	131081,04	106562,25	82043,46	57671,49	42255,48
3,33	293153,64	256987,55	230637,98	187497,00	144356,02	101473,38	74348,81
5	649900,36	569722,77	511307,67	415667,25	320026,83	224959,12	164825,92
10	2553808,95	2238747,95	2009203,51	1633380,75	1257557,99	883985,66	647689,91

Table 5.10. Buckling load factors for clamped elliptical FGM plate (α=1, β=0)

	n						
	0,1	0,3	0,5	1	2	5	15
a/b	**λ'**						
1	20660,63	18111,74	16254,70	13214,25	10173,80	7151,55	5239,89
1,11	23190,00	20329,07	18244,68	14832,00	11419,32	8027,08	5881,38
1,25	26996,36	23665,85	21239,33	17266,50	13293,67	9344,63	6846,74
1,43	32909,95	28849,88	25891,83	21048,75	16205,67	11391,58	8346,53
1,67	42450,50	37213,42	33397,84	27150,75	20903,66	14693,99	10766,18
2	58741,89	51494,96	46215,05	37570,50	28925,95	20333,15	14897,96
2,5	89168,21	78167,61	70152,89	57030,75	43908,61	30865,04	22614,59
3,33	155684,66	136477,99	122484,56	99573,75	76662,94	53889,31	39484,31
5	350217,50	307011,50	275532,84	223994,25	172455,66	121225,69	88821,19
10	1423732,83	1248088,25	1120118,63	910599,75	701080,87	492816,58	361083,15

Table 5.11. Buckling load factors for clamped elliptical FGM plate (α=1, β=0,2)

	n						
	0,1	0,3	0,5	1	2	5	15
a/b	**λ'**						
1	16530,61	14491,25	13005,42	10572,75	8140,08	5721,97	4192,45
1,11	18553,40	16264,49	14596,85	11866,50	9136,15	6422,15	4705,46
1,25	21592,87	18928,98	16988,14	13810,50	10632,86	7474,24	5476,32
1,43	26306,86	23061,40	20696,86	16825,50	12954,14	9105,96	6671,87
1,67	33909,04	29725,71	26677,86	21687,75	16697,64	11737,41	8599,92
2	46872,50	41089,88	36876,83	29979,00	23081,17	16224,63	11887,67
2,5	71086,21	62316,37	55926,91	45465,75	35004,59	24606,06	18028,69
3,33	124104,48	108793,82	97638,92	79375,50	61112,08	42958,02	31475,03
5	279388,10	244920,25	219807,97	178692,75	137577,53	96708,52	70857,63
10	1135912,32	995775,89	893676,49	726513,75	559351,01	393189,24	288086,92

Table 5.12. Buckling load factors for clamped elliptical FGM plate (α=1, β=0,4)

	n						
	0,1	0,3	0,5	1	2	5	15
a/b	**λ'**						
1	13526,33	11857,60	10641,81	8651,25	6660,69	4682,06	3430,51
1,11	15179,74	13307,03	11942,63	9708,75	7474,87	5254,38	3849,84
1,25	17663,38	15484,26	13896,62	11297,25	8697,88	6114,07	4479,74
1,43	21508,44	18854,96	16921,72	13756,50	10591,28	7445,02	5454,91
1,67	27699,94	24282,63	21792,87	17716,50	13640,13	9588,17	7025,18
2	38253,64	33534,33	30095,97	24466,50	18837,03	13241,27	9701,78
2,5	57971,47	50819,59	45608,93	37077,75	28546,57	20066,48	14702,56
3,33	101220,54	88733,05	79635,03	64739,25	49843,47	35036,88	25671,27
5	228040,83	199907,65	179410,62	145851,75	112292,88	78934,97	57835,08
10	927202,35	812814,27	729474,39	593025,75	456577,11	320945,54	235154,48

Table 5.13. Buckling load factors for clamped elliptical FGM plate (α=1, β=0,6)

	n						
	0,1	0,3	0,5	1	2	5	15
a/b	**λ'**						
1	11271,35	9880,82	8867,71	7209,00	5550,29	3901,51	2858,61
1,11	12650,37	11089,70	9952,65	8091,00	6229,35	4378,85	3208,35
1,25	14715,38	12899,95	11577,29	9411,75	7246,21	5093,64	3732,07
1,43	17913,15	15703,22	14093,13	11457,00	8820,87	6200,53	4543,08
1,67	23052,80	20208,80	18136,74	14744,25	11351,76	7979,59	5846,59
2	31808,85	27884,62	25025,54	20344,50	15663,46	11010,44	8067,27
2,5	48181,16	42237,09	37906,42	30816,00	23725,58	16677,62	12219,57
3,33	84148,17	73766,89	66203,38	53820,00	41436,62	29127,38	21341,42
5	189709,79	166305,48	149253,76	121335,75	93417,74	65666,91	48113,67
10	771355,86	676194,42	606862,51	493348,50	379834,49	267000,21	195629,13

Table 5.14. Buckling load factors for clamped elliptical FGM plate (α=1, β=0,8)

	n						
	0,1	0,3	0,5	1	2	5	15
a/b	**λ'**						
1	9544,06	8366,62	7508,77	6104,25	4699,73	3303,62	2420,54
1,11	10708,49	9387,39	8424,88	6849,00	5273,12	3706,68	2715,86
1,25	12456,88	10920,09	9800,43	7967,25	6134,07	4311,88	3159,28
1,43	15151,60	13282,36	11920,48	9690,75	7461,02	5244,63	3842,71
1,67	19489,17	17084,81	15333,06	12465,00	9596,94	6746,06	4942,79
2	26876,76	23561,00	21145,23	17190,00	13234,77	9303,23	6816,41
2,5	40691,55	35671,47	32013,99	26025,75	20037,51	14085,14	10320,08
3,33	71093,24	62322,54	55932,45	45470,25	35008,05	24608,50	18030,47
5	160381,06	140595,00	126179,44	102577,50	78975,56	55514,94	40675,40
10	652084,98	571637,87	513026,41	417064,50	321102,59	225715,31	165379,98

Table 5.15. Buckling load factors for clamped elliptical FGM plate (α=1, β=1)

	n						
	0,1	0,3	0,5	1	2	5	15
a/b	**λ'**						
1	8189,67	7179,32	6443,21	5238,00	4032,79	2834,81	2077,04
1,11	9188,75	8055,15	7229,23	5877,00	4524,77	3180,63	2330,43
1,25	10683,86	9365,80	8405,50	6833,25	5261,00	3698,15	2709,61
1,43	12991,60	11388,84	10221,12	8309,25	6397,38	4496,97	3294,89
1,67	16702,99	14642,36	13141,04	10683,00	8224,96	5781,64	4236,17
2	23017,62	20177,96	18109,06	14721,75	11334,44	7967,41	5837,66
2,5	34841,28	30542,95	27411,30	22284,00	17156,70	12060,10	8836,35
3,33	60898,37	53385,39	47911,65	38949,75	29987,85	21079,60	15444,87
5	137465,46	120506,48	108150,65	87921,00	67691,35	47582,85	34863,61
10	558874,70	489926,86	439693,43	357448,50	275203,57	193451,13	141740,25

Once the buckling load factors for each case are achieved in accordance with the α and β parameters, the critical buckling temperatures of elliptical FGM plates with variable thicknesses can be found. The methodology for the thermal buckling of plates is applied here for the FGM plates. The critical temperature results under the uniform temperature rise for the simply supported and the clamped elliptical FGM plates with variable thicknesses are presented in the tabular form. Tables from Table 5.16 to Table 5.21 give the critical temperature results for the fully simly supported case whereas tables from Table 5.22 to Table 5.27 give the critical temperature results for the fully clamped case.

Table 5.16. Critical buckling temperatures for simply supported elliptical FGM plates, (α=1, β=0)

	n								
	Ceramic	0,1	0,3	0,5	1	2	5	15	Metal
a/b	**Tcr (ºC)**								
1	14,54	12,20	9,78	8,54	7,08	6,05	5,28	4,89	4,68
1,11	16,34	13,71	10,99	9,59	7,95	6,79	5,93	5,49	5,26
1,25	19,07	16,00	12,83	11,20	9,29	7,93	6,92	6,42	6,14
1,43	23,37	19,61	15,72	13,73	11,38	9,71	8,48	7,86	7,52
1,67	30,35	25,47	20,42	17,83	14,78	12,62	11,01	10,21	9,77
2	42,29	35,48	28,45	24,84	20,59	17,58	15,34	14,22	13,61
2,5	64,33	53,97	43,27	37,78	31,32	26,74	23,33	21,64	20,7
3,33	110,8	92,96	74,54	65,07	53,94	46,06	40,19	37,27	35,65
5	239,32	200,79	161	140,55	116,51	99,49	86,81	80,5	77
10	918,62	770,72	617,98	539,5	447,22	381,9	333,22	308,99	295,55

Table 5.17. Critical buckling temperatures for simply supported elliptical FGM plates, (α=1, β=0,2)

	n								
	Ceramic	0,1	0,3	0,5	1	2	5	15	Metal
a/b	**Tcr (ºC)**								
1	19	15,95	12,78	11,16	9,25	7,90	6,89	6,39	6,11
1,11	21,34	17,91	14,36	12,53	10,39	8,87	7,74	7,18	6,87
1,25	24,93	20,92	16,77	14,64	12,14	10,36	9,04	8,39	8,02
1,43	30,55	25,63	20,55	17,94	14,87	12,70	11,08	10,28	9,83
1,67	39,72	33,32	26,72	23,33	19,34	16,51	14,41	13,36	12,78
2	55,43	46,51	37,29	32,55	26,99	23,04	20,11	18,64	17,83
2,5	84,55	70,94	56,88	49,66	41,16	35,15	30,67	28,44	27,2
3,33	146,26	122,71	98,39	85,90	71,20	60,80	53,07	49,20	47,06
5	317,47	266,36	213,57	186,45	154,56	131,98	115,16	106,79	102,14
10	1224,13	1027,05	823,51	718,94	595,96	508,91	444,05	411,75	393,85

Table 5.18. Critical buckling temperatures for simply supported elliptical FGM plates, (α=1, β=0,4)

	n								
	Ceramic	0,1	0,3	0,5	1	2	5	15	Metal
a/b	**Tcr (ºC)**								
1	25,74	21,59	17,31	15,11	12,53	10,70	9,34	8,66	8,28
1,11	28,91	24,26	19,45	16,98	14,08	12,02	10,49	9,73	9,3
1,25	33,77	28,34	22,72	19,84	16,44	14,04	12,25	11,36	10,87
1,43	41,41	34,75	27,86	24,32	20,16	17,22	15,02	13,93	13,32
1,67	53,89	45,21	36,25	31,65	26,23	22,40	19,55	18,13	17,34
2	75,33	63,20	50,68	44,24	36,67	31,32	27,32	25,34	24,24
2,5	115,23	96,68	77,52	67,67	56,10	47,90	41,80	38,76	37,07
3,33	216	167,94	134,66	117,56	97,45	83,21	72,61	67,33	64,4
5	436,7	366,39	293,78	256,48	212,6	181,55	158,41	146,89	140,5
10	1691,61	1419,27	1138	993,49	823,55	703,26	613,62	569	544,26

Table 5.19. Critical buckling temperatures for simply supported elliptical FGM plates, (α=1, β=0,6)

	n								
	Ceramic	0,1	0,3	0,5	1	2	5	15	Metal
a/b	**Tcr (ºC)**								
1	36,51	30,63	24,56	21,44	17,58	15,18	13,24	12,28	11,75
1,11	41,03	34,42	27,60	24,09	19,97	17,06	14,88	13,80	13,2
1,25	47,92	40,21	32,24	28,11	23,33	19,92	17,38	16,12	15,42
1,43	58,79	49,33	39,55	34,53	28,62	24,44	21,33	19,77	18,92
1,67	76,56	64,23	51,50	44,96	37,27	31,83	27,77	25,75	24,63
2	107,2	89,94	72,11	62,96	52,19	44,56	38,89	36,06	34,49
2,5	164,41	137,94	110,61	96,56	80,04	68,35	59,64	55,30	52,9
3,33	286,82	240,65	192,95	168,45	139,64	119,24	104,04	96,48	92,28
5	629,05	527,78	423,18	369,44	306,25	261,52	228,19	211,59	202,39
10	2448,04	2053,91	1646,86	1437,74	1191,81	1017,73	888,01	823,43	787,63

Table 5.20. Critical buckling temperatures for simply supported elliptical FGM plates, (α=1, β=0,8)

	n								
	Ceramic	0,1	0,3	0,5	1	2	5	15	Metal
a/b	Tcr (ºC)								
1	55,02	46,16	37,02	32,32	26,79	22,87	19,96	18,51	17,7
1,11	61,82	51,87	41,59	36,31	30,10	25,70	22,43	20,79	19,89
1,25	72,24	60,61	48,60	42,43	35,17	30,03	26,21	24,30	23,24
1,43	88,66	74,39	59,64	52,07	43,16	36,86	32,16	29,82	28,53
1,67	115,55	96,95	77,73	67,86	56,25	48,04	41,91	38,87	37,18
2	162,03	135,94	109,00	95,16	78,88	67,36	58,78	54,50	52,13
2,5	249,19	209,07	167,64	145,35	121,32	103,60	90,39	83,82	80,17
3,33	436,59	366,30	293,71	256,41	212,55	181,50	158,37	146,85	140,47
5	962,62	807,64	647,58	565,35	468,64	400,19	349,19	323,79	309,71
10	3764,03	3158,03	2532,17	2210,62	1832,49	1564,82	1365,38	1266,08	1211,04

Table 5.21. Critical buckling temperatures for simply supported elliptical FGM plates, (α=1, β=1)

	n								
	Ceramic	0,1	0,3	0,5	1	2	5	15	Metal
a/b	Tcr (ºC)								
1	90,09	75,59	60,61	52,91	43,86	37,45	32,68	30,30	28,98
1,11	101,24	84,94	68,11	59,46	49,29	42,09	36,72	34,05	32,57
1,25	118,32	99,27	79,60	69,49	57,60	49,19	42,92	39,80	38,07
1,43	145,27	121,88	97,73	85,32	70,72	60,39	52,70	48,86	46,74
1,67	189,47	158,97	127,46	111,28	92,24	78,77	68,73	63,73	60,96
2	266,07	223,23	179,00	156,26	129,53	110,61	96,51	89,50	85,6
2,5	410,26	344,21	276,00	240,95	199,73	170,56	148,82	138,00	132
3,33	721,86	605,65	485,62	423,95	351,43	310,00	261,85	242,81	232,25
5	1600,32	1342,67	1076,58	939,87	779,1	665,3	580,51	538,29	514,89
10	6288,52	5276,08	4230,46	3693,26	3061,52	2614,33	2281,13	2115,23	2023,26

Table 5.22. Critical buckling temperatures for clamped elliptical FGM plates (α=1, β=0)

	n								
	Ceramic	0,1	0,3	0,5	1	2	5	15	Metal
a/b	**Tcr (ºC)**								
1	50,87	42,68	34,22	29,88	24,77	21,15	18,45	17,11	16,37
1,11	57,1	47,91	38,41	33,54	27,80	23,74	20,71	19,21	18,37
1,25	66,48	55,77	44,72	39,04	32,36	27,64	24,11	22,36	21,39
1,43	81,04	67,99	54,52	47,59	39,45	33,69	29,40	27,26	26,07
1,67	104,53	87,70	70,32	61,39	50,89	43,46	37,92	35,16	33,63
2	144,65	121,36	97,31	84,95	70,42	60,13	52,47	48,65	46,54
2,5	219,57	184,22	147,71	128,95	106,89	91,28	79,65	73,85	70,64
3,33	383,36	321,64	257,90	225,15	186,63	159,37	139,06	128,95	123,34
5	862,38	723,54	580,15	506,48	419,84	358,52	312,82	290,07	277,46
10	3505,81	2941,38	2358,46	2058,97	1706,78	1457,47	1271,72	1179,23	1127,96

Table 5.23. Critical buckling temperatures for clamped elliptical FGM plates (α=1, β=0,2)

	n								
	Ceramic	0,1	0,3	0,5	1	2	5	15	Metal
a/b	**Tcr (ºC)**								
1	40,7	34,15	27,38	23,91	19,82	16,92	14,77	13,69	13,1
1,11	45,69	38,33	30,73	26,83	22,24	18,99	16,57	15,37	14,7
1,25	53,17	44,61	35,77	31,23	25,89	22,10	19,29	17,88	17,11
1,43	64,78	54,35	43,58	38,04	31,54	26,93	23,50	21,79	20,84
1,67	83,5	70,05	56,17	49,04	40,65	34,71	30,29	28,09	26,86
2	115,42	96,84	77,65	67,79	56,19	47,98	41,87	38,82	37,13
2,5	175,04	146,86	117,76	102,80	85,22	72,77	63,50	58,88	56,32
3,33	305,6	256,40	205,58	179,48	148,78	127,05	110,85	102,79	98,32
5	687,97	577,21	462,81	404,04	334,93	286,01	249,56	231,41	221,35
10	2797,08	2346,76	1881,67	1642,73	1361,74	1162,83	1014,63	940,84	899,93

Table 5.24. Critical buckling temperatures for clamped elliptical FGM plates (α=1, β=0,4)

	n								
	Ceramic	0,1	0,3	0,5	1	2	5	15	Metal
a/b	**Tcr (ºC)**								
1	33,31	27,94	22,41	19,56	16,21	13,85	12,08	11,20	10,72
1,11	37,38	31,36	25,15	21,95	18,20	15,54	13,56	12,57	12,03
1,25	43,49	36,49	29,26	25,54	21,17	18,08	15,78	14,63	13,99
1,43	52,96	44,44	35,63	31,10	25,78	22,02	19,21	17,81	17,04
1,67	68,21	57,23	45,89	40,06	33,21	28,36	24,74	22,94	21,94
2	94,2	79,03	63,37	55,32	45,86	39,16	34,17	31,68	30,31
2,5	142,75	119,77	96,03	83,84	69,50	59,34	51,78	48,02	45,93
3,33	249,25	209,12	167,67	146,38	121,34	103,62	90,41	83,84	80,19
5	561,53	471,12	377,76	329,79	273,38	233,44	203,69	188,88	180,67
10	2283,15	1915,57	1535,94	1340,9	1111,53	949,17	828,2	767,97	734,58

Table 5.25. Critical buckling temperatures for clamped elliptical FGM plates (α=1, β=0,6)

	n								
	Ceramic	0,1	0,3	0,5	1	2	5	15	Metal
a/b	**Tcr (ºC)**								
1	27,75	23,29	18,67	16,30	13,51	11,54	10,07	9,34	8,93
1,11	31,15	26,15	20,96	18,29	15,16	12,95	11,30	10,48	10,02
1,25	36,23	30,40	24,38	21,28	17,64	15,06	13,14	12,19	11,66
1,43	44,11	37,01	29,67	25,91	21,47	18,34	16,00	14,84	14,19
1,67	56,76	47,63	38,19	33,34	27,64	23,60	20,59	19,09	18,26
2	78,33	65,72	52,69	46,00	38,13	32,56	28,41	26,35	25,2
2,5	118,64	99,54	79,81	69,68	57,76	49,32	43,04	39,91	38,17
3,33	207,21	173,85	139,39	121,69	100,88	86,14	75,06	69,70	66,67
5	510,46	428,27	343,4	299,79	248,51	212,21	185,16	171,7	164,23
10	1899,39	1593,6	1277,77	1115,52	924,70	789,64	689	638,89	611,11

Table 5.26. Critical buckling temperatures for clamped elliptical FGM plates (α=1, β=0,8)

	n								
	Ceramic	0,1	0,3	0,5	1	2	5	15	Metal
a/b	Tcr (ºC)								
1	23,5	19,72	15,81	13,80	11,44	9,77	8,52	7,90	7,56
1,11	26,37	22,12	17,74	15,49	12,84	10,96	9,56	8,87	8,48
1,25	30,67	25,73	20,63	18,01	14,93	12,75	11,13	10,32	9,87
1,43	37,31	31,30	25,10	21,91	18,16	15,51	13,53	12,55	12
1,67	47,99	40,26	32,28	28,18	23,36	19,95	17,41	16,14	15,44
2	66,18	55,53	44,52	38,87	32,22	27,51	24,01	22,26	21,29
2,5	100,2	84,07	67,41	58,85	48,78	41,66	36,35	33,70	32,24
3,33	175,06	146,88	117,77	102,81	85,23	72,78	63,50	58,88	56,32
5	394,92	331,34	265,68	231,94	192,27	164,18	143,26	132,84	127,06
10	1605,7	1347,19	1080,2	943,03	781,72	667,54	582,46	540,1	516,62

Table 5.27. Critical buckling temperatures for clamped elliptical FGM plates (α=1, β=1)

	n								
	Ceramic	0,1	0,3	0,5	1	2	5	15	Metal
a/b	Tcr (ºC)								
1	20,17	16,92	13,57	11,84	9,82	8,38	7,31	6,78	6,49
1,11	22,63	18,98	15,22	13,29	11,01	9,41	8,21	7,61	7,28
1,25	26,31	22,07	17,70	15,45	12,81	10,94	9,54	8,85	8,46
1,43	31,99	26,84	21,52	18,79	15,57	13,30	11,60	10,76	10,29
1,67	41,13	34,51	27,67	24,15	20,02	17,10	14,92	13,83	13,23
2	56,68	47,55	38,13	33,29	27,59	23,56	20,56	19,06	18,23
2,5	85,79	71,98	57,72	50,39	41,77	35,67	31,12	28,86	27,6
3,33	149,96	125,81	100,88	88,07	73,00	62,34	54,40	50,44	48,25
5	338,5	284	227,72	198,8	164,79	140,72	122,79	113,86	108,91
10	1376,18	1154,62	925,79	808,23	669,98	572,12	499,2	462,9	442,77

As it is seen from the tables, again, a wide range of a/b ratio is considered. According to the results obtained in each case, the variation of the critical temperatures vs. dimensionless geometrical parameters a/b are plotted for each case. Seven arbitrary values of the power law index, *n*= 0.1, 0.3, 0.5, 1, 2, 5, 15 are taken in the calculations. As it is mentioned before, the value of *n*=0 represents a fully ceramic plate and the variation of the composition of ceramics and metal is linear for *n*=1. In the figures, critical buckling temperatures of the simply supported and clamped elliptical FGM plates with variable thicknesses are given. Each figure is plotted according to the variation of the α and β

parameters. Figures from Figure 5.1 to Figure 5.6 represent the critical buckling temperatures of the simply supported elliptical FGM plates in accordance with the variable thicknesses.

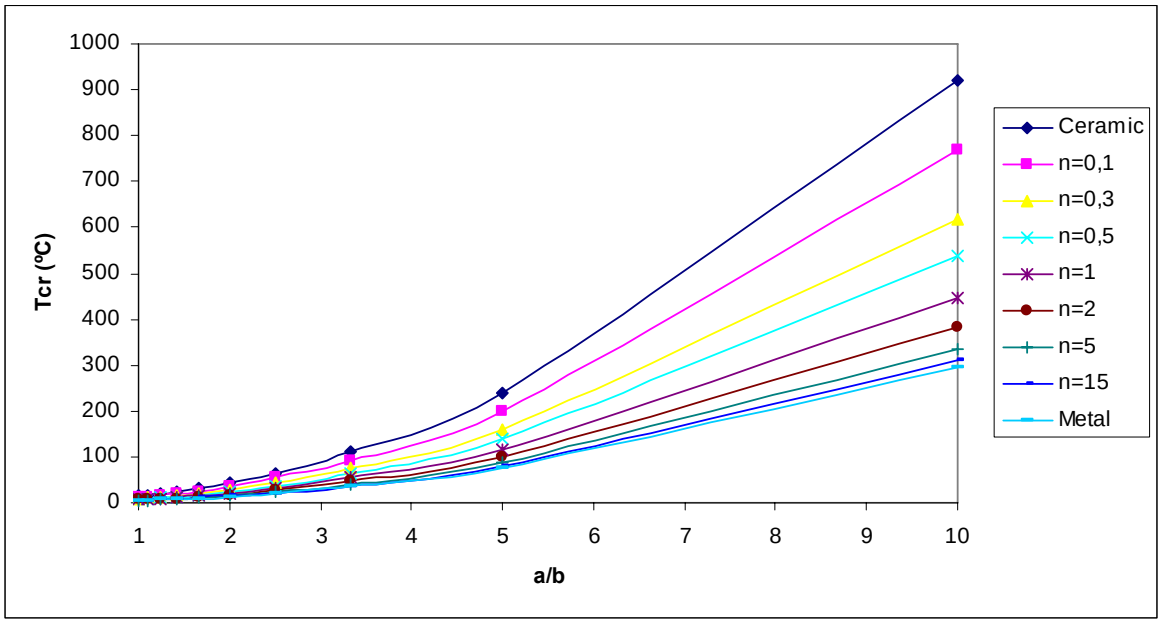

Figure 5.1. Critical buckling temperatures of simply supported elliptical FGM plates under linear temperature change across the thickness (α=1, β=0) vs a/b

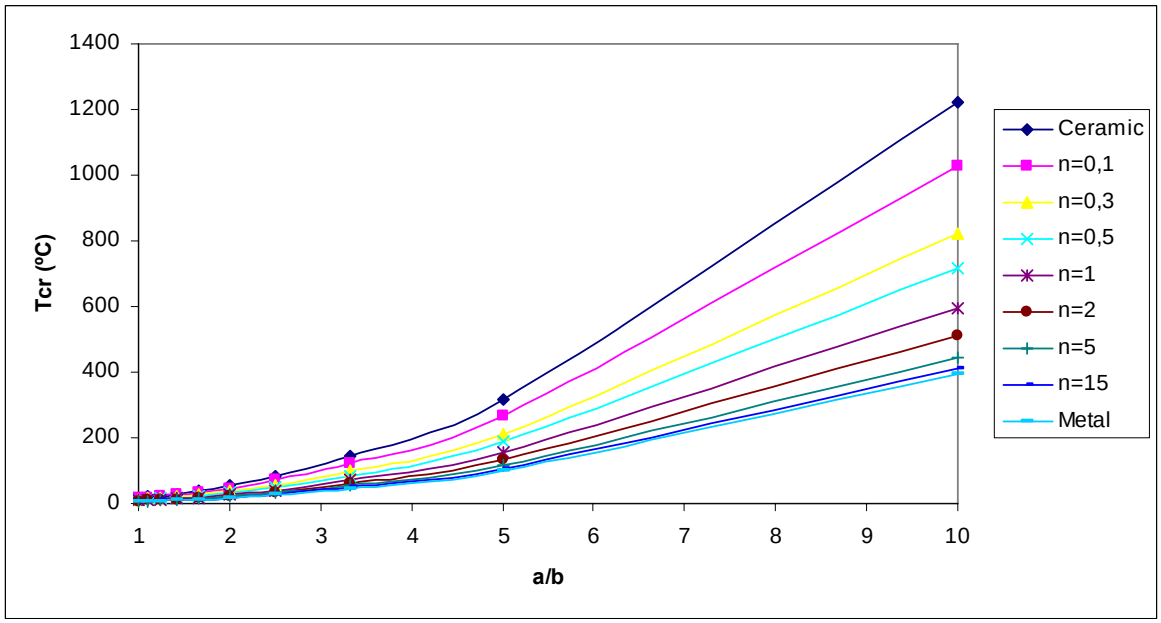

Figure 5.2. Critical buckling temperatures of simply supported elliptical FGM plates under linear temperature change across the thickness (α=1, β=0,2) vs a/b

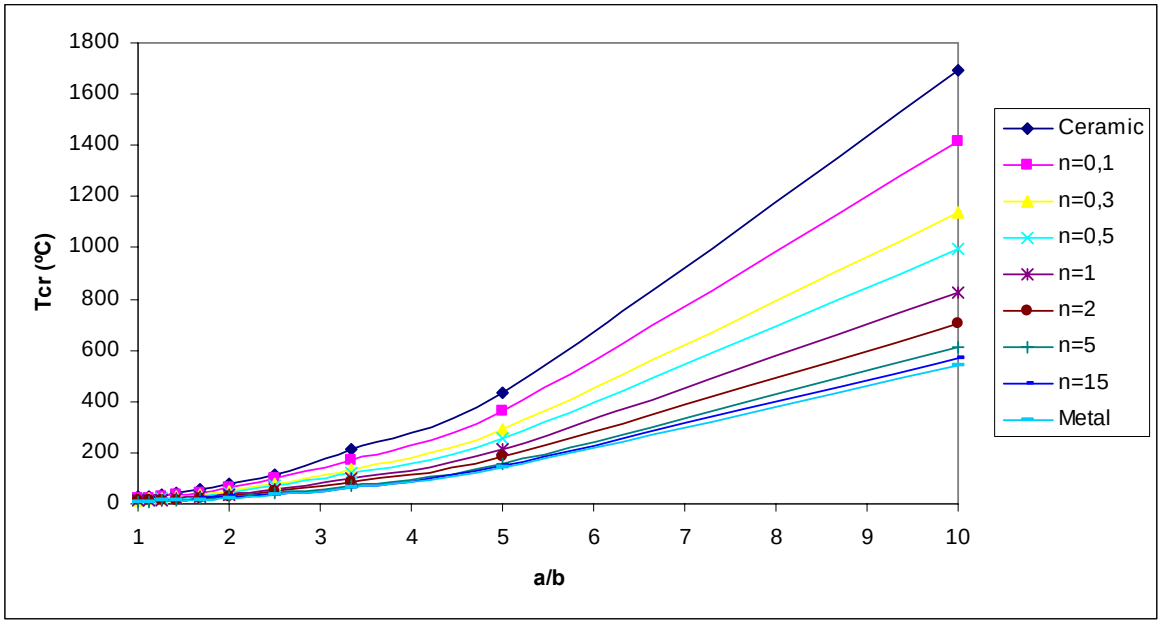

Figure 5.3. Critical buckling temperatures of simply supported elliptical FGM plates under linear temperature change across the thickness (α=1, β=0,4) vs a/b

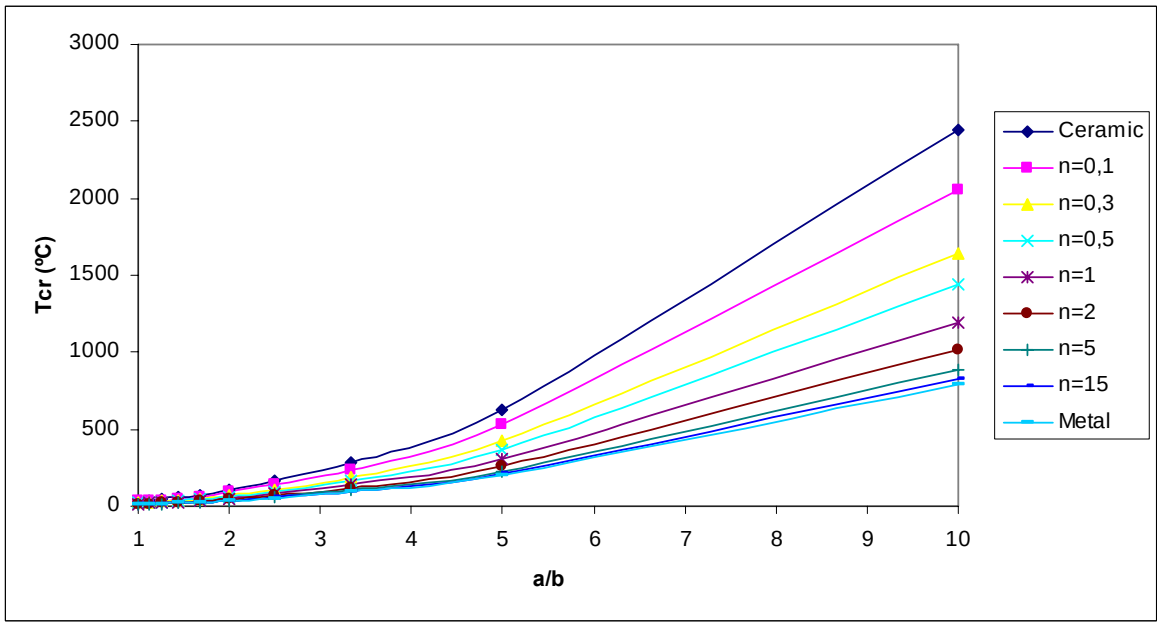

Figure 5.4. Critical buckling temperatures of simply supported elliptical FGM plates under linear temperature change across the thickness (α=1, β=0,6) vs a/b

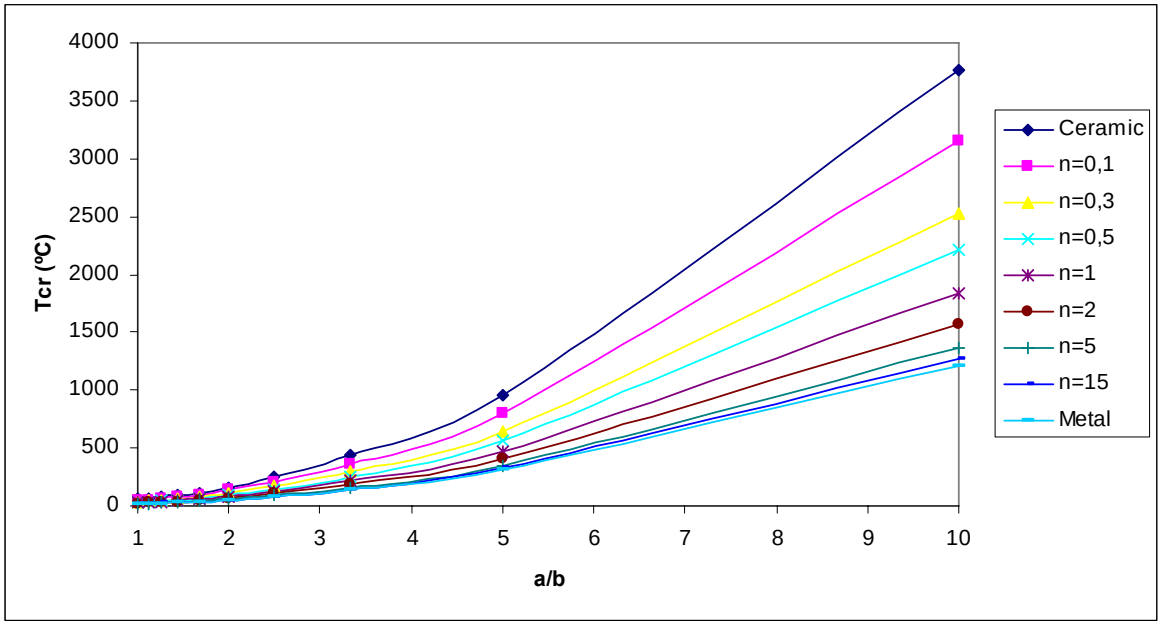

Figure 5.5. Critical buckling temperatures of simply supported elliptical FGM plates under linear temperature change across the thickness (α=1, β=0,8) vs a/b

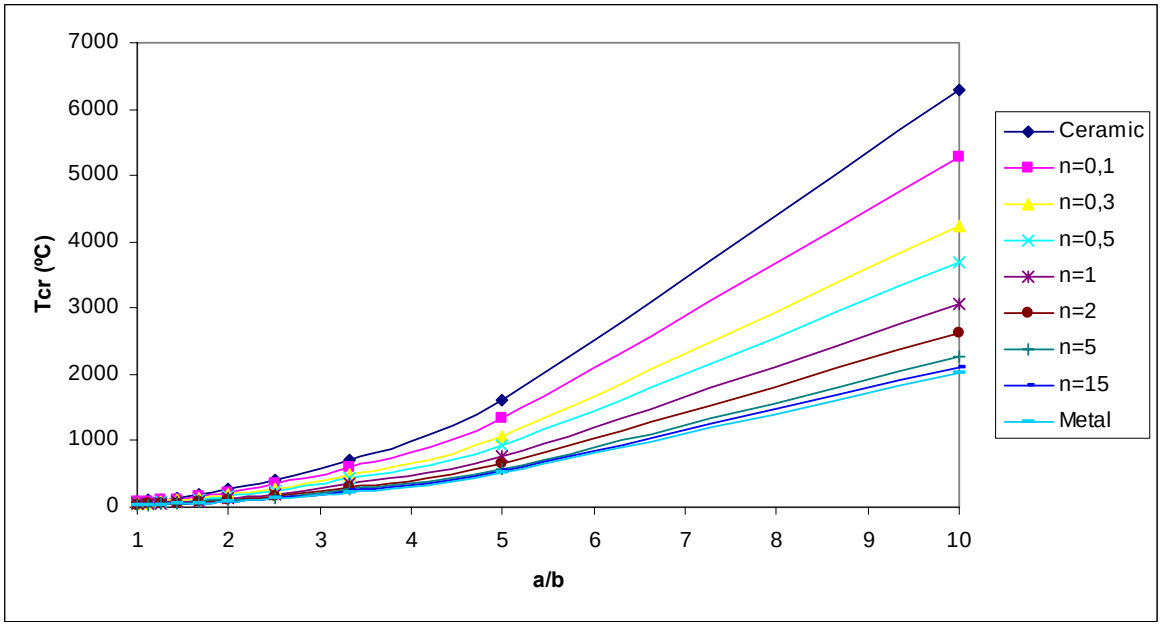

Figure 5.6. Critical buckling temperatures of simply supported elliptical FGM plates under linear temperature change across the thickness (α=1, β=1) vs a/b

Here, figures from Figure 5.7 to Figure 5.12 represent the critical buckling temperatures of the clamped elliptical FGM plates in accordance with the different aspect ratios, a/b, and variable thicknesses.

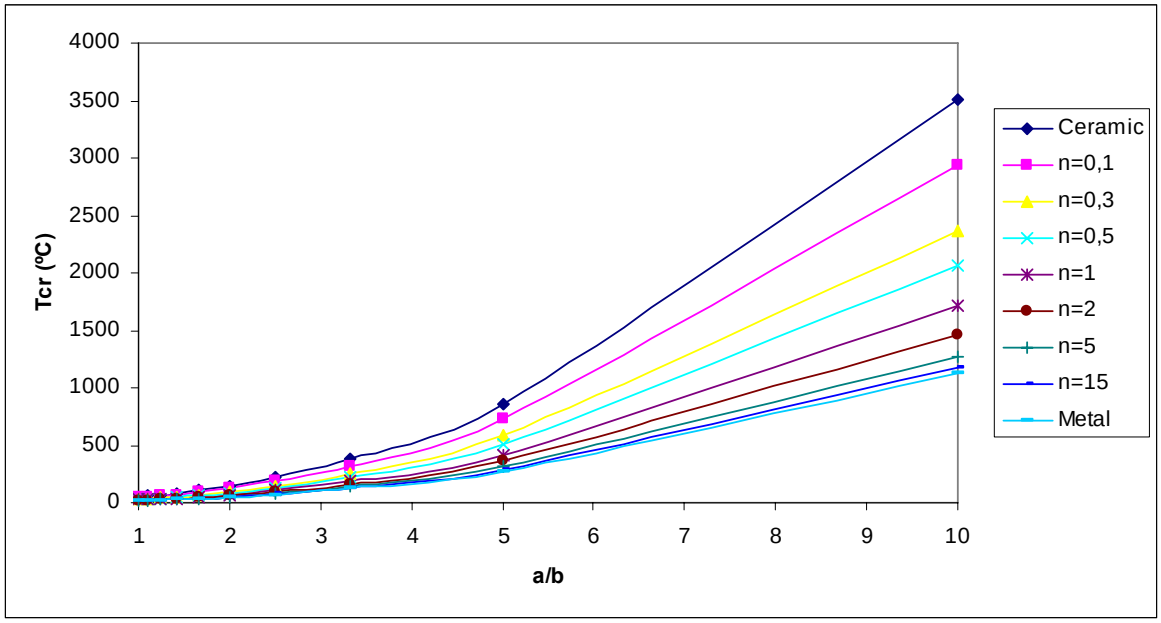

Figure 5.7. Critical buckling temperatures of clamped elliptical FGM plates under linear temperature change across the thickness (α=1, β=0) vs a/b

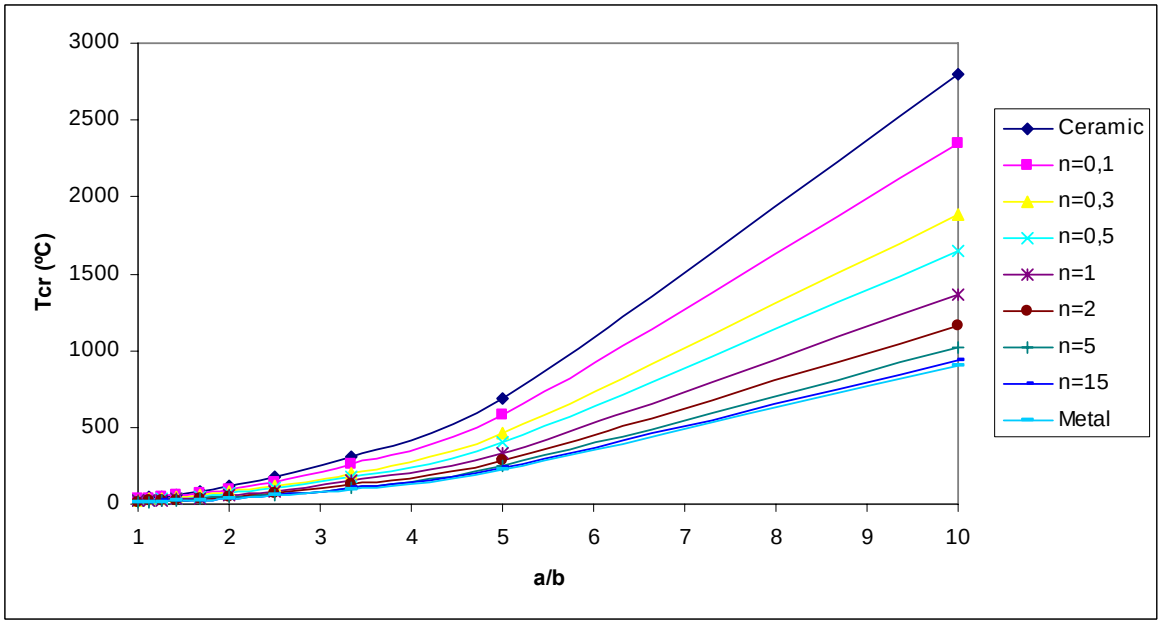

Figure 5.8. Critical buckling temperatures of clamped elliptical FGM plates under linear temperature change across the thickness (α=1, β=0,2) vs a/b

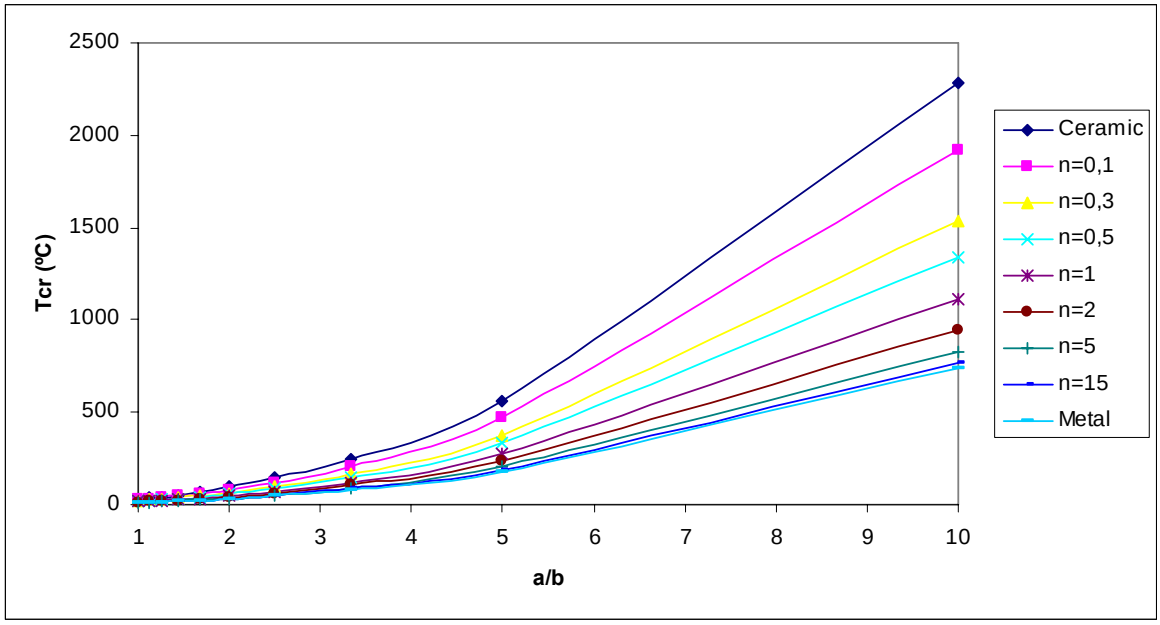

Figure 5.9. Critical buckling temperatures of clamped elliptical FGM plates under linear temperature change across the thickness (α=1, β=0,4) vs a/b

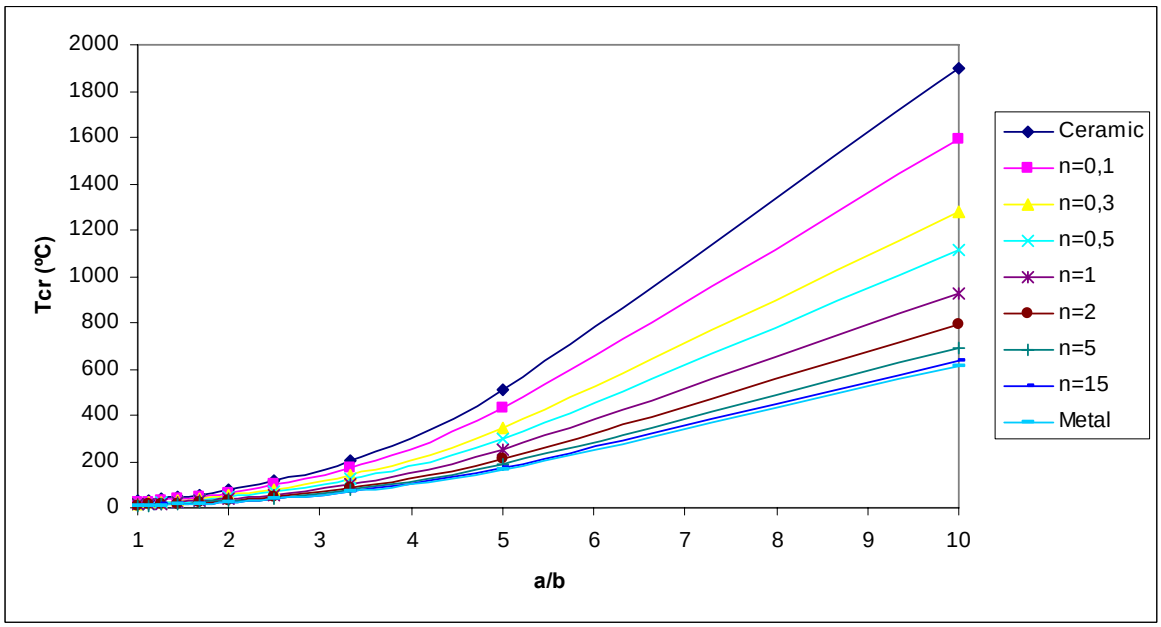

Figure 5.10. Critical buckling temperatures of clamped elliptical FGM plates under linear temperature change across the thickness (α=1, β=0,6) vs a/b

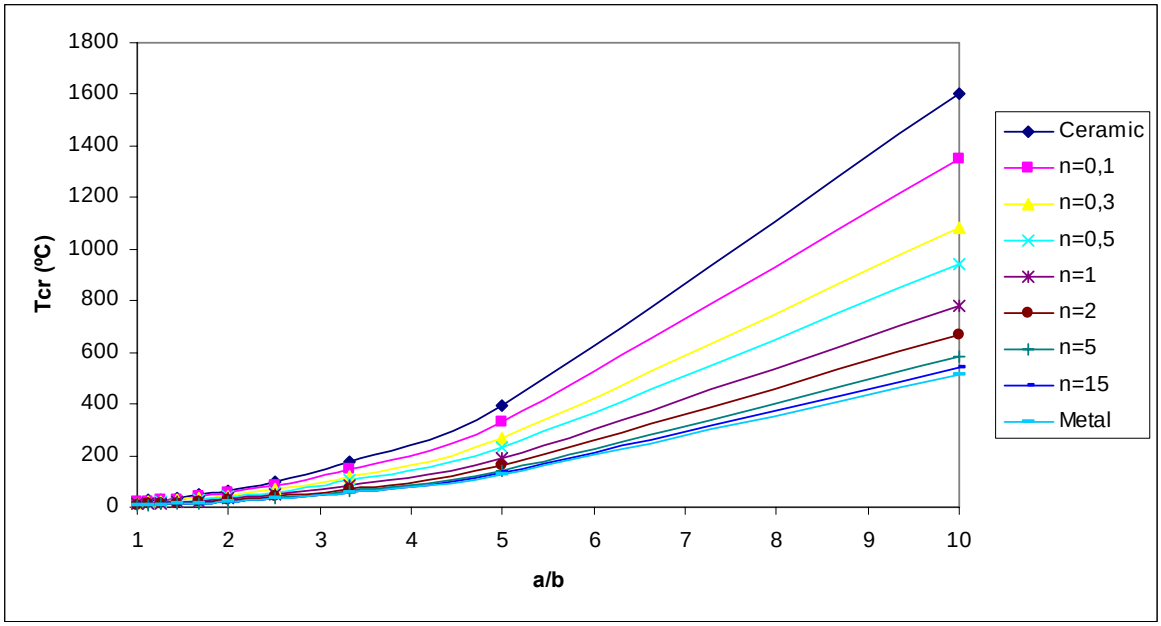

Figure 5.11. Critical buckling temperatures of clamped elliptical FGM plates under linear temperature change across the thickness (α=1, β=0,8) vs a/b

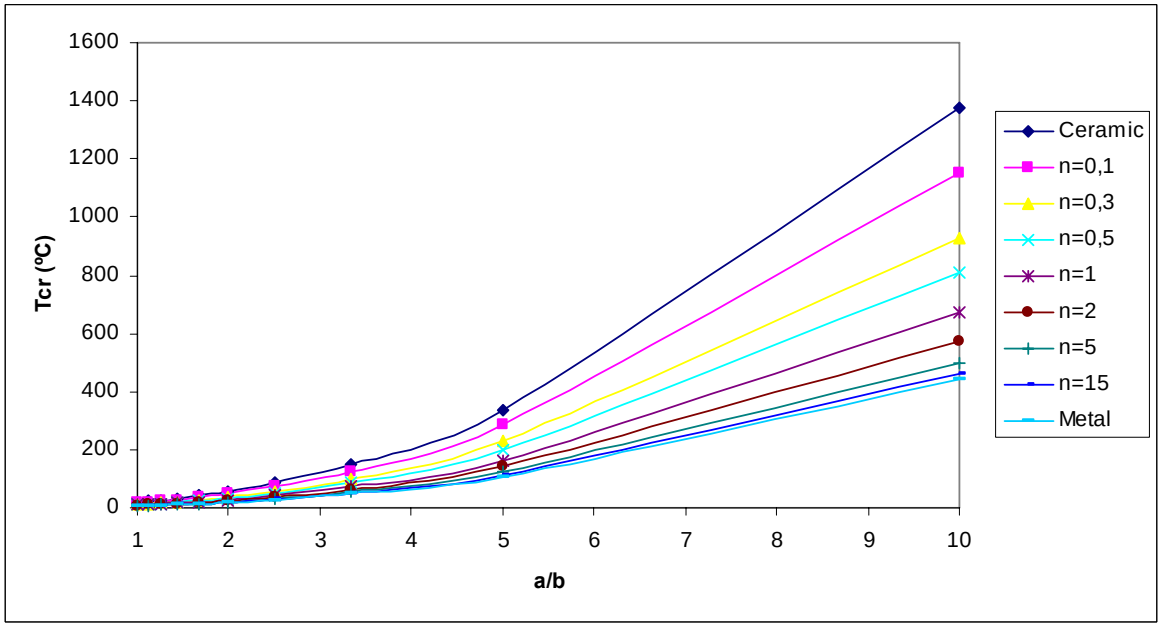

Figure 5.12. Critical buckling temperatures of clamped elliptical FGM plates under linear temperature change across the thickness (α=1, β=1) vs a/b

5.3. Thermal Buckling Problem of Rectangular FGM Plates with Variable Thickness

In the problem of thermal buckling of rectangular FGM plates with variable thickness, two different rectangular plates with different edge boundary condition combinations are considered. In the first case, three edges clamped, one edge simply supported rectangular FGM plate with variable thickness is studied whereas in the second case two edges clamped, two edges simply supported rectangular FGM plate with variable thickness is analyzed.

5.3.1. Basic Assumptions and Equations

In this problem, thermal buckling analyses are done for a rectangular FGM plate whose three edges are clamped and one edge is simply supported and for the one whose two edges are simply supported and two edges are clamped. The thicknesses of the plates vary parabolically according to the formulations given in Section 5.1. The configuration of the studied plates is given in Figure 5.13. Here, CL represents the clamped edges and SS represents the simply supported edges.

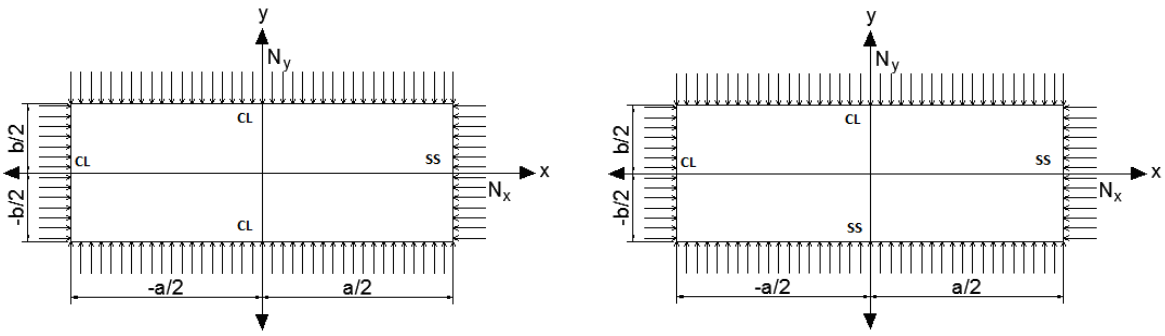

Figure 5.13. Configuration of the analyzed rectangular FGM plates

For the given rectangular plates, the boundary shape equation can be represented by Eq. (5.11).

$$\phi(x,y) = (x - a/2)^{\Omega}(x + a/2)^{\Omega}(y - b/2)^{\Omega}(y + b/2)^{\Omega} \tag{5.11}$$

For the edges whose external boundary condition is simply supported Ω=1 in the boundary shape equation whereas for the clamped edges Ω=2. According to this, the displacement functions for the three edges clamped, one edge simply supported rectangular plate and the two edges simply supported, two edges clamped rectangular plate are represented by Eq. (5.12) and Eq. (5.13), respectively.

$$w(x,y)=\sum_{i}^{r}\sum_{j}^{r}\alpha_{ij}(x-a/2)(x+a/2)^2(y-b/2)^2(y+b/2)^2x^iy^j \tag{5.12}$$

$$w(x,y)=\sum_{i}^{r}\sum_{j}^{r}\alpha_{ij}(x-a/2)(x+a/2)^2(y-b/2)^2(y+b/2)x^iy^j \tag{5.13}$$

where, $i+j\le r$, so r is the degree of the polynomial trial function and α_{ij} are the coefficients to be determined. In order to apply the Rayleigh-Ritz method, displacement functions given in Eq. (5.12) and Eq. (5.13), at the length of r=6 is selected. Since the thicknesses are not uniform, the parabolic variation of the plate thicknesses is again considered with respect to the Eq. (5.2), (5.4) and (5.6). Due to the plate thickness assumptions where the thickness in the middle of the plate is less than the one at the edges the configuration of the analyzed rectangular plates becomes as it is shown in Figure 5.14.

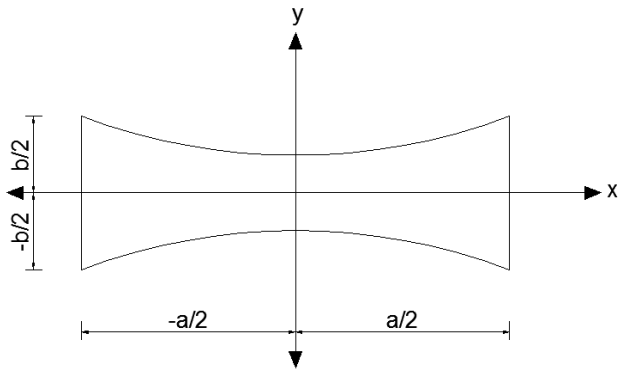

Figure 5.14. Configuration of the analyzed rectangular FGM plates with parabolically varying thickness

Therefore, the total energy equation for the buckling problem of the given rectangular plates can be recalled from Eq. (5.8). According to this, in order to obtain the

critical buckling load factors, Rayleigh-Ritz method is conducted by considering the thickness variation.

As stated in Section 4.1.1, for the solution of FGM plates, effective material properties are obtained due to the variation of the power law index, *n*. As a result of the analyses, thermal buckling load factor, λ, changes due to the change in the material properties and the variation of the α and β parameters. According to this, λ_{eff} is calculated for the different values of a/b ratios and used in the calculation of the critical buckling temperature of the rectangular FGM plates with variable thicknesses. By the help of the obtained buckling load factors, critical buckling temperatures are calculated by using Eq. (3.4) and Eq. (3.5).

5.3.2. Numerical Results

In order to obtain the critical buckling temperatures of the given rectangular FGM plates with a parabolic variation of their plate thicknesses, first of all the buckling parameters are obtained. The buckling parameters depending on the α and β parameters are calculated by Rayleigh-Ritz method for the three edges clamped, one edge simply supported rectangular plate and for the two edges simply supported and two edges clamped rectangular plate for different a/b ratios (1≤a/b≤10). In the analyses, Poisson's ratio is taken to be 0.3. The critical buckling parameters for the three edges clamped, one edge simply supported rectangular plate and for the two edges simply supported and two edges clamped rectangular plate are presented in Table 5.28 and Table 5.29, respectively.

Table 5.28. Buckling parameters for the three edges clamped, one edge simply supported rectangular plate with variable thickness

		a/b									
		1	1,11	1,25	1,43	1,67	2	2,5	3,33	5	10
α	**β**	**λ=Na²/D**									
1,0	0,0	43,07	50,53	61,52	78,31	105,24	151,32	238,07	421,79	937,97	3858,30
1,0	0,2	34,93	41,04	50,01	63,69	85,58	122,94	192,88	342,60	771,64	3144,61
1,0	0,4	28,96	34,05	41,53	52,89	71,02	101,81	158,97	281,30	635,28	2579,29
1,0	0,6	24,44	28,77	35,10	44,70	59,94	85,71	133,25	235,33	531,73	2155,80
1,0	0,8	20,96	24,68	30,11	38,33	51,33	73,20	113,41	200,06	452,04	1831,18
1,0	1,0	18,20	21,45	26,17	33,29	44,51	63,31	97,82	172,43	389,58	1577,17

Table 5.29. Buckling parameters for the two edges simply supported, two edges clamped rectangular plate with variable thickness

		a/b									
		1	1,11	1,25	1,43	1,67	2	2,5	3,33	5	10
α	**β**	**λ=Na²/D**									
1,0	0,0	34,03	38,11	44,07	53,11	67,51	92,02	138,04	238,67	527,95	2093,29
1,0	0,2	27,61	30,92	35,73	42,98	54,51	74,08	110,74	190,76	420,27	1659,09
1,0	0,4	22,92	25,66	29,62	35,58	45,01	60,98	90,80	155,72	341,45	1342,93
1,0	0,6	19,39	21,70	25,02	30,01	37,87	51,14	75,84	129,49	282,71	1108,69
1,0	0,8	16,66	18,64	21,48	25,72	32,38	43,58	64,38	109,44	238,00	931,07
1,0	1,0	14,52	16,24	18,70	22,35	28,06	37,65	55,41	93,81	203,30	793,56

After the buckling load factors for each case are achieved in accordance with the α and β parameters, the critical buckling temperatures of the given rectangular FGM plates with variable thicknesses are found. The critical temperature results under the uniform temperature rise for the given boundary condition combinations of the rectangular FGM plates with variable thicknesses are presented in the tabular form. Tables from Table 5.30 to Table 5.35 give the critical temperature results for the three edges clamped, one edge simply supported case.

Table 5.30. Critical buckling temperatures for the three edges clamped, one edge simply supported rectangular FGM plate, (α=1, β=0)

	n								
	Ceramic	0,1	0,3	0,5	1	2	5	15	Metal
a/b	**Tcr (ºC)**								
1	37,31	31,30	25,10	21,91	18,16	15,51	13,53	12,55	12,00
1,11	43,77	36,72	29,45	25,71	21,31	18,20	15,88	14,72	14,08
1,25	53,29	44,71	35,85	31,30	25,94	22,15	19,33	17,92	17,15
1,43	67,84	56,91	45,63	39,84	33,02	28,20	24,61	22,82	21,82
1,67	91,16	76,49	61,33	53,54	44,38	37,90	33,07	30,66	29,33
2	131,08	109,98	88,18	76,98	63,81	54,59	47,55	44,09	42,17
2,5	206,23	173,03	138,73	121,12	100,40	85,73	74,81	69,37	66,35
3,33	365,38	306,55	245,80	214,59	177,88	151,90	132,54	122,90	117,56
5	812,52	681,7	546,6	477,19	395,57	337,79	294,74	273,3	261,42
10	3342,26	2804,16	2248,43	1962,91	1627,15	1389,48	1212,39	1124,21	1075,33

Table 5.31. Critical buckling temperatures for the three edges clamped, one edge simply supported rectangular FGM plate, (α=1, β=0,2)

	n								
	Ceramic	0,1	0,3	0,5	1	2	5	15	Metal
a/b	**Tcr (ºC)**								
1	30,26	25,39	20,35	17,77	14,73	12,58	10,98	10,18	9,73
1,11	35,55	29,83	23,92	20,88	17,31	14,78	12,90	11,96	11,44
1,25	43,32	36,35	29,14	25,44	21,09	18,01	15,71	14,57	13,94
1,43	55,17	46,29	37,11	32,40	26,86	22,94	20,01	18,56	17,75
1,67	74,13	62,20	49,87	43,54	36,09	30,82	26,89	24,94	23,85
2	106,5	89,35	71,64	62,55	51,85	44,27	38,63	35,82	34,26
2,5	167,08	140,18	112,40	98,13	81,34	69,46	60,61	56,20	53,76
3,33	296,78	249,00	199,65	174,30	144,48	123,38	107,65	99,82	95,48
5	668,43	560,82	449,67	392,57	325,42	277,89	242,47	224,84	215,06
10	2724,02	2285,46	1832,52	1599,82	1326,17	1132,46	988,12	916,26	876,42

Table 5.32. Critical buckling temperatures for the three edges clamped, one edge simply supported rectangular FGM plate, (α=1, β=0,4)

	n								
	Ceramic	0,1	0,3	0,5	1	2	5	15	Metal
a/b	**Tcr (ºC)**								
1	25,09	21,05	16,88	14,73	12,21	10,43	9,10	8,44	8,07
1,11	29,5	24,75	19,84	17,32	14,36	12,26	10,70	9,92	9,49
1,25	35,97	30,18	24,20	21,13	17,51	14,96	13,05	12,10	11,57
1,43	45,82	38,44	30,82	26,91	22,30	19,05	16,62	15,41	14,74
1,67	61,52	51,62	41,39	36,13	29,95	25,58	22,32	20,69	19,79
2	88,19	73,99	59,33	51,80	42,94	36,66	31,99	29,66	28,37
2,5	137,71	115,54	92,64	80,88	67,04	57,25	49,95	46,32	44,31
3,33	243,68	204,44	163,93	143,11	118,63	101,30	88,39	81,96	78,4
5	550,31	461,71	370,21	323,2	267,91	228,78	199,62	185,1	177,06
10	2234,31	1874,59	1503,08	1312,22	1087,76	928,87	810,49	751,54	718,87

Table 5.33. Critical buckling temperatures for the three edges clamped, one edge simply supported rectangular FGM plate, (α=1, β=0,6)

	n								
	Ceramic	0,1	0,3	0,5	1	2	5	15	Metal
a/b	**Tcr (ºC)**								
1	21,17	17,76	14,24	12,43	10,31	8,80	7,68	7,12	6,81
1,11	24,92	20,91	16,77	14,64	12,13	10,36	9,04	8,38	8,02
1,25	30,4	25,51	20,45	17,86	14,80	12,64	11,03	10,23	9,78
1,43	38,72	32,49	26,05	22,74	18,85	16,10	14,05	13,02	12,46
1,67	51,92	43,56	34,93	30,49	25,28	21,59	18,83	17,46	16,71
2	74,25	62,29	49,95	43,60	36,15	30,87	26,93	24,97	23,89
2,5	115,43	96,84	77,65	67,79	56,19	47,99	41,87	38,82	37,14
3,33	203,85	171,03	137,14	119,72	99,24	84,75	73,95	68,57	65,59
5	460,61	386,45	309,87	270,52	224,24	191,49	167,08	154,93	148,2
10	1867,46	1566,81	1256,29	1096,76	909,16	776,36	677,41	628,15	600,84

Table 5.34. Critical buckling temperatures for the three edges clamped, one edge simply supported rectangular FGM plate, (α=1, β=0,8)

	n								
	Ceramic	0,1	0,3	0,5	1	2	5	15	Metal
a/b	**Tcr (ºC)**								
1	18,16	15,23	12,21	10,66	8,84	7,55	6,59	6,11	5,84
1,11	21,38	17,94	14,38	12,56	10,41	8,89	7,75	7,19	6,88
1,25	26,08	21,88	17,55	15,32	12,70	10,84	9,46	8,77	8,39
1,43	33,2	27,86	22,34	19,50	16,16	13,80	12,04	11,17	10,68
1,67	44,46	37,31	29,91	26,11	21,65	18,48	16,13	14,96	14,31
2	63,41	53,20	42,66	37,24	30,87	26,36	23,00	21,33	20,4
2,5	98,24	82,42	66,09	57,70	47,83	40,84	35,64	33,04	31,61
3,33	173,3	145,40	116,58	101,78	84,37	72,05	62,86	58,29	55,76
5	391,58	328,54	263,43	229,98	190,64	162,79	142,04	131,71	125,99
10	1586,26	1330,88	1067,12	931,61	772,26	659,46	575,41	533,56	510,36

Table 5.35. Critical buckling temperatures for the three edges clamped, one edge simply supported rectangular FGM plate, (α=1, β=1)

	n								
	Ceramic	0,1	0,3	0,5	1	2	5	15	Metal
a/b	Tcr (°C)								
1	15,77	13,23	10,61	9,26	7,67	6,55	5,72	5,30	5,07
1,11	18,58	15,59	12,50	10,91	9,05	7,72	6,74	6,25	5,98
1,25	22,67	19,02	15,25	13,31	11,04	9,42	8,22	7,62	7,29
1,43	28,84	24,19	19,40	16,94	14,04	11,99	10,46	9,70	9,28
1,67	38,56	32,35	25,94	22,64	18,77	16,03	13,99	12,97	12,4
2	54,84	46,01	36,89	32,21	26,70	22,80	19,89	18,45	17,65
2,5	84,74	71,09	57,00	49,77	41,25	35,23	30,74	28,50	27,26
3,33	149,37	125,32	100,48	87,72	72,72	62,10	54,18	50,24	48,06
5	337,47	283,14	227,03	198,2	164,3	140,3	122,42	113,51	108,58
10	1366,22	1146,27	919,1	802,39	665,14	567,98	495,59	459,55	439,57

According to the critical temperatures obtained in each case, the variation of the critical temperatures vs. aspect ratios is plotted for each case. Each figure is also plotted according to the variation of the α and β parameters. Figures from Figure 5.15 to Figure 5.20 represent the critical buckling temperatures of the three edges clamped, one edge simply supported rectangular FGM plates in accordance with the variable thicknesses.

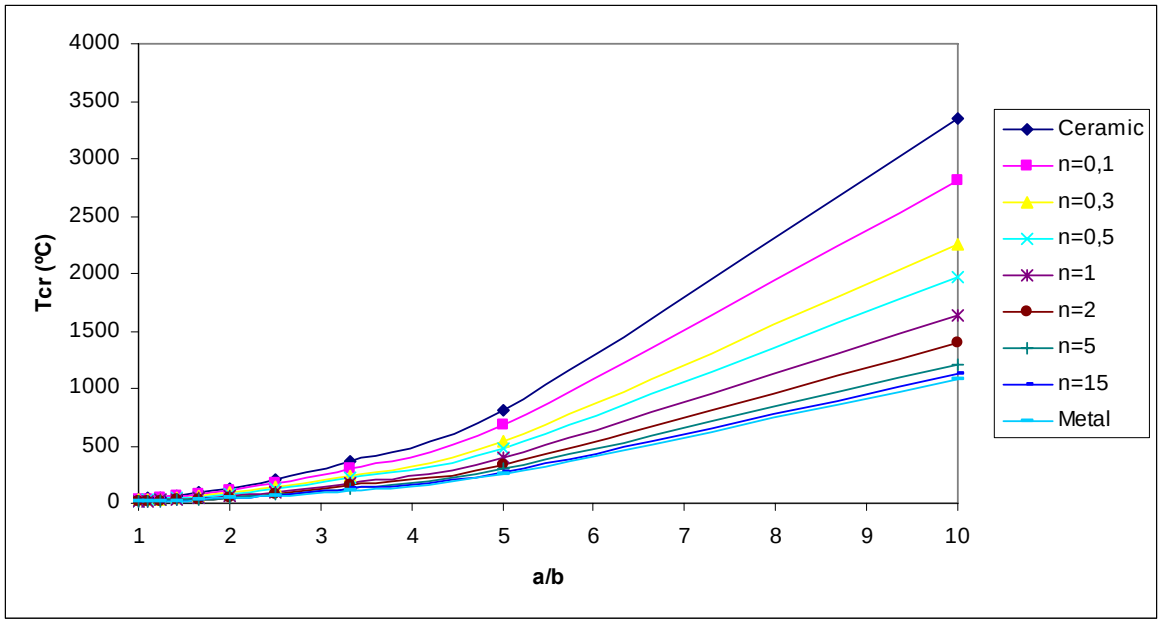

Figure 5.15. Critical buckling temperatures of the three edges clamped, one edge simply supported rectangular FGM plates under linear temperature change across the thickness (α=1, β=0) vs a/b

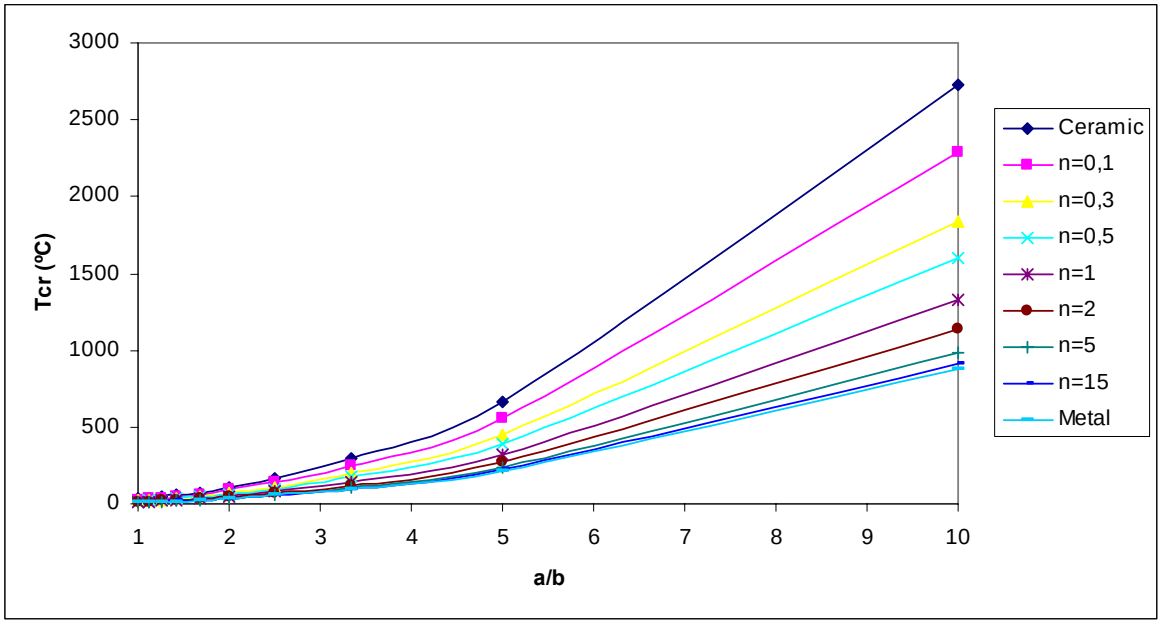

Figure 5.16. Critical buckling temperatures of the three edges clamped, one edge simply supported rectangular FGM plates under linear temperature change across the thickness (α=1, β=0,2) vs a/b

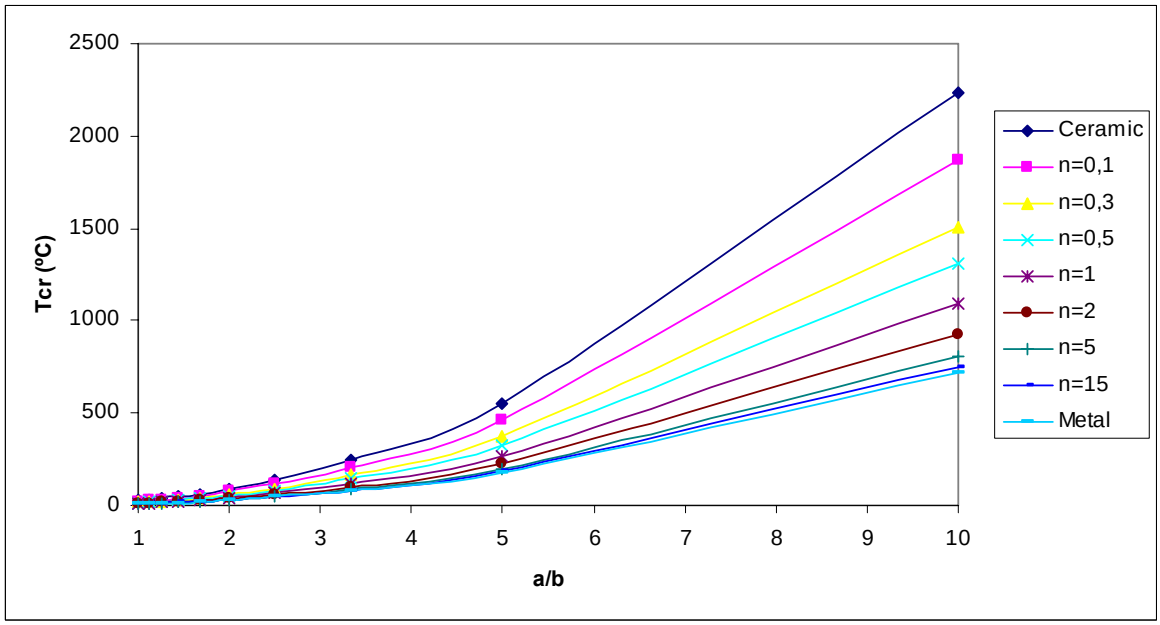

Figure 5.17. Critical buckling temperatures of the three edges clamped, one edge simply supported rectangular FGM plates under linear temperature change across the thickness (α=1, β=0,4) vs a/b

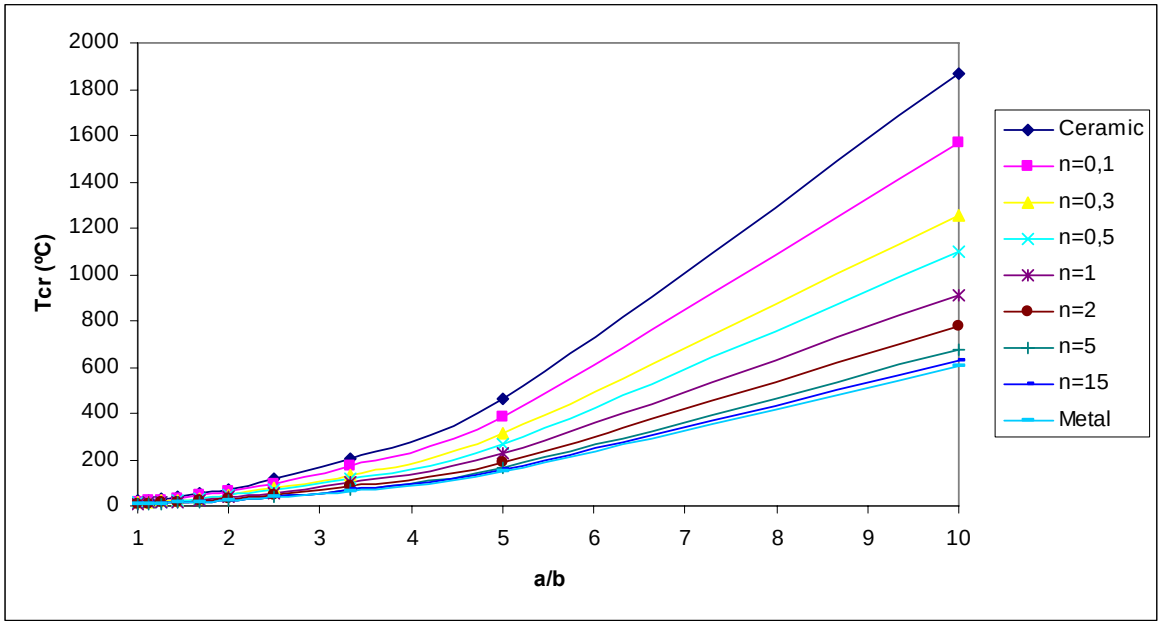

Figure 5.18. Critical buckling temperatures of the three edges clamped, one edge simply supported rectangular FGM plates under linear temperature change across the thickness (α=1, β=0,6) vs a/b

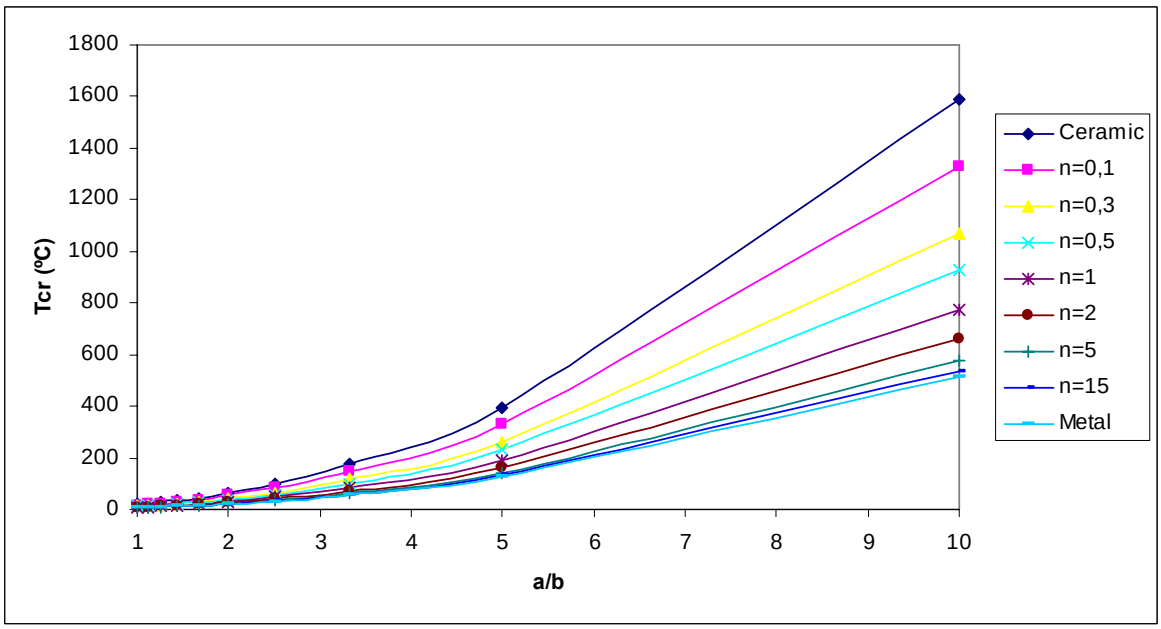

Figure 5.19. Critical buckling temperatures of the three edges clamped, one edge simply supported rectangular FGM plates under linear temperature change across the thickness (α=1, β=0,8) vs a/b

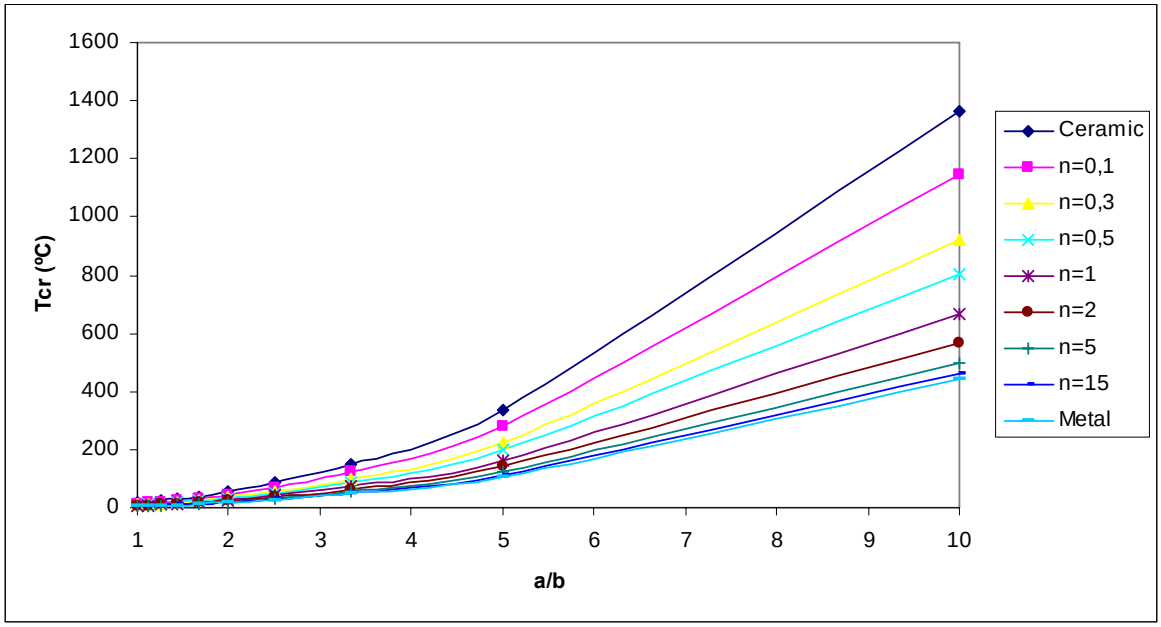

Figure 5.20. Critical buckling temperatures of the three edges clamped, one edge simply supported rectangular FGM plates under linear temperature change across the thickness (α=1, β=1) vs a/b

The critical temperature results under the uniform temperature rise for the two edges simply supported, two edges clamped rectangular FGM plates with variable thicknesses are also obtained and presented in the tabular form. Tables from Table 5.36 to Table 5.41 show the critical temperature results for the two edges simply supported, two edges clamped case.

Table 5.36. Critical buckling temperatures for the two edges simply supported, two edges clamped rectangular FGM plate, (α=1, β=0)

	n								
	Ceramic	0,1	0,3	0,5	1	2	5	15	Metal
a/b	**Tcr (ºC)**								
1	29,48	24,73	19,83	17,31	14,35	12,25	10,69	9,91	9,48
1,11	33,01	27,70	22,21	19,39	16,07	13,72	11,97	11,10	10,62
1,25	38,18	32,03	25,68	22,42	18,58	15,87	13,85	12,84	12,28
1,43	46,01	38,60	30,95	27,02	22,40	19,13	16,69	15,47	14,8
1,67	58,48	49,06	39,34	34,34	28,47	24,31	21,21	19,67	18,81
2	79,71	66,88	53,62	46,81	38,81	33,14	28,91	26,81	25,65
2,5	119,58	100,33	80,44	70,23	58,21	49,71	43,38	40,22	38,47
3,33	206,75	173,46	139,08	121,42	100,65	85,95	75,00	69,54	66,52
5	457,34	383,71	307,66	268,59	222,65	190,13	165,9	153,83	147,14
10	1813,31	1521,37	1219,87	1064,96	882,8	753,85	657,77	609,93	583,41

Table 5.37. Critical buckling temperatures for the two edges simply supported, two edges clamped rectangular FGM plate, (α=1, β=0,2)

	n								
	Ceramic	0,1	0,3	0,5	1	2	5	15	Metal
a/b	Tcr (ºC)								
1	23,92	20,07	16,09	14,05	11,64	9,94	8,68	8,04	7,69
1,11	26,78	22,47	18,02	15,73	13,04	11,13	9,71	9,01	8,62
1,25	30,95	25,97	20,82	18,18	15,07	12,87	11,23	10,41	9,96
1,43	37,23	31,24	25,05	21,87	18,13	15,48	13,50	12,52	11,98
1,67	47,22	39,62	31,77	27,73	22,99	19,63	17,13	15,88	15,19
2	64,17	53,84	43,17	37,69	31,24	26,68	23,28	21,58	20,65
2,5	95,93	80,48	64,53	56,34	46,70	39,88	34,80	32,27	30,86
3,33	165,25	138,64	111,17	97,05	80,45	68,70	59,94	55,58	53,17
5	364,06	305,45	244,91	213,81	177,24	151,35	132,06	122,46	117,13
10	1437,19	1205,8	966,84	844,06	699,68	597,48	521,33	483,42	462,4

Table 5.38. Critical buckling temperatures for the two edges simply supported, two edges clamped rectangular FGM plate, (α=1, β=0,4)

	n								
	Ceramic	0,1	0,3	0,5	1	2	5	15	Metal
a/b	Tcr (ºC)								
1	19,85	16,66	13,36	11,66	9,67	8,25	7,20	6,68	6,39
1,11	22,23	18,65	14,95	13,05	10,82	9,24	8,06	7,48	7,15
1,25	25,66	21,53	17,26	15,07	12,49	10,67	9,31	8,63	8,25
1,43	30,82	25,86	20,73	18,10	15,00	12,81	11,18	10,37	9,92
1,67	38,99	32,71	26,23	22,90	18,98	16,21	14,14	13,11	12,54
2	52,82	44,32	35,54	31,02	25,72	21,96	19,16	17,77	16,99
2,5	78,66	65,99	52,91	46,19	38,29	32,70	28,53	26,46	25,31
3,33	134,89	113,17	90,75	79,22	65,67	56,08	48,93	45,37	43,4
5	295,78	248,16	198,98	173,71	144	122,96	107,29	99,49	95,16
10	1163,31	976,02	782,59	683,22	566,35	483,62	421,99	391,3	374,28

Table 5.39. Critical buckling temperatures for the two edges simply supported, two edges clamped rectangular FGM plate, (α=1, β=0,6)

	n								
	Ceramic	0,1	0,3	0,5	1	2	5	15	Metal
a/b	Tcr (ºC)								
1	16,8	14,09	11,30	9,86	8,18	6,98	6,09	5,65	5,4
1,11	18,8	15,77	12,65	11,04	9,15	7,81	6,82	6,32	6,05
1,25	21,67	18,18	14,58	12,73	10,55	9,01	7,86	7,29	6,97
1,43	26,00	21,81	17,49	15,27	12,66	10,81	9,43	8,74	8,36
1,67	32,8	27,52	22,07	19,27	15,97	13,64	11,90	11,03	10,55
2	44,30	37,17	29,80	26,02	21,57	18,42	16,07	14,90	14,25
2,5	65,70	55,12	44,20	38,58	31,98	27,31	23,83	22,10	21,14
3,33	112,17	94,11	75,46	65,88	54,61	46,63	40,69	37,73	36,09
5	244,90	205,47	164,75	143,83	119,23	101,81	88,83	82,37	78,79
10	960,40	805,78	646,09	564,05	467,56	399,27	348,38	323,04	309,00

Table 5.40. Critical buckling temperatures for the two edges simply supported, two edges clamped rectangular FGM plate, (α=1, β=0,8)

	n								
	Ceramic	0,1	0,3	0,5	1	2	5	15	Metal
a/b	Tcr (ºC)								
1	14,43	12,11	9,71	8,48	7,03	6,00	5,23	4,85	4,64
1,11	16,15	13,55	10,86	9,48	7,86	6,71	5,86	5,43	5,19
1,25	18,61	15,61	12,52	10,93	9,06	7,73	6,75	6,26	5,99
1,43	22,28	18,69	14,99	13,08	10,85	9,26	8,08	7,49	7,17
1,67	28,05	23,53	18,87	16,47	13,65	11,66	10,17	9,43	9,02
2	37,75	31,67	25,40	22,17	18,38	15,69	13,69	12,70	12,15
2,5	55,77	46,79	37,52	32,75	27,15	23,18	20,23	18,76	17,94
3,33	94,8	79,54	63,78	55,68	46,15	39,41	34,39	31,89	30,5
5	206,17	172,97	138,69	121,08	100,37	85,71	74,79	69,35	66,33
10	806,54	676,69	542,58	473,68	392,66	335,3	292,57	271,29	259,5

Table 5.41. Critical buckling temperatures for the two edges simply supported, two edges clamped rectangular FGM plate, (α=1, β=1)

	n								
	Ceramic	0,1	0,3	0,5	1	2	5	15	Metal
a/b	**Tcr (ºC)**								
1	12,58	10,55	8,46	7,39	6,12	5,23	4,56	4,23	4,05
1,11	14,07	11,80	9,46	8,26	6,85	5,85	5,10	4,73	4,53
1,25	16,2	13,59	10,90	9,51	7,89	6,73	5,88	5,45	5,21
1,43	19,36	16,24	13,02	11,37	9,43	8,05	7,02	6,51	6,23
1,67	24,31	20,39	16,35	14,27	11,83	10,10	8,82	8,17	7,82
2	32,61	27,36	21,94	19,15	15,88	13,56	11,83	10,97	10,49
2,5	48,00	40,27	32,29	28,19	23,37	19,95	17,41	16,14	15,44
3,33	81,26	68,18	54,67	47,73	39,56	33,78	29,48	27,33	26,14
5	176,11	147,76	118,47	103,43	85,74	73,21	63,88	59,24	56,66
10	687,42	576,75	462,45	403,72	334,67	285,78	249,36	231,22	221,17

According to the results obtained, the variation of the critical temperatures vs. dimensionless geometrical parameters a/b are again plotted for each case. Seven arbitrary values of the power law index, *n*= 0.1, 0.3, 0.5, 1, 2, 5, 15 are taken in the calculations like the previous cases. Again, a wide range of a/b ratio is considered and each figure is plotted according to the variation of the α and β parameters. Figures from Figure 5.21 to Figure 5.26 represent the critical buckling temperatures of the two edges simply supported, two edges clamped rectangular FGM plates with variable thicknesses.

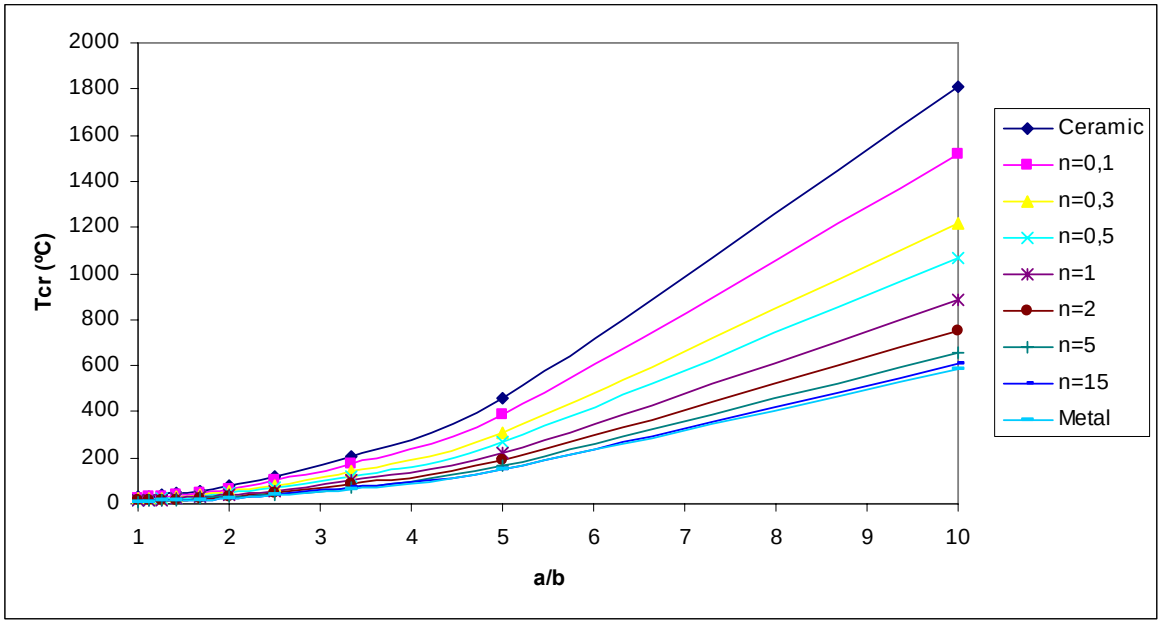

Figure 5.21. Critical buckling temperatures of the two edges simply supported, two edges clamped rectangular FGM plates under linear temperature change across the thickness (α=1, β=0) vs a/b

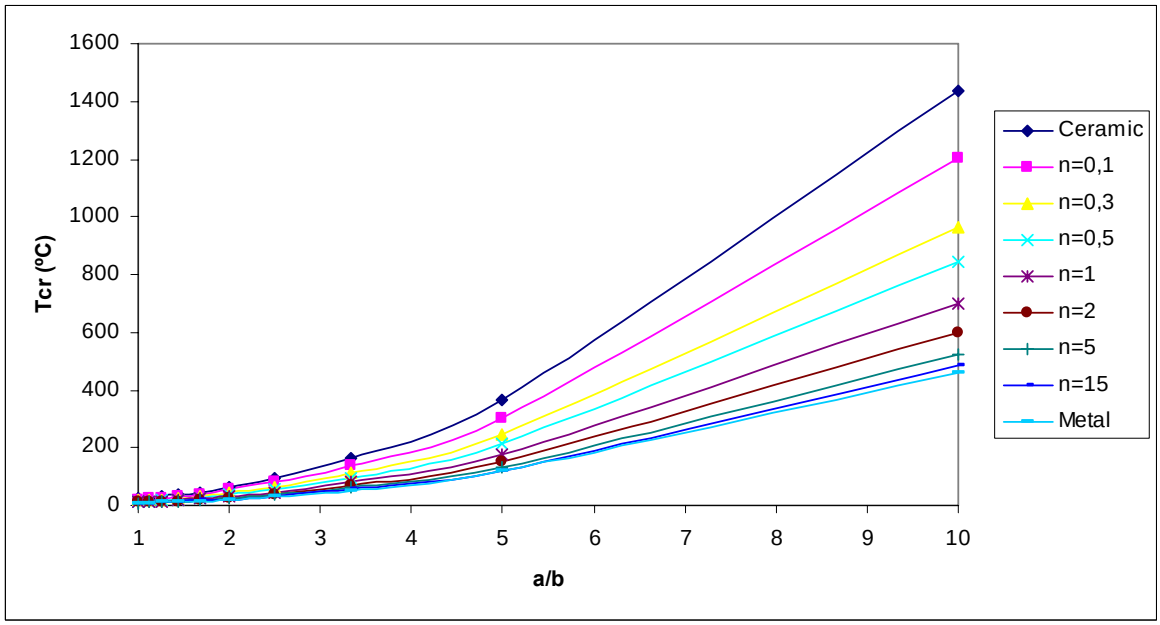

Figure 5.22. Critical buckling temperatures of the two edges simply supported, two edges clamped rectangular FGM plates under linear temperature change across the thickness (α=1, β=0,2) vs a/b

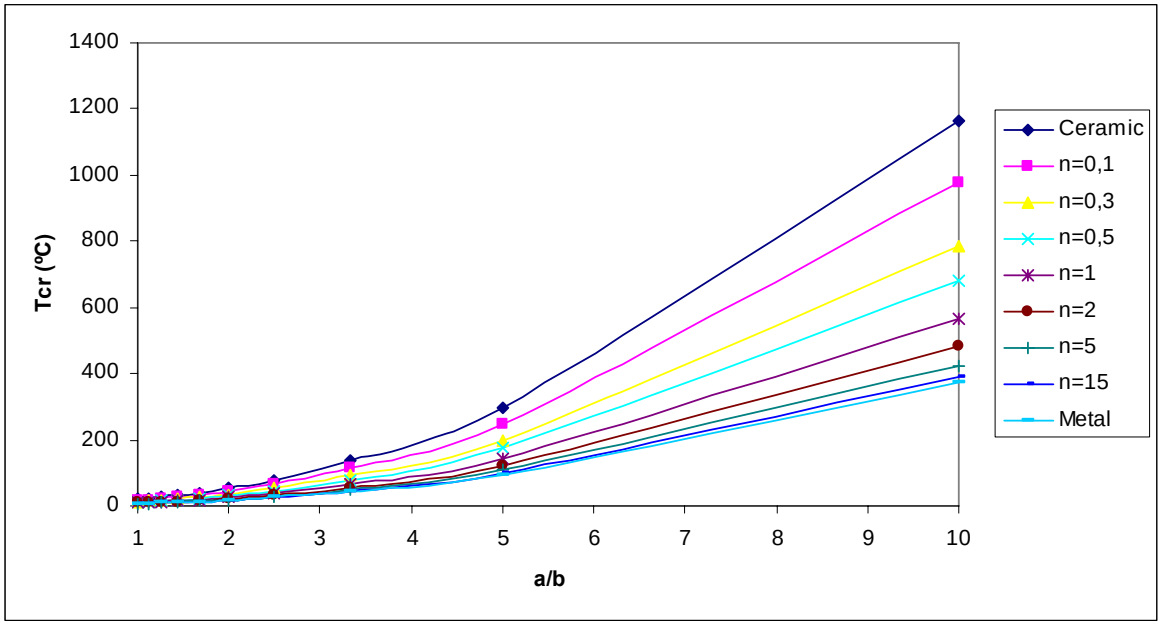

Figure 5.23. Critical buckling temperatures of the two edges simply supported, two edges clamped rectangular FGM plates under linear temperature change across the thickness (α=1, β=0,4) vs a/b

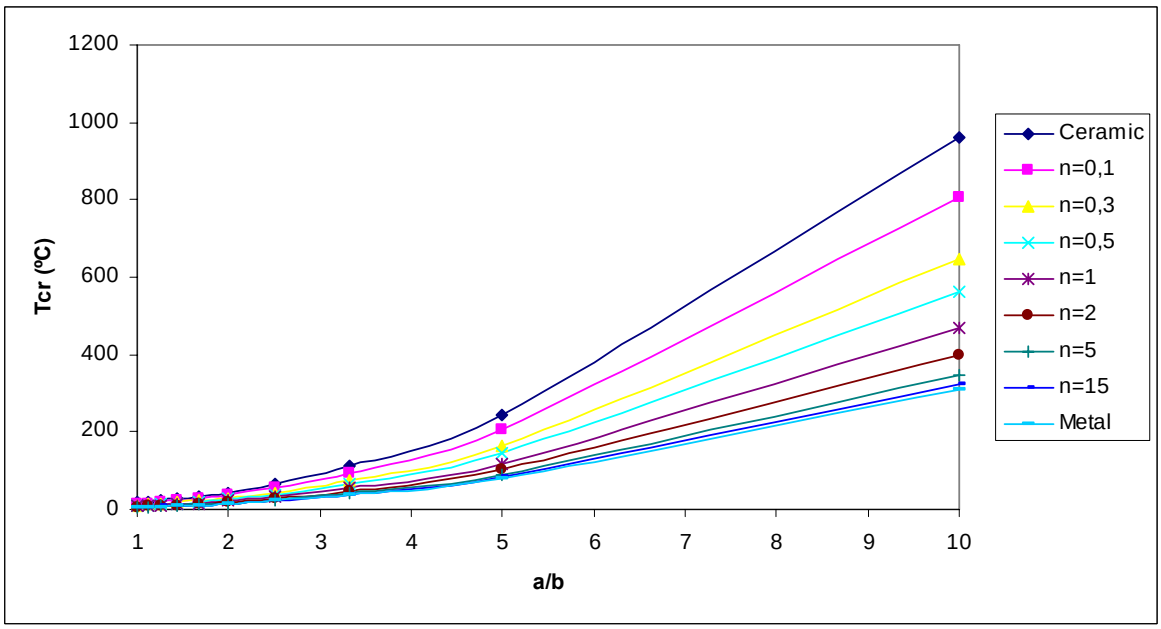

Figure 5.24. Critical buckling temperatures of the two edges simply supported, two edges clamped rectangular FGM plates under linear temperature change across the thickness (α=1, β=0,6) vs a/b

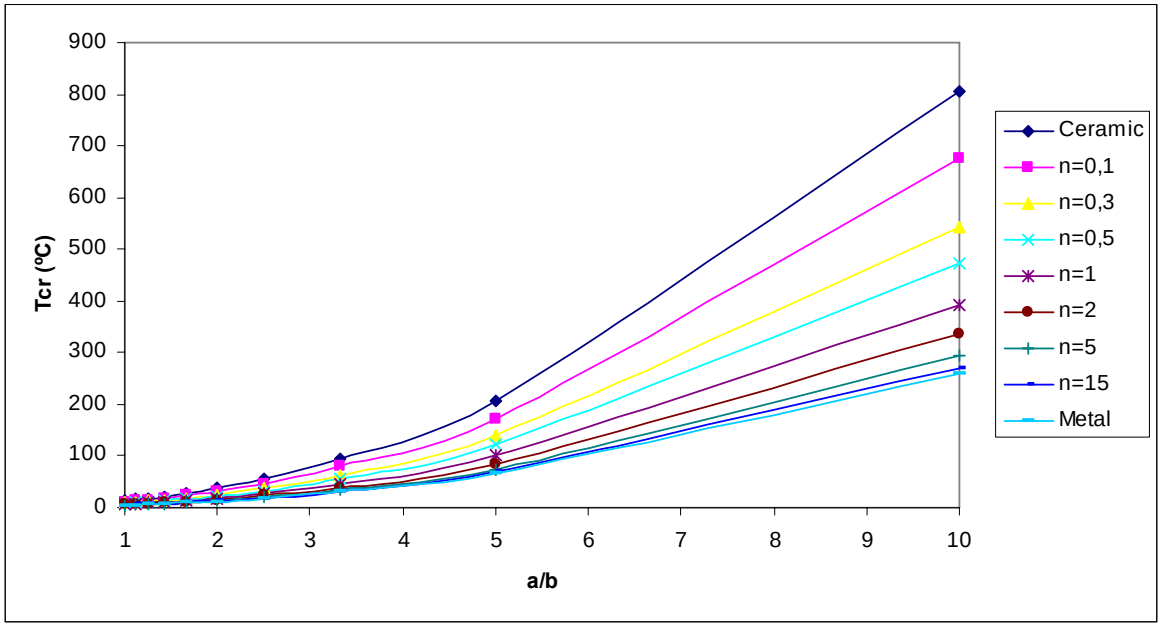

Figure 5.25. Critical buckling temperatures of the two edges simply supported, two edges clamped rectangular FGM plates under linear temperature change across the thickness (α=1, β=0,8) vs a/b

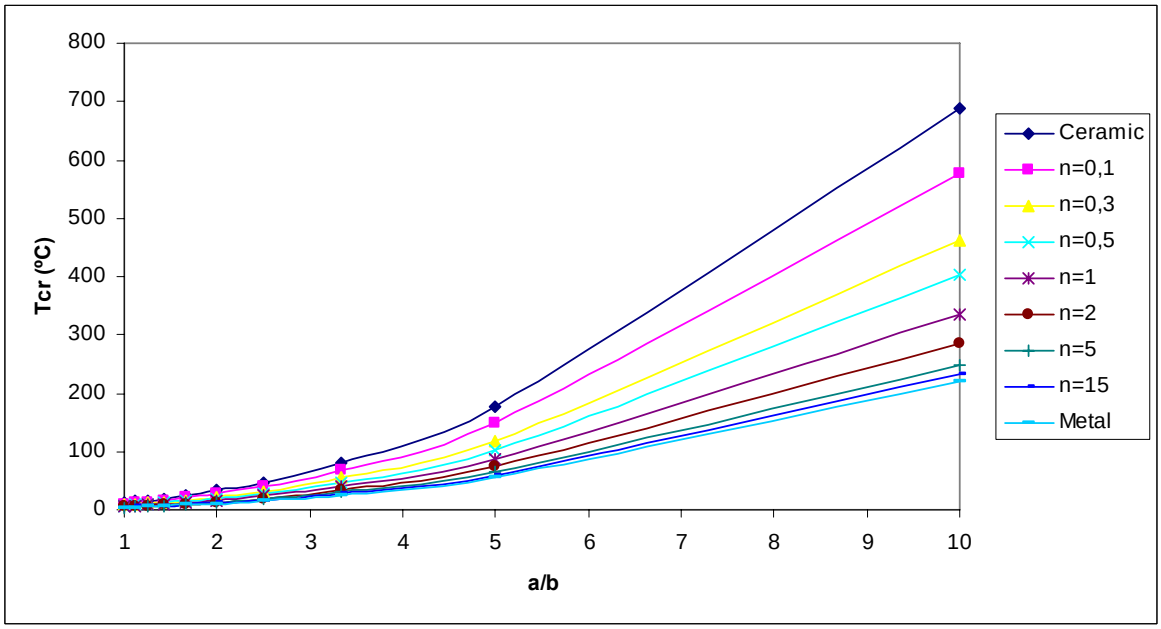

Figure 5.26. Critical buckling temperatures of the two edges simply supported, two edges clamped rectangular FGM plates under linear temperature change across the thickness (α=1, β=1) vs a/b

6. CONCLUSIONS

In this thesis, thermal buckling analyses of rectangular and elliptical plates are studied with Kirchhoff plate model. Rayleigh Ritz method is applied and presented. The method is employed both for homogenous and FGM plates. In addition to this, plates with constant thickness and those with the parabolic thickness variation are studied. In each case, various combinations of boundary conditions are taken into account. Here, some concluding remarks are explained as follows:

Buckling behavior of homogenous, isotropic rectangular and elliptical plates with constant thicknesses for various aspect ratios, a/b, are presented in Chapter 3 and compared with the results in Ref. [49]. By comparing the buckling factors for the rectangular and elliptical plates, it is observed that the difference is maximum when the aspect ratio a/b is equal to 1.0. This maximum difference of about 15% and 12% for simply supported and clamped plates, respectively, decreases as the aspect ratio moves away from unity. When a/b gets higher, the buckling parameters of the rectangular and elliptical plates with the same boundary conditions become very similar. As it is expected from this point, critical buckling temperatures for rectangular and elliptical plates increase for both simply supported and clamped cases, as the aspect ratio increases. As the plates get thicker, critical buckling temperature rises parabolically. Also, as the t/a ratio of the rectangular and elliptical plates increase, the variation of the critical temperature results for the clamped boundary condition is sharper than those for the simply supported case.

After the thermal buckling analyses of homogenous, isotropic plates, buckling behavior of FGM plates with constant thickness are investigated in Chapter 4. The results are obtained for the rectangular and elliptical FGM plates both for fully simply supported and clamped edges. As explained earlier, variation of the composition of ceramics and metal is linear for n=1. The value of n=0 represents a homogenous, fully ceramic, plate. During the analyses done for the rectangular and elliptical plates, it is observed that the critical buckling temperatures of FGM plates increase by the increase of the aspect ratio a/b and decrease by the increase of the power law index, n from 0 to 15. It is also seen that after the value of n=5, for the higher values of n, there is no significant change in the

temperatures for the FGM plates. As n increases, critical buckling temperature of the linear temperature distribution increase. If the FGM plate results are compared with the ones obtained for the homogenous plates, it is concluded that the critical buckling temperatures for the homogenous plates are considerably higher than those for the FGM plates especially for the comparatively longer and thicker plates. The critical buckling temperatures obtained for the clamped case are higher than those obtained for the simply supported case for both rectangular and elliptical FGM plates.

In the case of the parabolic variation of the plate thicknesses in Chapter 5, for all the boundary conditions, controlling parameter of the constant part of the plate is kept constant ($\alpha=1$) and the controlling parameter of the thickness variation is changed between 0 and 1 ($0\leq\beta\leq1$). It should be noted that the results of $\alpha=1$, $\beta=0$ represents the plates with constant thickness. While the controlling parameter of the thickness variation, β decreases, the buckling load factors and as a result of this, critical buckling temperatures decrease as well. The critical buckling temperatures for both elliptical and rectangular plates, increase by the increase of a/b and decrease by the increase of the power law index n from 0 to 15. It is also observed that for the higher values of n, there is no significant difference in the temperatures for the FGM plates with variable thicknesses. When the results of the rectangular plates with different boundary condition combinations are compared, it is seen that the critical buckling temperatures of the rectangular plates with three edges clamped, one edge simply supported are higher than those of the two edges simply supported, two edges clamped case. Since it is more difficult to buckle for the clamped cases, as the plates get closer to the clamped condition, the critical buckling temperatures of the plates increase. On the other hand, in the case of parabolic variation of the plate thickness, no matter what the boundary conditions are, the buckling load factor increases according to the constant thickness values.

For the future work, this study can be widened with the application of different boundary conditions, different shapes of plates, different plate materials and different solution techniques. Also, plate thickness variation can be assumed to be changed differently, e.g. exponentially. Magnetic and piezoelectric effects can be added into this study. Especially, thermal post-buckling behavior of FGM plates can be studied in the future as the extension of the present study.

APPENDIX A1: THERMAL BUCKLING SOFTWARE EXAMPLE OF RECTANGULAR AND ELLIPTICAL PLATES PREPARED BY USING MATHEMATICA 5.2

(*Buckling of clamped rectangular plates-Ritz, 10 terms*)

a=1; (**L1 Reference plate dimension**)

$\nu = 0.3$

<<LinearAlgebraMatrixManupulation'

<<Calculus'VectorAnalysis'

r=1.0; (**L2 Plate aspect ratio a/b**)

$b = \frac{a}{r}$

d=1;(* $d = \frac{Et^3}{12(1-\nu^2)}$ *is the flexural rigidity of the plate**)

$w = ((x^2 - a^2/4) + (y^2 - b^2/4))^2 (a_{00} + a_{20}x^2 + a_{02}y^2 + a_{22}x^2y^2 + a_{40}x^4 + a_{04}y^4 + a_{24}x^2y^4 + a_{42}x^4y^2 + a_{60}x^6 + a_{06}y^6)$ (**L3 Displacement function**)

$uUt = \frac{d}{2} * Integrate\left[\begin{matrix}((D[w,\{x,2\}] + D[w,\{y,2\}])^2 + 2(1-\nu)((D[D[w,y],x])^2 - D[w,\{x,2\}] * D[w,\{y,2\}]),\\ \{y,-b/2,\ b/2\}\end{matrix}\right]$

$uU = Integrate[uUt, \{x,-a/2, a/2\}]$ (**L4 uU is the strain energy due to bending**)

$tTt = (-n/2) * Integrate[((D[w,x])^2 + (D[w,y])^2), \{y,-b/2,\ b/2\}]$

$tT = Integrate[tTt, \{x,-a/2, a/2\}]$ (**L5 tT is the potential energy of inplane uniform pressure, n**)

Print[thesis*fF*]

$fF = uU + tT$ (**L6 fF is the total energy function**)

$eq1 = D[fF, a_{00}];$
$eq2 = D[fF, a_{20}];$
$eq3 = D[fF, a_{02}];$
$eq4 = D[fF, a_{22}];$
$eq5 = D[fF, a_{40}];$
$eq6 = D[fF, a_{04}];$

$eq7 = D[fF, a_{24}];$
$eq8 = D[fF, a_{42}];$
$eq9 = D[fF, a_{60}];$
$eq10 = D[fF, a_{06}];$

$$eqs = LinearEquationsToMatrices\left[\begin{Bmatrix} eq1 == 0, eq2 == 0, eq3 == 0, eq4 == 5, eq6 == 0, eq7 == 0, \\ eq8 == 0, eq9 == 0, eq10 == 0 \end{Bmatrix}, \{a_{00}, a_{20}, a_{02}, a_{22}, a_{40}, a_{04}, a_{24}, a_{42}, a_{60}, a_{06}\}\right];$$

Dettt

deteqs=eqs[[1]];

Print [theequation]

polpolpol

polinomialeq=Det[deteqs] (*_determinant of the equations_*)

Print [rootsoftheequation]

sol=Solve[polinomialeq==0,n]

TimeUsed []

Null

(*Buckling of simply supported elliptical plates-Ritz, 10 terms*)

a=1; (*_L1 Reference plate dimension_*)

$\nu = 0.3$

<<LinearAlgebraMatrixManupulation'

<<Calculus'VectorAnalysis'

r=1.0; (*_L2 Plate aspect ratio a/b_*)

$b = \frac{a}{r}$

d=1;(* $d = \frac{Et^3}{12(1-\nu^2)}$ _is the flexural rigidity of the plate_*)

$w = ((4x^2/a^2) + (4y^2/b^2) - 1)^1 (a_{00} + a_{20}x^2 + a_{02}y^2 + a_{22}x^2y^2 + a_{40}x^4 + a_{04}y^4 + a_{24}x^2y^4 + a_{42}x^4y^2 + a_{60}x^6 + a_{06}y^6)$ (*_L3 Displacement function_*)

$$uUt = \frac{d}{2} * Integrate\left[\begin{Bmatrix} (D[w,\{x,2\}] + D[w,\{y,2\}])^2 + 2(1-\nu)\left((D[D[w,y],x])^2 - D[w,\{x,2\}] * D[w,\{y,2\}]\right), \\ \{y, -b/2 * \sqrt{1-(x^2/(a^2/4))},\ b/2 * \sqrt{1-(x^2/(a^2/4))}\} \end{Bmatrix}\right]$$

$uU = Integrate[uUt, \{x, -a/2, a/2\}]$ (*L4 *uU is the strain energy due to bending**)

$tTt = (-n/2) * Integrate\left[\left((D[w,x])^2 + (D[w,y])^2\right), \left\{y, -b/2 * \sqrt{1-(x^2/(a^2/4))},\ b/2 * \sqrt{1-(x^2/(a^2/4))},\right\}\right]$

$tT = Integrate[tTt, \{x, -a/2, a/2\}]$ (*L5 *tT is the potential energy of inplane uniform pressure, n**)

Print[thesis*fF*]

$fF = uU + tT$ (*L6 *fF is the total energy function**)

$eq1 = D[fF, a_{00}];$
$eq2 = D[fF, a_{20}];$
$eq3 = D[fF, a_{02}];$
$eq4 = D[fF, a_{22}];$
$eq5 = D[fF, a_{40}];$
$eq6 = D[fF, a_{04}];$
$eq7 = D[fF, a_{24}];$
$eq8 = D[fF, a_{42}];$
$eq9 = D[fF, a_{60}];$
$eq10 = D[fF, a_{06}];$

$$eqs = LinearEquationsToMatrices\left[\begin{Bmatrix} eq1 == 0, eq2 == 0, eq3 == 0, eq4 == 5, eq6 == 0, eq7 == 0, \\ eq8 == 0, eq9 == 0, eq10 == 0 \end{Bmatrix}, \{a_{00}, a_{20}, a_{02}, a_{22}, a_{40}, a_{04}, a_{24}, a_{42}, a_{60}, a_{06}\}\right];$$

Dettt

deteqs=eqs[[1]];

Print [theequation]

polpolpol

polinomialeq=Det[deteqs] (**determinant of the equations**)

Print [rootsoftheequation]

sol=Solve[polinomialeq==0,n]

TimeUsed []

Null

REFERENCES

1. Szilard, R., *Theory and Applications of Plate Analysis: Classical, Numerical and Engineering Methods,* John Wiley, New Jersey, 2003.

2. Timoshenko, S. and S. Woinowsky-Kreiger, *Theory of Plates and Shells,* Mc Graw-Hill, New York, 1959.

3. Tauchert, T. R., "Thermally Induced Flexure, Buckling and Vibration of Plates", *ASME Applied Mechanics Reviews,* Vol. 44, pp. 347-360, 1991.

4. Thornton, E. A., "Thermal Buckling of Plates and Shells", *ASME Applied Mechanics Reviews,* Vol. 46, pp. 485-506, 1993.

5. Murphy, K. D. and D. Ferreira, "Thermal Buckling of Rectangular Plates", *International Journal of Solids and Structures*, Vol. 38, pp. 3979-3994, 2001.

6. Shariyat, M., "Thermal Buckling Analysis of Rectangular Composite Plates with Temperature Dependent Properties Based on a Layerwise Theory", *Thin-Walled Structures*, Vol. 45, pp. 439-452, 2007.

7. Bert, C. W. and K. K. Devarakonda, "Buckling of Rectangular Plates Subjected to Nonlinearly Distributed In-Plane Loading", *International Journal of Solids and Structures*, Vol. 40, pp. 4097-4106, 2003.

8. Kabir, H. R. H., M. A. M. Hamad, J. Al-Duaij and M. J. John, "Thermal Buckling Response of All-Edge Clamped Rectangular with Symmetric Angle-Ply Lamination", *Composite Structures*, Vol. 79, pp. 148-155, 2007.

9. Li, S. R., R. C. Batra and L. Sheng, "Vibration of Thermally Post-Buckled Orthotropic Circular Plates", *Journal of Thermal Stresses*, Vol. 30, pp. 43-57, 2007.

10. Laura, P. A. A. and C. A. Rossit, “Thermal Bending of Thin, Anisotropic, Clamped Elliptic Plates”, *Ocean Engineering*, Vol. 29, pp. 485-488, 1999.

11. Liew, K. M., J. -B. Han and Z. M. Xiao, “Vibration Analysis of Circular Mindlin Plates”, *Journal of Sound and Vibration*, Vol. 205, No. 5, pp. 617-630, 1997.

12. Kalyan, J. B. and K. Bhaskar, “An Analytical Parametric Study on Buckling of Non-Uniformly Compressed Orthotropic Rectangular Plates”, *Composite Structures*, Vol. 82, pp. 10-18, 2006.

13. Belinha, J. and L. M. J. S. Dinis, “Nonlinear Analysis of Plates and Laminates Using the Element Free Galerkin Method”, *Composite Structures*, Vol. 78, pp. 337-350, 2007.

14. Çeribaşı, S., G. Altay and M. C. Dökmeci, “Static Analysis of Superelliptical Clamped Plates by Galerkin’s Method”, *Thin-Walled Structures,* Vol. 46, pp.122-127, 2008.

15. Lee, D. –M. and I. Lee, “Vibration Behaviors of Thermally Post-Buckled Anisotropic Plates Using First Order Shear Deformable Plate Theory”, *Computers and Structures*, Vol. 63, pp. 371-378, 1997.

16. Park, J. -S., J. -H. Kim and S. -H. Moon, “Vibration of Thermally Post-Buckled Composite Plates Embedded with Shape Memory Alloy Fibers”, *Composite Structures*, Vol. 63, pp. 179-188, 2004.

17. Shen, H. -S., J. Yang and L. Zhang, “Dynamic Response of Reissner-Mindlin Plates under Thermomechanical Loading and Resting on Elastic Foundations”, *Journal of Sound and Vibration,* Vol. 232, pp. 309-329, 2000.

18. Shen, H. -S., “Thermal Postbuckling Analysis of Imperfect Reissner-Mindlin Plates on Softening Nonlinear Elastic Foundations”, *Journal of Engineering Mathematics,* Vol. 33, pp. 259-270, 1998.

19. Shen, H. -S., "Thermal Postbuckling Analysis of Imperfect Shear Deformable Plates on Two Parameter Elastic Foundations", *Computers and Structures,* Vol. 63, pp. 1187-1193, 1997.

20. Shen, H. -S., "Thermomechanical Postbuckling of Imperfect Moderately Thick Plates on Nonlinear Elastic Foundations", *Mechanics of Structures and Machines,* Vol. 24, pp. 513-530, 1996.

21. Ganapathi, M. and M. Touratier, "A Study on Thermal Postbuckling Behavior of Laminated Composite Plates Using a Shear Flexible Finite Element", *Finite Elements in Analysis and Design*, Vol. 28, pp. 115-135, 1997.

22. Prabhu, M. R. and R. Dhanaraj, "Thermal Buckling of Laminated Composite Plates", *Computers and Structures*, Vol. 53, pp. 1193-1204, 1994.

23. Huang, N. N. and T. R. Tauchert, "Thermal Buckling of Clamped Symmetrical Laminated Plates", *Thin-Walled Structures*, Vol. 13, pp. 259-273, 1992.

24. Giorgi, C. and M. G. Naso, "Mathematical Models of Reissner-Mindlin Thermoviscoelastic Plates", *Journal of Thermal Stresses*, Vol. 29, pp. 699-716, 2006.

25. Lee, J. J., I. K. Oh and I. Lee, "Thermal Postbuckling Behavior of Patched Laminated Panels under Uniform and Non-Uniform Temperature Distributions", *Composite Structures,* Vol. 55, pp. 137-145, 2002.

26. Shen, H. -S., "Postbuckling of Shear Deformable Laminated Plates with Piezoelectric Actuators under Complex Loading Conditions", *International Journal of Solids and Structures,* Vol. 38, pp. 7703-7721, 2001.

27. Shen, H. -S., "Thermal Postbuckling of Shear Deformable Laminated Plates with Piezoelectric Actuators", *Composite Science and Technology,* Vol. 61, pp. 1931-1943, 2001.

28. Shen, H. -S., "Thermal Postbuckling Behavior of Imperfect Shear Deformable Laminated Plates with Temperature Dependent Properties", *Computer Methods in Applied Mechanics and Engineering,* Vol. 190, pp. 5377-5390, 2001.

29. Shen, H. -S., "Thermomechanical Postbuckling of Imperfect Shear Deformable Laminated Plates on Elastic Foundations", *Computer Methods in Applied Mechanics and Engineering,* Vol. 189, pp. 761-784, 2000.

30. Cheng, Z. Q. and S. Kitipornchai, "Exact Eigenvalue Correspondences Between Laminated Plate Theories via Membrane Vibration", *International Journal of Solids and Structures,* Vol. 37, pp. 2253-2264, 2000.

31. Shen, H. -S., "Thermal Postbuckling of Imperfect Shear Deformable Laminated Plates on Two Parameter Elastic Foundations", *Mechanics of Composite Materials and Structures,* Vol. 6, pp. 207-228, 1999.

32. Yapici, A., "Thermal Buckling Behavior of Hybrid-Composite Angle-Ply Laminated Plates with an Inclined Crack", *Mechanics of Composite Materials,* Vol. 41, pp. 131-138, 2005.

33. Singha, M. K. and M. Ganapathi, "A Parametric Study on Supersonic Flutter Behavior of Laminated Composite Skew Flat Panels", *Composite Structures,* Vol. 69, pp. 55-63, 2005.

34. Zhu, Y. A., F. Wang and R. H. Liu, "Thermal Buckling of Axisymmetrically Laminated Cylindrically Orthotropic Shallow Spherical Shells Including Transverse Shear", *Applied Mathematics and Mechanics,* Vol. 29, pp. 291-300, 2008.

35. Pradeep, V. and N. Ganesan, "Thermal Buckling and Vibration Behavior of Multi-Layer Rectangular Viscoelastic Sandwich Plates", *Journal of Sound and Vibration,* Vol. 310, pp. 169-183, 2008.

36. Aydogdu, M., "Thermal Buckling Analysis of Cross-Ply Laminated Composite Beams with General Boundary Conditions", *Composites Science and Technology,* Vol. 67, pp. 1096-1104, 2007.

37. Matsunaga, H., "Free Vibration and Stability of Angle-Ply Laminated Composite and Sandwich Plates under Thermal Loading", *Composite Structures,* Vol. 77, pp. 249-262, 2007.

38. Avci, A., O. S. Sahin and N. Ataberk, "Thermal Buckling Behavior of Cross- Ply Hybrid Composite Laminates with Inclined Crack", *Composites Science and Technology,* Vol. 66, pp. 2965-2970, 2006.

39. Zakeri, A. A. and M. M. Alinia, "An Analytical Study on Postbuckling Behavior of Imperfect Sandwich Panels Subjected to Uniform Thermal Stresses", *Thin-Walled Structures,* Vol. 44, pp. 344-353, 2006.

40. Matsunaga, H., "Thermal Buckling of Angle-Ply Laminated Composite and Sandwich Plates According to a Global Higher Order Deformation Theory", *Composite Structures,* Vol. 72, pp. 177-192, 2006.

41. Sahin, O. S., "Thermal Buckling of Hybrid Angle-Ply Laminated Composite Plates with a Hole", *Composite Science and Technology,* Vol. 65, pp. 1780-1790, 2005.

42. Avci, A., O. S. Sahin and M. Uyaner, "Thermal Buckling of Hybrid Laminated Composite Plates with a Hole", *Composite Structures,* Vol. 68, pp. 247-254, 2005.

43. Avci, A., S. Kaya and B. Daghan, "Thermal Buckling of Rectangular Laminated Plates with a Hole", *Journal of Reinforced Plastics and Composites,* Vol. 24, pp. 259-272, 2005.

44. Shen, H. -S. and Q. S. Li, "Postbuckling of Shear Deformable Laminated Plates Resting on a Tensionless Elastic Foundation Subjected to Mechanical or Thermal

Loading", *International Journal of Solids and Structures,* Vol. 41, pp. 4769-4785, 2005.

45. Vangipuram, P. and N. Ganesan, "Buckling and Vibration of Rectangular Composite Viscoelastic Sandwich Plates under Thermal Loads", *Composite Structures,* Vol. 77, pp. 419-429, 2007.

46. Morimoto, T., Y. Tanigawa and R. Kawamura, "Thermal Buckling Analysis of Inhomogeneous Rectangular Plate due to Uniform Heat Supply", *Journal of Thermal Stresses,* Vol. 26, pp. 1151-1170, 2003.

47. Girish, J. and L. S. Ramachandra, "Thermal Postbuckled Vibrations of Symmetrically Laminated Composite Plates with Initial Geometric Imperfections", *Journal of Sound and Vibration,* Vol. 282, pp. 1137-1153, 2005.

48. Zhang, N. H. and J. J. Xing, "Vibration Analysis of Linear Coupled Thermoviscoelastic Thin Plates by a Variational Approach", *International Journal of Solids and Structures*, Vol. 45, pp. 2583-2597, 2008.

49. Wang, C. M., L. Wang and K. M. Liew, "Vibration and Buckling of Super Elliptical Plates", *Journal of Sound and Vibration*, Vol. 171, pp. 301-314, 1994.

50. Singha, M. K., L. S. Ramachandra and J. N. Bandyopadhyay, "Thermal Postbuckling Analysis of Laminated Composite Plates", *Composite Structures*, Vol. 54, pp. 453-458, 2001.

51. Gossard, M. L., P. Seide and W. M. Roberts, *Thermal Buckling of Plates*, NACA TND, Washington, 1952.

52. Nath, Y. and K. K. Shukla, "Postbuckling of Angle Ply Laminated Plates under Thermal Loading", *Commun Nonlinear Sci Numer Simul*, Vol. 6, pp. 1-16, 2001.

53. Shiau, L. C., S. Y. Kuo and C. Y. Chen, "Thermal Buckling Behavior of Composite Laminated Plates", *Composite Structures*, Vol. 92, pp. 508-514, 2010.

54. Javaheri, R. and M. R. Eslami, "Buckling of Functionally Graded Plates under In-plane Compressive Loading", *Journal of Applied Mathematics and Mechanics,* Vol. 82, pp. 277-283, 2001.

55. Javaheri, R. and M. R. Eslami, "Thermal Buckling of Functionally Graded Plates", *AIAA Journal,* Vol. 40, pp. 162-169, 2002.

56. Javaheri, R. and M. R. Eslami, "Thermal Buckling of Functionally Graded Plates based on Higher Order Theory", *Journal of Thermal Stresses,* Vol. 25, pp. 603-625, 2002.

57. Na, K. -S. and J. H. Kim, "Thermal Postbuckling Investigations of Functionally Graded Plates Using 3-D Finite Element Method", *Finite Elements in Analysis and Design,* Vol. 42, pp. 749-756, 2006.

58. Na, K. -S. and J. H. Kim, "Three Dimensional Thermal Buckling Analysis of Functionally Graded Materials", *Composites Part B,* Vol. 35, pp. 429-437, 2004.

59. Najafizadeh, M.M. and H. R. Heydari, "An Exact Solution for Buckling of Functionally Graded Circular Plates based on Higher Order Shear Deformation Plate Theory under Uniform Radial Compression", *International Journal of Mechanical Sciences*, Vol. 50, pp. 603-612, 2008.

60. Najafizadeh, M.M. and H. R. Heydari, "Thermal Buckling of Functionally Graded Circular Plates based on Higher Order Shear Deformation Plate Theory", *European Journal of Mechanics A/Solids*, Vol. 23, pp.1085-1100, 2004.

61. Ganapathi, M. and T. Prakash, "Thermal Buckling of Simply Supported Functionally Graded Skew Plates", *Composite Structures*, Vol. 74, pp. 247-250, 2006.

62. Prakash, T., M. K. Singha and M. Ganapathi, “Thermal Post-buckling Analysis of FGM Skew Plates”, *Engineering Structures,* Vol. 30, pp. 22-32, 2008.

63. Yang, J. and H.-S. Shen, “Non-linear Bending Analysis of Shear Deformable Functionally Graded Plates subjected to Thermo-Mechanical Loads under Various Boundary Conditions”, *Composites Part B,* Vol. 34, pp. 103-115, 2003.

64. Yang, J. and H.-S. Shen, “Non-linear Analysis of Functionally Graded Plates under Transverse and In-Plane Loads”, *International Journal of Non-Linear Mechanics,* Vol. 38, pp. 467-482, 2003.

65. Yang, J., K. M. Liew and S. Kitipornchai, “Imperfection Sensitivity of the Postbuckling Behavior of Higher-Order Shear Deformable Functionally Graded Plates”, *International Journal of Solids and Structures,* Vol. 43, pp. 5247-5266, 2006.

66. Saidi, A. R. and A. H. Baferani, “Thermal Buckling Analysis of Moderately Thick Functionally Graded Annular Sector Plates”, *Composite Strucures,* Vol. 92, pp. 1744-1752, 2010.

67. Wu, L., “Thermal Buckling of Simply Supported Moderately Thick Rectangular FGM Plate”, *Composite Structures*, Vol. 64, pp. 211-218, 2004.

68. Wu, T.-L., K. K. Shukla and J. H. Huang, “Postbuckling Analysis of Functionally Graded Rectangular Plates”, *Composite Structures*, Vol. 81, pp. 1-10, 2007.

69. Park, J. S. and J. –H. Kim, “Thermal Post-buckling and Vibration Analyses of Functionally Graded Plates”, *Journal of Sound and Vibration,* Vol. 289, pp. 77-93, 2006.

70. Shariat, B. A. S. and M. R. Eslami, “Effect of Initial Imperfections on Thermal Buckling of Functionally Graded Plates”, *Journal of Thermal Stresses,* Vol. 28, pp. 1183-1198, 2005.

71. Shariat, B. A. S. and M. R. Eslami, "Thermal Buckling of Imperfect Functionally Graded Plates", *International Journal of Solids and Structures*, Vol. 43, pp. 4082-4096, 2006.

72. Shariat, B. A. S. and M. R. Eslami, "Buckling of Thick Functionally Graded Plates under Mechanical and Thermal Loads", *Composite Structures,* Vol. 78, pp. 433-439, 2007.

73. Shen, H. -S., "Postbuckling of FGM Plates with Piezoelectric Actuators under Thermo-Electro-Mechanical Loadings", *International Journal of Solids and Structures,* Vol. 42, pp. 6101-6121, 2005.

74. Shen, H. -S. and S. R. Li, "Postbuckling of Sandwich Plates with FGM Face Sheets and Temperature Dependent Properties", *Composites Part B-Engineering,* Vol. 39, pp. 332-344, 2008.

75. Chen, X. L. and K. M. Liew, "Buckling of Rectangular Functionally Graded Material Plates subjected to Nonlinearly Distributed In-Plane Edge Loads", *Smart Materials and Structures*, Vol. 13, pp. 1430-1437, 2004.

76. Chen, X. L., Z. Y. Zhao and K. M. Liew, "Stability of Piezoelectric FGM Rectangular Plates subjected to Non-Uniformly Distributed Load, Heat and Voltage", *Advances in Engineering Software*, Vol. 39, pp. 121-131, 2008.

77. Shen, H. –S., "Thermal Post-Buckling Behavior of Shear Deformable FGM Plates with Temperature-Dependent Properties", *International Journal of Mechanical Sciences,* Vol. 49, pp. 466-478, 2007.

78. Liew, K. M., J. Yang and S. Kitipornchai, "Postbuckling of Piezoelectric FGM Plates subject to Thermo-Electro-Mechanical Loading", *International Journal of Solids and Structures*, Vol. 40, pp. 3869-3892, 2003.

79. Kim, Y. -W., "Temperature Dependent Vibration Analysis of Functionally Graded Rectangular Plates", *Journal of Sound and Vibration,* Vol. 284, pp. 531-549, 2005.

80. Kitipornchai, S., J. Yang and K. M. Liew, "Random Vibration of the Functionally Graded Laminates in Thermal Environments", *Computer Methods in Applied Mechanics and Engineering,* Vol. 195, pp. 1075-1095, 2006.

81. Reddy, J. N., "Analysis of Functionally Graded Plates", *International Journal for Numerical Methods in Engineering,* Vol. 47, pp. 663-684, 2000.

82. Lanhe, W., "Thermal Buckling of a Simply Supported Moderately Thick Rectangular FGM Plate", *Composite Structures,* Vol. 64, pp. 211-218, 2004.

83. Yang, J., K. M. Liew and S. Kitipornchai, "Second-order Statistics of the Elastic Buckling of Functionally Graded Rectangular Plates", *Composites Science and Technology*, Vol. 65, pp. 1165-1175, 2005.

84. Morimoto, T., Y. Tanigawa and R. Kawamura, "Thermal Buckling of Functionally Graded Rectangular Plates subjected to Partial Heating", *International Journal of Mechanical Sciences,* Vol. 48, pp. 926-937, 2006.

85. Park, J.-S., J.-H. Kim and S.-H., Moon, "Thermal Postbuckling and Flutter Characteristics of Composite Plates Embedded with Shape Memory Alloy Fibers", *Composites Part B-Engineering*, Vol. 36, pp. 627-636, 2005.

86. Sohn, K. J. and J. H. Kim, "Structural Stability of Functionally Graded Panels Subjected to Aero-Thermal Loads", *Composite Structures,* Vol. 82, pp. 317-325, 2008.

87. Navazi, H. M. and H. Haddadpour, "Aero-Thermoelastic Stability of Functionally Graded Plates", *Composite Structures*, Vol. 80, pp. 580-587, 2007.

88. Zhao, X., Y. Y. Lee and K. M. Liew, "Mechanical and Thermal Buckling Analysis of Functionally Graded Plates", *Composite Structures,* Vol. 90, pp. 161-171, 2009.

89. Singh, B. and D. K. Tyagi, "Transverse Vibrations of an Elliptic Plate with Variable Thickness", *Journal of Sound and Vibration,* Vol. 99, No. 3, pp.379-391, 1985.

90. Singh, B. and S. Chakraverty, "Transverse Vibration of Circular and Elliptic Plates with Quadratically Varying Thickness", *Applied Mathematical Modeling,* Vol. 16, No. 5, pp. 269-274, 1992.

91. Singh, B. and V. Saxena, "Transverse Vibration of a Quarter of a Circular Plate with Variable Thickness", *Journal of Sound and Vibration,* Vol. 183, No. 1, pp. 49-67, 1995.

92. Singh, B. and V. Saxena, "Transverse Vibration of a Quarter of an Elliptic Plate with Variable Thickness", *International Journal of Mechanical Sciences,* Vol. 37, No. 10, pp.1103-1132, 1995.

93. Singh, B. and S. M. Hassan, "Transverse Vibration of a Circular Plate with Arbitrary Thickness Variation", *International Journal of Mechanical Sciences,* Vol. 40, No. 11, pp.1089-1104, 1998.

94. Gupta, U. S. and R. Lal, "Buckling and Vibrations of Circular Plates with Variable Thickness", *Journal of Sound and Vibration,* Vol. 58, No. 4, pp. 501-507, 1978.

95. Gupta, U. S., R. Lal and S. Sharma, "Vibration of Non-Homogenous Circular Mindlin Plates with Variable Thickness", *Journal of Sound and Vibration,* Vol. 302, pp. 1-17, 2007.

96. Gupta, A. K. and A. Khanna, "Vibration of Visco-Elastic Rectangular Plate with Linearly Thickness Variations in Both Directions", *Journal of Sound and Vibration,* Vol. 301, pp. 450-457, 2007.

97. Bayer, I., U. Güven and G. Altay, "A Parametric Study on Vibrating Clamped Elliptical Plates with Variable Thickness", *Journal of Sound and Vibration,* Vol. 254, No. 1, pp. 179-188, 2002.

98. Çeribaşı, S. and G. Altay, "Free Vibration of Super Elliptical Plates with Constant and Variable Thickness by Ritz Method", *Journal of Sound and Vibration,* Vol. 319, pp. 668-680, 2009.

99. Gupta, A. P. and N. Bhardwaj, "Vibration of Rectangular Orthotropic Elliptic Plates of Quadratically Varying Thickness Resting on Elastic Foundation", *Journal of Vibration and Acoustics,* Vol. 126, No. 1, pp. 132-140, 2004.

100. Chakraverty, S., R. Jindal and V. K. Agarwal, "Vibration of Nonhomogenous Orthotropic Elliptic and Circular Plates with Variable Thickness", *Journal of Vibration and Acoustics,* Vol. 129, pp. 256-259, 2007.

101. Wang, C. M., G. M. Hong and T. J. Tan, "Elastic Buckling of Tapered Circular Plates", *Computers and Structures,* Vol. 55, No. 6, pp. 1055-1061, 1995.

102. Kobayashi, H. and K. Sonada, "Buckling of Rectangular Plates with Tapered Thickness", *Journal of Structural Engineering,* Vol. 116, No. 5, pp. 1278-1289, 1990.

103. Nerantzaki, M. S. and J. T. Katsikadelis, "Buckling of Plates with Variable Thickness- an Analog Equation Solution", *Engineering Analysis with Boundary Elements,* Vol. 18, pp. 149-154, 1996.

104. Eisenberger, M. and A. Alexandrov, "Buckling Loads of Variable Thickness Thin Isotropic Plates", *Thin-Walled Structures,* Vol. 41, pp. 871-889, 2003.

105. Wang, C. M., J. N. Reddy and K. H. Lee, *Shear Deformable Beams and Plates: Relationships with Classical Solutions*, Elsevier Science Ltd., Amsterdam, 2000.

106. Boley, B. A. and J. H. Weiner, *Theory of Thermal Stresses*, John Wiley, New York, 1960.

107. Kaliakin, V. N., *Introduction to Approximate Solution Techniques, Numerical Modeling, and Finite Element Methods,* Marcel Dekker, New York, 2002.

108. Solecki, R. and R. J. Conant, *Advanced Mechanics of Materials,* Oxford University Press, New York, 2003.

109. Shames, I. H. and C. L. Dym, *Energy and Finite Element Methods in Structural Mechanics,* Hemisphere, Washington, 1991.

110. Birman, V. and L. W. Byrd, "Modeling and Analysis of Functionally Graded Materials and Structures", *ASME Applied Mechanics Reviews,* Vol. 60, pp. 195-215, 2007.

111. Shen, H. –S., *Functionally Graded Materials: Nonlinear Analysis of Plates and Shells,* CRC Press, New York, 2009.

112. Çeribaşı, S., *Statics and Dynamics of Super Elliptical Homogenous and FGM Plates,* Ph.D. Thesis, Boğaziçi University, 2007.

113. Delale, F. and F. Erdoğan, "The Crack Problem for a Non-Homogenous Plane", *ASME Journal of Applied Mechanics,* Vol. 50, pp. 609-614, 1983.